2013

# Novel insights into the function and regulation of group X secretory phospholipase $A_2$

Joseph D. Layne Jr
*University of Kentucky*, jdlayn3@uky.edu

STUDENT AGREEMENT:

I represent that my thesis or dissertation and abstract are my original work. Proper attribution has been given to all outside sources. I understand that I am solely responsible for obtaining any needed copyright permissions. I have obtained and attached hereto needed written permission statements(s) from the owner(s) of each third-party copyrighted matter to be included in my work, allowing electronic distribution (if such use is not permitted by the fair use doctrine).

I hereby grant to The University of Kentucky and its agents the non-exclusive license to archive and make accessible my work in whole or in part in all forms of media, now or hereafter known. I agree that the document mentioned above may be made available immediately for worldwide access unless a preapproved embargo applies.

I retain all other ownership rights to the copyright of my work. I also retain the right to use in future works (such as articles or books) all or part of my work. I understand that I am free to register the copyright to my work.

REVIEW, APPROVAL AND ACCEPTANCE

The document mentioned above has been reviewed and accepted by the student's advisor, on behalf of the advisory committee, and by the Director of Graduate Studies (DGS), on behalf of the program; we verify that this is the final, approved version of the student's dissertation including all changes required by the advisory committee. The undersigned agree to abide by the statements above.

Joseph D. Layne Jr, Student

Dr. Nancy Webb, Major Professor

Dr. Howard Glauert, Director of Graduate Studies

# NOVEL INSIGHTS INTO THE FUNCTION AND REGULATION OF GROUP X SECRETORY PHOSPHOLIPASE $A_2$

---

DISSERTATION

---

A dissertation submitted in partial fulfillment of the
requirements for the degree of Doctor of Philosophy in the
Graduate Center for Nutritional Sciences
at the University of Kentucky

By
Joseph D. Layne Jr.

Lexington, KY

Director: Dr. Nancy R Webb, PhD

Lexington, KY

2013

ABSTRACT OF DISSERTATION

# NOVEL INSIGHTS INTO THE FUNCTION AND RGULATION OF GROUP X SECRETORY PHOSPOLIPASE $A_2$

Group X secretory phospholipase $A_2$ (GX $sPLA_2$) hydrolyzes membrane phospholipids producing free fatty acids and lysophospholipids. Previous studies from our lab suggest that mice with targeted deletion of GX $sPLA_2$ (GX KO) have increased age-related weight gain due to an increase in overall adiposity. Paradoxically, this increased adiposity is associated with improved age-related glucose intolerance. GX KO mice also demonstrate a reduced inflammatory response to lipopolysaccharide injection. *In vitro* studies indicate this phenotype may be attributable to blunted macrophage mediated inflammatory responses. Given the role of macrophages in promoting adipose tissue (AT) inflammation and metabolic dysfunction in response to diet-induced obesity, we hypothesized that GX KO mice would be protected from the obesity related metabolic derangements associated with overfeeding. Unexpectedly, GX KO mice were only partially protected from high fat (HFD) diet-induced glucose intolerance and showed no improvement in HFD-induced insulin resistance. Moreover, GX KO mice were not protected against HFD-induced AT inflammation.

GX $sPLA_2$ is produced as a proenzyme (pro-GX $sPLA_2$), and propeptide cleavage is required for enzymatic activity. Furin-like proprotein convertases (PCs) have recently been implicated in the proteolytic activation of pro-GX $sPLA_2$; however the identity of individual PCs involved is unclear. Previous findings from our lab have shown that GX $sPLA_2$ is expressed in the adrenals where it regulates glucocorticoid production. GX KO mice have increased plasma corticosterone levels under both basal and ACTH-induced stress conditions. However, how GX $sPLA_2$ is regulated in the adrenals is still uncertain. We hypothesized that PCs may be involved in the proteolytic activation of pro-GX $sPLA_2$ in the adrenals. Here we report the novel findings that the PCs, furin and PCSK6, proteolytically activate pro-GX $sPLA_2$ in Y1 adrenal cells. Furthermore, we demonstrate that PC dependent processing of pro-GX $sPLA_2$ is necessary for GX $sPLA_2$ dependent suppression of steroidogenesis. Finally, we provide evidence that pro-GX $sPLA_2$ processing by PCs is enhanced in response to adrenocorticotropic hormone (ACTH), suggesting a novel mechanism for negatively regulating adrenal steroidogenesis. Cumulatively, these studies provide valuable insight into the function and regulation of GX $sPLA_2$.

Keywords: Phospholipase $A_2$, nuclear receptor, glucocorticoid, obesity, convertase

_Joseph D. Layne Jr._____
Student Signature

_12.13.2013_____
Date

NOVEL INSIGHTS INTO THE FUNCTION AND REGULATION OF GROUP X SECRETORY PHOSPHOLIPASE $A_2$

By

Joseph D. Layne Jr.

_Nancy R. Webb, Ph.D._____
Director of Dissertation

_Howard Glauert, Ph.D._____
Director of Graduate Studies

_12.13.2013_____
Date

Table of Contents

List of Tables

List of Figures

# Chapter 1

# Introduction

## 1.1 The secretory phospholipase $A_2$ ($sPLA_2$) family of enzymes

### 1.1.1 General properties of $sPLA_2$s

The phospholipase $A_2$'s are a unique class of enzymes that catalyze the hydrolysis of the sn-2 ester bond of glycerophospholipids liberating free fatty acids and lysophospholipids. The distinct biochemical properties of $PLA_2$s including cellular localization, requirement for $Ca^{2+}$, substrate specificity, and sequence homology allows for classification of these enzymes into several families including the $Ca^{2+}$ dependent arachidonoyl-specific cytosolic ($cPLA_2$), the $Ca^{2+}$ independent ($iPLA_2$), the platelet-activating-factor (PAF) hydrolases, and the low molecular weight (~14-18 kDa) secreted ($sPLA_2$)[1].

The $sPLA_2$ enzyme family is characterized by their requirement for millimolar concentrations of $Ca^{2+}$, utilization of a highly conserved catalytic histidine within their active site, and their ability to hydrolyze phospholipids with distinct polar head groups and fatty acyl chains. Thus far, eleven $sPLA_2$ isoforms have been identified (IB, IIA, IIC, IID, IIE, IIF, III, V, X, XIIA, and XIIB $PLA_2$-like protein that lacks catalytic activity) and placed into different groups based on the number and position of multiple conserved cysteine residues which pair up with one another to form disulfide bridges, generating a rigid three-dimensional structure (Figure 1.1).

The disparity in substrate specificity among the different $sPLA_2$ isoforms is attributable to the interfacial binding properties intrinsic to each one. For example, in human tears, GIIA $sPLA_2$ is the foremost bactericidal factor against gram-positive bacteria[2]. This may reflect the preference of the highly cationic GIIA $sPLA_2$ for anionic phospholipids including phosphatidylserine and phosphatidylglycerol[3]. Conversely, the outer leaflet of mammalian cell membranes are rich in phosphatidylcholine (PtdCho), and GIIA $sPLA_2$ exhibits virtually no enzymatic activity toward PtdCho rich liposomes in vitro[4]. GV and GX $sPLA_2$ on the other hand, potently hydrolyze zwitterionic membrane phospholipids including PtdCho[3,5]. This preference for condensed zwitterionic phospholipids like those found in mammalian membranes may be due, at least in part, to the presence of interfacial tryptophan residues. To this effect, tryptophan-67 in human GX $sPLA_2$ is necessary for efficient membrane hydrolysis[6]. Importantly, GIIA $sPLA_2$ contains no tryptophan residues and insertion of a unique tryptophan at amino acid position 3 (V3W GIIA $sPLA_2$) increased its hydrolytic activity toward PtdCho ~250 fold[7].

There is now evidence from in vitro studies supporting a role for several $sPLA_2$s in the release of arachidonic acid (AA) from cell membranes, thereby providing substrates for eicosanoid generation[6,8]. Among the most potent $sPLA_2$s capable of yielding AA is, in descending order, GX, -V, and, -III $sPLA_2$, likely reflecting their preference for phosphatidylcholine, the most abundant phospholipid in the outer leaflet of mammalian cell membranes[5,8,9]. Furthermore, there are reports that $sPLA_2$s may also indirectly lead to eicosanoid generation through the coordinated activation of $cPLA_2\alpha$. Indeed, GV $sPLA_2$ deficiency in bone marrow-derived mast cells (BMMCs) results in the

diminished TLR2 dependent generation of eicosanoids, likely due to decreases in the sequential phosphorylation and subsequent activation of ERK1/2 and cPLA$_2$α[10]. On the other hand, in mouse spleen cells GX sPLA$_2$ potently releases AA leading to prostaglandin E$_2$ (PGE$_2$) production in the presence of Pyrrophenone, a cPLA$_2$α-specific inhibitor[11].

### 1.1.2 sPLA$_2$ functional diversity

The diversity of tissue distribution and substrate specificity implies broad and distinct physiological functions of sPLA$_2$s (Figure 1.1, Table 1.1). To be certain, a role for sPLA$_2$s has been defined in regulating physiological processes including digestion of dietary phospholipids, inflammation, and host defense against infection among others.

The first sPLA$_2$ to be identified was GIB sPLA$_2$ in the pancreas[12]. GIB is secreted as a proenzyme into the duodenum by pancreatic acinar cells. Upon propeptide cleavage in the gastrointestinal tract by trypsin, GIB is able to digest dietary phospholipids, predominantly PtdCho. Mice deficient in GIB sPLA$_2$ are protected against diet-induced obesity (DIO) and insulin resistance[13]. Additional studies went on to suggest that GIB sPLA$_2$ deficiency protects mice from diet induced metabolic dysfunction by decreasing the absorption of dietary lysophospholipids, and in particular, lysophoshatidylcholine (LysoPtdCho)[14].

The investigation into both acute and chronic inflammatory disorders including sepsis, rheumatoid arthritis, and atherosclerosis has suggested a role for sPLA$_2$s as mediators of the inflammatory response. GIIA sPLA$_2$ is increased in the synovial fluid from patients with rheumatoid arthritis[15]. It has also been shown that GIIA sPLA$_2$ binds

integrins alphavbeta3 and alpha4beta1 and induces monocyte proliferation and inflammation[16], thus making it an attractive target for clinical intervention[17]. Plasma levels of GIIA $sPLA_2$ are increased in patients with sepsis, and appear to correlate with the severity of disease[18]. When antisense oligonucleotides to GIIA $sPLA_2$ are administered to Sprague-Dawley rats with sepsis, there is a reduction in overall mortality when compared to rats treated with either antibiotics or control oligonucleotides[19]. When the expression of several $sPLA_2$s is examined in rodent models of inflammation, there is increased expression of GV $sPLA_2$ and to a lesser extent GIID, IIE, and IIF, in response to lipopolysaccharide (LPS) injection[20]. However, to date, clinical trials using $sPLA_2$ inhibitors have proven disappointing with respect to their efficacy in treating both sepsis and rheumatoid arthritis[21-23]. Our lab has demonstrated a role for GV $sPLA_2$ in the hydrolysis of low density lipoproteins (LDL). GV $sPLA_2$ dependent hydrolysis of LDL increases its uptake by macrophages through a mechanism independent of scavenger receptors and requiring cell surface proteoglycans[24]. LDL-R deficient (LDL-$R^{-/-}$) mice overexpressing GV $sPLA_2$ by retrovirus mediated gene transfer have an ~2.7 fold increase in lesion area in the aortic root[25]. Conversely, GV $sPLA_2$ deficiency in bone marrow-derived cells (BMCs) results in significantly less lesion formation in LDL-$R^{-/-}$ mice when compared to LDL-$R^{-/-}$ mice who received WT BMCs[25]. Notably, recent evidence suggests that plasma $sPLA_2$ may provide prognostic information independent of traditional risk markers in patients with coronary artery disease[26,27]. On the other hand, GIID $sPLA_2$ is produced by regulatory T cells (Tregs) where, independent of its catalytic activity, it suppresses the proliferation of CD4+ and CD8+ T cells[28]. Importantly,

administration of a GIID-Fc fusion protein inhibits disease development in a mouse model of ulcerative colitis[28].

Several members of the $sPLA_2$ family have been shown to play a role in host defense against bacterial infection. The bactericidal properties of several $sPLA_2$s including groups I, II, V, X, and XII $sPLA_2$s toward Listeria Monocytogenes has been characterized, and bactericidal potency was found to be dependent on the overall positive charge, and to a lesser extent, the positive charge within the membrane binding surface of the $sPLA_2$[29]. The bactericidal properties of GIIA have been most clearly defined. In vitro studies suggest GIIA $sPLA_2$ kills Gram-positive bacteria including staphylococci and streptococci[30,31]. GIIA $sPLA_2$ has also been found in the mouse intestine, where it was shown to kill both Escherichia coli and Listeria monocytogenes[32].

### 1.1.3 $sPLA_2$ binding proteins

Several $sPLA_2$s are able to exert physiological affects through means independent of their hydrolytic activity. A class of $sPLA_2$ receptors in the brain has been identified based on their ability to bind snake venom $sPLA_2$ ($OS_2$) with picomolar level affinity. The binding affinity of snake venom $sPLA_2$ for these so-called neuronal-type (N-type) receptors appears to strongly correlate with its level of neurotoxicity, with higher affinity binding associated with increased toxicity[33]. Later, another $sPLA_2$ receptor was identified in rabbit skeletal muscle and hence named the muscle-type (M-type) receptor[34]. Through the binding of the M-type receptor, GIB $sPLA_2$ is able to influence cell proliferation, migration and lipid mediator production[35]. Additionally, the M-type receptor may be involved in GX $sPLA_2$ clearance and degradation[36]. There is also a soluble form of the M-type receptor that may act as an endogenous inhibitor of $sPLA_2$s[37]. Moreover, GV,

GIIA, and GIID $sPLA_2$ bind the heparan sulfate proteoglycan, glypican, and this binding is required for AA release and $PGE_2$ production[5].

### 1.1.4 GX $sPLA_2$

Within the $sPLA_2$ family, GX $sPLA_2$ has the most potent hydrolytic activity toward PtdCho, leading to the production of free fatty acids and LysoPtdCho (Figure 1.2)[38]. GX $sPLA_2$ has a wide tissue distribution[39], which is reflected in the diversity of physiological processes GX $sPLA_2$ is suggested to modulate. To this effect, a role for GX $sPLA_2$ in the regulation of inflammation, lipoprotein metabolism, myocardial infarction, and innate immunity have all been described[29,35,40-43].

A role for eicosanoids as mediators of inflammatory processes including atherosclerosis is now well established (reviewed in[44]). GX $sPLA_2$ appears to preferentially hydrolyze arachidonate and linoleate at the sn-2 position of PtdCho containing plasma lipoproteins[45,46]. Indeed, the preference of GX $sPLA_2$ for AA has important consequences with respect to eicosanoid generation. GX $sPLA_2$ has been implicated in the production of eicosanoids including $PGE_2$, $PGD_2$, leukotriene B4, and cysteinylleukotrienes (cysLTs) in a Th2 cytokine-driven mouse model of asthma[41]. Importantly, both GX $sPLA_2$ expression and cysLTs are increased in the airways of patients with asthma[47]. Our group has recently demonstrated a role for GX $sPLA_2$ in the production of $PGE_2$ in mouse pancreatic islet cells resulting in decreased glucose-stimulated insulin secretion (Shridas et al., unpublished data).

The pathophysiology of several disease processes stems from aberrant inflammatory responses in which GX $sPLA_2$ has been shown to be involved. GX $sPLA_2$

deficiency (GX KO) partially protects mice from myocardial ischemia/reperfusion injury, at least partly through the reduction of neutrophil cytotoxic responses[42]. Similarly, in a model of abdominal aortic aneurism (AAA) formation induced by $CaCl_2$ application to the external surface of the aorta, GX KO mice are partially protected from AAA formation, likely through reduced production of neutrophil derived matrix metalloproteinase (MMP-9), elastase, and gelatinase[48]. Results from our lab have demonstrated a role for GX $sPLA_2$ in promoting AAA formation in response to chronic subcutaneous infusion of angiotensin II (Ang II)[49]. Furthermore, gene expression analysis revealed that the mRNA levels of several inflammatory cytokines including cyclooxygenase-2 (COX-2), interleukin-6 (IL-6), matrix metalloproteinase-2 (MMP-2), MMP-13 and MMP-14 are significantly decreased GX $sPLA_2^{-/-}$/$apoE^{-/-}$ (GX DKO) mice compared to $apoE^{-/-}$ control mice. Additionally, GX KO mice show a marked reduction in allergen-induced interstitial edema and infiltration of inflammatory cells into the bronchoalveolar fluid and lung tissue[41]. Previous studies from our lab demonstrated GX KO mice have reduced plasma inflammatory cytokine expression in response to LPS injection, likely attributable to decreased toll like receptor 4 (TLR4) signaling in macrophages[43].

The lipolytic activity of GX $sPLA_2$ may increase the atherogenicity of lipoproteins. GX $sPLA_2$ expression is increased in atherosclerotic lesions[35]. To this effect, GX $sPLA_2$ hydrolytic modification of LDL has been shown to result in increased cholesterol ester uptake by macrophages[35]. LDL phospholipid hydrolysis also led to increased levels of LysoPtdCho, which may contribute to the production of inflammatory cytokines[50]. Furthermore, in vitro studies in human umbilical cord endothelial cells

(HUVECs) suggest that GX $sPLA_2$ modified LDL may increase adhesion molecule expression resulting in increased monocyte adhesion[40]. GX $sPLA_2$ can also hydrolyze PtdCho in high density lipoproteins (HDL). The lipolytic modification of HDL by GX $sPLA_2$ leads to decreased cholesterol efflux capacity from lipid loaded macrophages[51]. However, it should also be noted that when irradiated LDL-R deficient mice were reconstituted with bone marrow from GX $sPLA_2$ deficient mice it had a proatherogenic effect, possibly due to enhanced plaque infiltration if T lymphocytes[52]. Hence, a complete understanding of the role of GX $sPLA_2$ in the atherogenesis will likely only come from studies involving its tissue specific deletion.

Recent studies from our lab have defined a role GX $sPLA_2$ as a negative regulator of liver X receptor (LXR) transcriptional activation. Accordingly, *in vitro* studies have demonstrated that exogenous addition recombinant GX $sPLA_2$ or transgenic overexpression results in the suppression of LXR transcriptional activity and decreased target gene expression (Figure 1.3A). Conversely, in GX KO mice, LXR target gene expression is enhanced when compared to WT mice (Figure 1.3B). GX KO mice have enhanced LXR target gene expression peritoneal macrophages isolated from GX KO mice had increased expression of ATP-binding cassette transporter A1 (ABCA1) and G1 (ABCG1), leading to enhanced cholesterol efflux capacity in these cells (Figure 1.4)[53]. Conversely, GX $sPLA_2$ overexpression in J774 macrophages resulted in increased plasma membrane free cholesterol and lipid raft content[43]. The altered lipid raft content in GX $sPLA_2$ overexpressing macrophages was associated with enhanced TLR4 signaling and an augmented inflammatory response to LPS[43]. Evidence from GX KO mice has also implicated GX $sPLA_2$ in the regulation of adipogenesis[54]. When compared to control

mice, GX KO mice had increased age-related weight gain (Figure 1.5A, B) attributed to an increase in overall adiposity. Stromal vascular fraction (SVF) cells were isolated from GX KO mice and differentiated into adipocytes ex vivo, they accumulated significantly more triglyceride compared to SVF derived adipocytes from wild type mice. Conversely, GX $sPLA_2$ overexpression resulted in decreased triglyceride accumulation in differentiated OP9 cells. Most notably, OP9 cells overexpressing GX $sPLA_2$ had decreased expression of several LXR target genes involved in lipogenesis including SREBP-1c, FAS, SCD-1, and DGAT-1. We recently reported a role for GX $sPLA_2$ in the adrenals where it modulates glucocorticoid (GC) production[55].

GX KO mice have increased plasma corticosterone levels under both basal and adrenocorticotropic hormone (ACTH)-induces stress conditions (Figure 1.6). Mouse adrenals stained positive for GX $sPLA_2$ in the zona reticularis and the zona fasciculata but not the zona glomerulosa regions of the adrenal cortex, consistent with GX $sPLA_2$s ability to modulate GC but not mineral corticoid production. Experiments in GX KO mice using dexamethasone ruled out a systemic effect of GX $sPLA_2$ on the hypothalamic-pituitary axis. Primary adrenals from GX KO mice demonstrated a trend toward enhanced corticosterone production under basal conditions when compared to adrenal cells from control mice; this trend became highly significant upon stimulation with ACTH. The rate-limiting protein involved in adrenal GC production is steroidogenic acute regulatory protein (StAR). StAR expression was enhanced in the adrenals of GX KO mice under basal and ACTH-stimulated conditions. Conversely, StAR expression is suppressed in GX $sPLA_2$ overexpressing Y1 (Y1-GX) cells. Importantly, Cummins et al. identified StAR as a bona fide LXR target gene[56]. StAR promoter activation in response

to the LXR agonist T0901317 was diminished in Y1-GX cells compared to control transfected (Y1-C) cells. Furthermore, Y1-GX cells had decreased progesterone levels compared to Y1-C cells under both basal and ACTH-stimulated conditions. Notably, GX $sPLA_2$ dependent suppression of progesterone production was dependent on its hydrolytic activity. Indeed, GX $sPLA_2$, but not thecatalytically inactive mutant H46Q, was able to inhibit progesterone production in Y1 cells. However, the regulatory mechanisms underlying GX $sPLA_2$ activation in the adrenals have yet to be investigated.

Given the potency with which GX $sPLA_2$ hydrolyzes PtdCho, its enzymatic activity must be tightly regulated. Recent evidence suggests that GX $sPLA_2$ may be transcriptionally regulated in response to certain inflammatory stimuli. Primary epithelial cells cultured in the presence of TNF-α/IL-1β, IL-13, and to a lesser extent IL-17 had enhanced GX $sPLA_2$ expression when compared to untreated cells[57]. Conversely, IL-4 and IL-25 decreased GX $sPLA_2$ expression. However, results from our own lab suggest that GX $sPLA_2$ mRNA is not increased in response to lipolysaccharide (LPS) in macrophages (Shridas et al., unpublished data). The $sPLA_2$ receptor ($sPLA_2$-R) has been implicated in GX $sPLA_2$degradation. In $sPLA_2$-R expressing Chinese hamster ovary (CHO) cells, GX $sPLA_2$ was rapidly internalized and degraded, and this was associated with diminished $PGE_2$ production when compared to control CHO cells not expressing the $sPLA_2$-R[36]. Moreover, a soluble form of $sPLA_2$-R was found to bind and inactivate GX $sPLA_2$. Indeed, in vitro incubation of GX $sPLA_2$ with plasma from WT mice but not $sPLA_2$-R deficient mice resulted in decreased phospholipase activity[37].

GX $sPLA_2$ is produced as an inactive proenzyme (pro-GX $sPLA_2$), and propeptide cleavage appears to be necessary for enzymatic activity[45]. In GX $sPLA_2$ transgenic mice,

the predominant form of the enzyme found in tissues is the inactive proenzyme[58]. It is only after the induced formation of inflammatory granulation tissue that proteolytic activation of pro-GX $sPLA_2$ was observed. Within the 11 amino acid propeptide there is a dibasic motif, suggesting cleavage by furin-like proproteinconvertases (PCs)[45] (Figure 1.7). Indeed, use of the broad specificity peptide inhibitor, dec-RVKR-cmk, in GX $sPLA_2$ expressing HEK293 cells resulted in diminished pro-GX $sPLA_2$ processing and phospholipase activity[59]. Furthermore, using both permeable and non-permeable PC inhibitors, it has been suggested that pro-GX $sPLA_2$ processing and AA release occurs intracellularly. However, the sub-cellular location of pro-GX $sPLA_2$ processing may vary between tissues. To this effect, while pro-GX $sPLA_2$ processing and AA release may take place extracellularly in HEK 293 cells, AA release from CHO cells occurred both before and after enzyme secretion[60]. While PCs appear to be necessary for pro-GX $sPLA_2$ processing, at least in HEK 293 cells expressing a GX $sPLA_2$ transgene, the identity of the individual PCs involved in a physiologically relevant system remains to be investigated.

## 1.2 Furin-like proprotein convertases

### 1.2.1 Mechanism of action and substrate specificity

The subtilisin/kexin like proprotein convertase family consists of at least nine members, of which there are a core of seven biochemically and structurally related enzymes, namely PCSK1, $PCSK_2$, furin, PCSK4, PCSK6, and PCSK7[61]. The furin-like proprotein convertases (PCs) proteolytically activate zymogen targets through the recognition of dibasic motifs found within the substrates proregion. PCs are a group of calcium dependent serine-proteases that are themselves synthesized as proenzymes[62].

Among the PCs, furin is the most extensively studied. In the case of furin, the propeptide is necessary for proper folding, and elimination or substitution of the native proregion resulted in an inactive enzyme[63]. This N-terminally located propeptide act as an "intramolecular chaperone" (IMC) and is autoproteolytically cleaved at -Arg-Thr-LysArg107↓- in the endoplasmic reticulum[64]. The non-covalently linked but tightly bound IMC has been shown to act as an autoinhibitory peptide until a second autoproteolytic cleavage event leads to its disassociation[63]. The sequential, autoproteolytic cleavage of the IMC appears to take place in the endoplasmic reticulum and then in the trans-Golgi network (TGN). However, there is also evidence to suggest select PCs, most notably PCSK5A, and perhaps PCSK6, may retain their propeptide at the cell surface thus providing a mechanism for zymogen activation. In fact, in Y1 adrenal cells, PC5A (PCSK5A) was retained at the cell surface complexed to its prosegment, and upon stimulation with ACTH, detection of the prosegment was decreased and only the active PCSK5A enzyme remained[65].

A clustering of negatively charged residues within the catalytic domain of these enzymes may account for their substrate specificity for dibasic motifs[66,67]. Proteolysis of substrates usually occurs at the recognition motif -Arg-X-Lys/Arg-Arg↓-, including a P1 and P4 arginine[68]. The catalytic domains of furin-like PCs are remarkably well conserved, providing redundancy in substrate cleavage preferences. Therefore, the differential regulation of PC substrate recognition is likely determined, at least in part, by the various other regulatory domains governing PC-protein interactions, sub-cellular localization and trafficking, and $Ca^{2+}$ and pH requirements. There is evidence that signal sequences within the cytoplasmic domain of PCs including furin, PCSK5B and PCSK7

are involved in their intracellular trafficking within the TGN[61]. PCSK5A and PCSK6 interact with tissue inhibitors of metalloproteases (TIMPs) and heparin sulfate proteoglycans (HSPGs) through interactions with their cysteine-rich domains (CRDs)[69]. Downstream of the catalytic domain, the P domain is involved in modulating PC $Ca^{2+}$ dependence and pH requirements[61].

### 1.2.2 Physiological functions

The involvement of furin-like PCs in both maintaining homeostatic balance and in disease pathophysiology in humans has been the subject of intense investigation. Undoubtedly, the functional redundancy in substrate specificity seen among PCs confounds our understanding of their physiological function in vivo. Nonetheless, an emerging role for PCs in cancer, Alzheimer's, infectious diseases, hyperlipidemia, and neuroendocrinopathies have all been described (reviewed in [61]).

Deficiency in PCSK1 and $_2$ in mice leads to severe neuroendocrinopathies resulting from inadequacies in prohormone processing. Deletion of PCSK1 has been linked to diminished processing of precursor hormones including growth hormone-releasing hormone (GHRH), proopiomelanocortin (POMC), proinsulin, and proglucagon, leading to dwarfism[70]. Interestingly, a mutation in PCSK1 was identified in mice that resulted in an obese phenotype accompanied by marked hyperproinsulinemia in the absence of glucose intolerance[71], perhaps reflecting alterations in substrate specificity[61]. Indeed, the obese phenotype of this mouse may be more representative of human PCSK1 deficiency[72]. Similarly, $PCSK_2$ deficiency results in glucoregulatory imbalances due to impaired processing of proglucagon, proinsulin, and prosomatostatin in pancreatic islet cells[73]. Recently, using a panel of non-specific protease inhibitors, Jemel et al.

demonstrated a role for PCs in the proteolytic activation of ectopically expressed pro-GX $sPLA_2$ in HEK 293 cells[59]. We have recently described a role for GX $sPLA_2$ in regulating GC production in the adrenals[55]. However the role of PCs in regulating pro-GX $sPLA_2$ dependent modulation of glucocorticoid production has not been explored.

## 1.3 Glucocorticoid physiology

### 1.3.1 Regulation of adrenal glucocorticoid production

The hypothalamic-pituitary-adrenal (HPA) axis controls the secretion of GCs by the adrenals through a tightly controlled negative feedback system. In the hypothalamus, corticotrophin releasing hormone (CRH) is released in response to stress. In response to CRH, the pituitary releases pro-opiomelanocortin (POMC), the precursor to ACTH. The release of ACTH by the pituitary then triggers GC production in the adrenal cortex, which in turn limits the stress response through a feedback loop that involves negatively regulating both CRH and POMC secretion from the hypothalamus and the pituitary respectively.

Within the zona fasciculata of the adrenal cortex, ACTH stimulation of G-protein coupled receptors results in cyclic-AMP (cAMP)/protein kinase A (PKA) dependent mobilization of cholesterol to the inner mitochondrial membrane (IMM) where cytochrome P450scc (CYP11A1) metabolizes cholesterol to form pregnenolone, the precursor to all other steroid hormones. Interestingly, GC production is regulated, not at the level of CYP11A1 enzymatic activity, but by modulating the amount of cholesterol delivered to the mitochondria. In the adrenals, ACTH increases the expression of the sterol regulatory binding protein-1 (SR-B1) while also enhancing the expression and

activation of hormone sensitive lipase (HSL) which cumulatively leads to increased cholesterol trafficking to the mitochondria. The increased SR-B1 expression in the adrenals in response to ACTH provides substrates for steroid hormone synthesis through the "selective uptake" of HDL cholesterol[74]. Coordinately, ACTH also promotes the direct interaction between HSL and the cholesterol binding protein StAR, resulting in increased HSL mediated cholesterol ester hydrolysis from lipid droplets[75].

### 1.3.2 Steroidogenic acute regulatory protein

The trafficking of cholesterol from the outer mitochondrial membrane (OMM) to the IMM in response to ACTH is mediated by StAR[76,77]. Mice deficient in StAR die shortly after birth due to adrenocortical insufficiencies[78]. The loss of negative-feedback regulation of the hypothalamic-pituitary-axis leads to the trophic hormone induced deposition of lipid in the adrenals of these mice, ultimately resulting in their death. The trophic hormone stimulation of StAR activity involves the rapid cAMP/PKA dependent phosphorylation of the 37-kDa precursor (p37), leading to its intramitochondrial processing and subsequent targeting of the mature phosphorylated form (pp30) to the inner mitochondria[79]. While StAR processing and activation is dependent on the synthesis of new StAR protein, it appears to precede increases in StAR gene expression. The transcriptional regulation of StAR in response to ACTH is facilitated by the PKA dependent activation of nuclear Janus kinase-signal transducer and activator of transcription (JAK/STAT), leading to the increased protein stability of the carbohydrate response element binding protein (CREB) and the transcription of steroidogenic genes including StAR[80]. Notably, a role for LXR in regulating adrenal cholesterol homeostasis has also been demonstrated[56]. In mice, LXRα/β deficiency leads to decreased ABCA1

expression and a derepression of StAR, resulting in a net decrease in cholesterol efflux and enhanced GC production. Most importantly, our lab has shown that adrenals harvested from GX KO mice have enhanced StAR gene expression under both basal and ACTH-induced stress conditions[55]. Furthermore, the enhanced StAR expression is associated with significantly increased plasma corticosterone levels.

### 1.3.3 Role of arachidonic acid in regulating glucocorticoid production

Importantly, several studies have now demonstrated a role for AA mediated steroid production in response to trophic hormone stimulation. $PLA_2$s have been implicated in the generation of AA in human chorionic gonadotropin (hCG)-stimulated Leydig cells[81]. Furthermore, the mitochondrial acyl-CoA thioesterase (MTE-I) mediates AA release from arachidonyl-coA in adrenal cortex cells and results in augmented steroid production[82]. It has also been demonstrated that knockdown of either MTE-1 or acyl-CoA synthetase (ACS4) by small interfering RNA leads to a marked reduction in cAMP stimulated steroidogenesis, probably by decreasing StAR expression[83]. The release of AA provides substrate for AA metabolizing enzymes including the cyclooxygenases (COX), lipoxygenases, and the cytochrome p450 endoperoxidases. Notably, treatment of MA-10 Leydig cells with NS398, a $COX_2$ inhibitor, results in increased cAMP stimulated StAR expression and steroidogenesis[84]. Similarly, prostaglandin $F_2\alpha$ has been shown to negatively regulateStAR expression through the AP-1 family member c-Fos[85]. Conversely, AA metabolites derived from 15-lipoxygenase together with cAMP, synergistically activated steroidogenesis in adrenal cells[86]. However, studies from our own lab suggest that hydrolytic products generated in

response to GX $sPLA_2$ overexpression in Y1 adrenal cells (i.e. AA) inhibits StAR expression through the suppression of LXR transcriptional activation[55].

### 1.3.4 Metabolic effects of glucocorticoids

There is now evidence to suggest that hyperglucocorticoidism may contribute to the pathophysiology of the metabolic syndrome. Indeed, increased secretion of GCs in patients suffering from Cushing's syndrome leads to central obesity, hyperglycemia, hyperlipidemia, glucose intolerance, and hypertension[87].

In the liver, GC administration leads to a marked increase in enzymes involved in fatty acid synthesis, including acetyl-CoA carboxylase[88]. In vitro stimulation of rat hepatocytes with GCs results to increased hepatic secretion of ApoB containing lipoproteins by enhancing protein synthesis of ApoB100 and ApoB48 while preventing the intracellular degradation of newly synthesized ApoB[89]. These findings are consistent with the idea that GC therapy induces lipid accumulation in the liver[90,91] and may thus contribute to hepatic insulin resistance[92]. GCs also stimulate hepatic gluconeogenesis via interaction with the GC receptor and subsequently increasing expression of phosphoenolpyruvate carboxykinase (PEPCK) and glucose-6-phosphatase (G6Pase), the consequences of which result in enhanced hepatic glucose output and hyperglycemia[93,94]. Interestingly, adrenalectomy in ob/ob mice reverses the obese phenotype and GC replacement leads to reestablishment of obesity in adrenolectomized mice[95]. GCs may also impair insulin-dependent glucose uptake in adipocytes though a mechanism that involves decreased translocation of glucose transporter type-4 (GLUT4) to the plasma membrane[96]. Quite strikingly, GX KO mice have improved age-related glucose

intolerance, even in the face of increased adrenal GC production (Shridas et al., unpublished data).

### 1.4 Metabolic syndrome and type-2 diabetes

While the definition of the metabolic syndrome is somewhat a matter of debate, it is generally well agreed upon that it is associated with increased central adiposity, dislipidemia, elevated fasting blood glucose, and increased blood pressure. The metabolic perturbations associated with DIO are multifaceted and likely stem from a state of chronic low-grade inflammation, ultimately resulting in glucose intolerance and insulin resistance. The multi-organ pathogenesis leading to the metabolic dysregulation linked to type-2 diabetes (T2D) results from a failure to adequately respond to insulin.

#### 1.4.1 Role of macrophage inflammation in DIO

The rapid expansion of adipose tissue (AT) in response to DIO is associated with AT remodeling and increased FFA flux which may contribute to insulin resistance and ectopic lipid deposition. The excessive accumulation of lipid into AT results in adipocyte hypertrophy and adipocyte cell death, which may lead to the infiltration of adipose tissue macrophages (ATMs)[97]. Monocyte chemoattractant proteins (MCPs) and their receptors play an integral role in recruiting immune cells to the sites of inflammation. Both genetically obese db/db mice and high fat diet (HFD) induced obese mice had increased AT expression of C-C motif chemokine ligand-2 (CCL2 or MCP-1)[98]. Furthermore, mice expressing an MCP-1 transgene under the control of the AP2 promoter show evidence of increased AT inflammation, diminished insulin sensitivity, and worsening hepatic steatosis[98]. There is evidence from genetically engineered mouse models to suggest that ATM recruitment to dysfunctional AT plays a causal role in the development of AT

inflammation and subsequently glucose intolerance and insulin resistance[98,99]. Macrophage dependent AT inflammation is mediated, at least in part by TLR4. TLR4 deficiency in mice attenuates AT inflammation and insulin resistance in response to HFD, in the absence of reduced ATM infiltration[100]. The absence of TLR4 in bone marrow derived cells protects mice from HFD induced hepatic and AT insulin resistance[101]. Lipid rafts/caveolae are thought to be essential components necessary for TLR4-dependent signal transduction[102]. Notably, macrophage ABCA1 reduced TLR4 trafficking to lipid rafts by altering lipid raft cholesterol content[103]. We have recently shown that GX $sPLA_2$ potentiates TLR4 dependent cytokine production in J774 macrophages[43]. We attributed the enhanced inflammatory response to perturbations in cholesterol efflux capacity due to blunted ABCA1 expression. Recent evidence suggests that TLR4 deficiency may also result in an alternatively activated phenotype in macrophages leading to a blunted inflammatory response[104].

The AT of lean mice is predominantly occupied by a less inflammatory "alternatively activated" M2 macrophage, characterized by the enhanced gene expression of Ym-1, arginase-1 and IL-10[105]. Whereas "classically activated" macrophages, secreting high levels of TNFα and iNOS, typify AT from diet induced obese mice. There is now evidence to suggest that this shift in macrophage polarity toward a pro-inflammatory M1 phenotype may be causally linked to the development of glucose intolerance and insulin resistance associated with DIO. Indeed, the macrophage-specific deletion of peroxisome proliferator activated receptor-γ (PPARγ) impairs alternative activation and resulted in enhanced AT inflammation, glucose intolerance, and insulin resistance[106]. The agonist activation of LXR has been shown to increase PPARγ gene

expression[107]. Moreover, bone marrow-derived macrophages from WT mice are more reminiscent of alternatively activated macrophages, secreting more IL-10 and less proinflammatory cytokines, than macrophages isolated from ABCA1 deficient mice[108]. Peritoneal macrophages isolated from GX KO mice have enhanced LXR target gene expression, including ABCA1 and ABCG1[53]. However, the role of GX $sPLA_2$ in promoting macrophage mediated inflammation in a model of DIO has not been investigated.

### 1.4.2 AT dysfunction in DIO

It has been suggested that it is not the expansion of AT per se but the dysfunctional expansion of AT that may lead to ATM recruitment and metabolic dysfunction. Indeed, large hypertrophic adipocytes have been associated with genetic or DIO are linked to ectopic lipid deposition, insulin resistance and glucose intolerance[109]. Alternatively, when AT expansion results in adipocyte hyperplasia, stemming from the recruitment and differentiation preadipocytes, a "metabolically healthy but obese" (MHO) phenotype, lacking the metabolic dysregulation associated with over-nutrition, prevails[110]. Thus, tipping the scale toward a more hyperplastic AT phenotype tends to lend itself to an improved metabolic profile. To this effect, in the face of massive subqutaneous AT expansion, adiponectin transgenic ob/ob (Ad Tgob/ob) mice have smaller adipocytes and improved insulin sensitivity and glucose tolerance compared to control ob/ob mice[111]. Ad Tgob/ob mice have increased expression PPARγ, the master regulator of preadipocyte differentiation, in the AT compared to control mice. Notably, administration of PPARγ agonists, thiazolidinediones (TZDs), has also been shown to result in healthy AT expansion resulting in smaller adipocytes and improved insulin

sensitivity[112]. LXR response elements have been identified in the promoter region of PPARγ[107]. The LXR agonist, T0901317, has been shown to promote adipocyte differentiation, demonstrating marked increases in PPARγ and several genes involved in lipid metabolism[107]. Furthermore, agonist activation of LXR improves glucose tolerance in a model of DIO[113]. Upon differentiation, stromal vascular fraction (SVF) cells isolated from GX KO mice have increased lipid accumulation compared to SVF from WT mice[54]. On the other hand, GX $sPLA_2$ overexpression in differentiated OP9 cells results in diminished lipogenic gene expression compared to control cells. Intriguingly, GX KO mice demonstrate increased age-related weight gain compared to WT control mice. This increased weight gain is due to increased adiposity and hypertrophic adipocytes. Paradoxically, GX KO mice are protected from age-related glucose intolerance compared to WT control mice. However, the role of GX $sPLA_2$ in promoting metabolic dysfunction in a model of DIO has not been explored.

| $sPLA_2$ collection | $sPLA_2$ subtype | Gene manipulation | Phenotype |
|---|---|---|---|
| conventional $sPLA_2$s | IB | Knockout | Reduced obesity, hepatic steatosis and insulin resistance due to decreased phospholipid digestion in the GI tract |
| | IIA | Natural Knockout | Increased colon cancer |
| | | Knockout | |
| | | Transgenic | Alopecia and epidermal hyperplasia<br>Increased skin cancer[a]<br>Increased atherosclerosis<br>Protection from bacterial infection due to bacterial killing |
| | V | Transgenic | Neonatal death due to respiratory failure resulting from destruction of lung surfactant |
| | | Knockout | Reduced zymosan-induced peritonitis<br>Defective phagocytotic clearance of fungi<br>Reduced asthma<br>Impaired Th2 response[b]<br>Reduced LPS-induced air pouch inflammation<br>Reduced bacteria-induced airway inflammation<br>Reduced ischemia/ reperfusion-induced myocardial injury<br>Reduced atherosclerosis[c]<br>Exacerbated arthritis |
| | X | Transgenic | Pulmonary inflammation[d]<br>Alopecia and epidermal hyperplasia<br>Increased peripheral pain nociception |
| | | Knockout | Reduced asthma<br>Reduced ischemia/reperfusioninduced myocardial injury<br>Reduced aneurysm<br>Accelerated atherosclerosis[e]<br>Reduced phospholipid digestion in the GI tract in association with reduced adiposity<br>Abnormal hair follicles<br>Reduced peripheral pain nociception<br>Increased adiposity due to accelerated lipogenesis<br>Increased adrenal corticosteroidogenesis<br>Reduced macrophage cholesterol efflux<br>Reduced LPS-induced cytokine production in macrophages<br>Reduced capacitation of spermatozoa |
| Atypical $sPLA_2$ (group III collection) | III | Transgenic | Increased atherosclerosis<br>Systemic inflammation |
| | | Knockout | Impaired sperm maturation and infertility |
| Atypical $sPLA_2$s (group XII collection) | XIIB | Knockout | Steatohepatitis due to impaired hepatic secretion of VLDL |

[a] Skin-specific.
[b] Adoptive transfer of dendritic cells.
[c] Adoptive transfer of bone marrow cells.
[d] Macrophage-specific.
[e] Bone marrow transfer into $Ldlr^{-/-}$ mice.

**Table 1.1: Phenotype of sPLA2 gene-manipulated mice.**

(Adapted from Murakami et al., Biochimie, 2013)

**Figure 1.1: The $sPLA_2$ family.**

(Adapted from Murakami et al., J. Biochem, 2011)

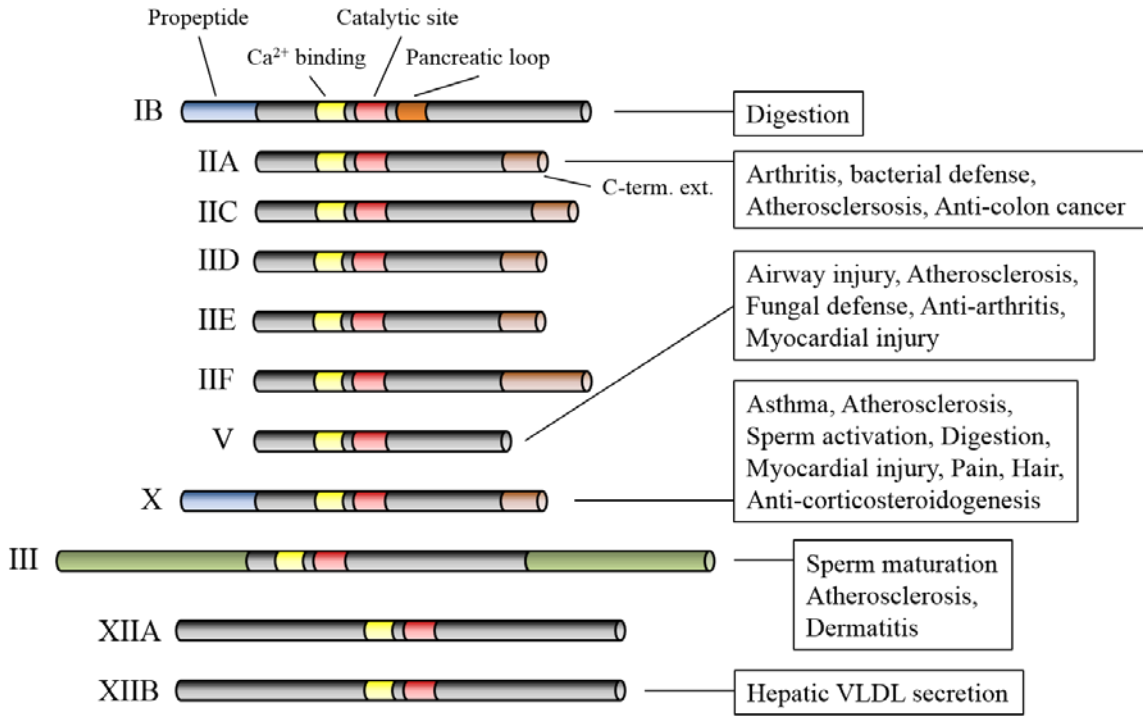

**Figure 1.2: GX sPLA$_2$ hydrolyzes phosphatidylcholine at the sn-2.**

GX sPla$_2$ cleaves the sn-$_2$ ester bond of phosphatidylcholine (PtdCho) producing free fatty acids (FFAs), most notably arachidonic acid (AA), and lysophsophosphatidylcholine (LysoPtdCho).

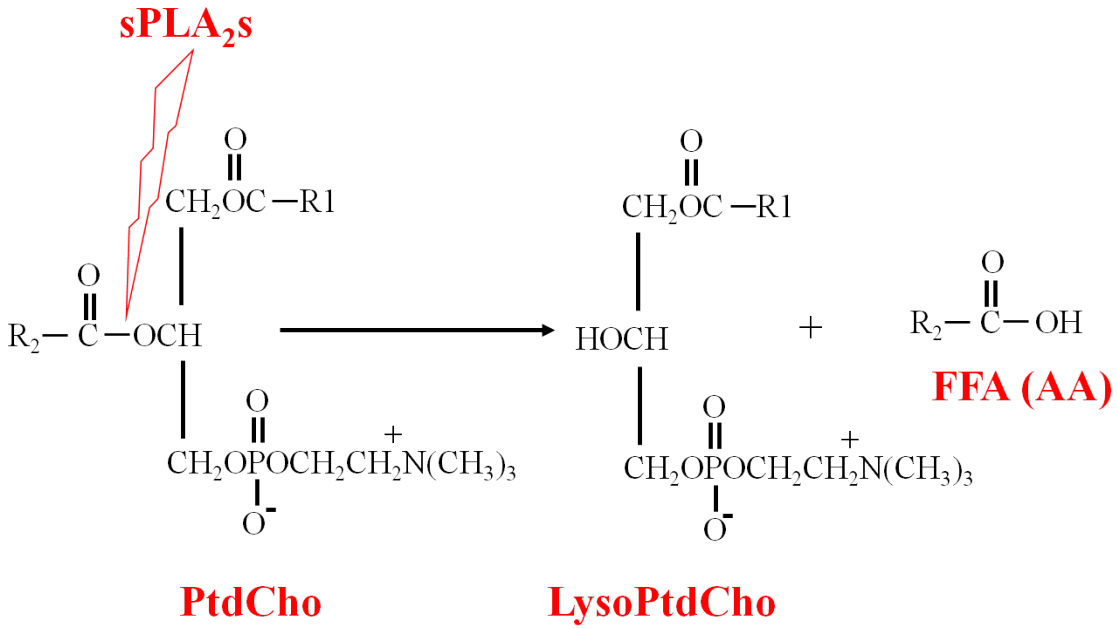

**Figure 1.3: GX $sPLA_2$ negatively regulates LXR transcriptional activity.**

A. GX KO mice have enhanced liver X receptor (LXR) target gene expression, resulting in a mouse with hypercorticosteronemia, increased adiposity, and a blunted inflammatory response. B. GX $sPLA_2$ overexpression results in blunted LXR target gene expression resulting in suppressed glucocorticoid production by adrenal cells, decreased triglyceride accumulation in adipocytes, and enhanced macrophage inflammatory responses.

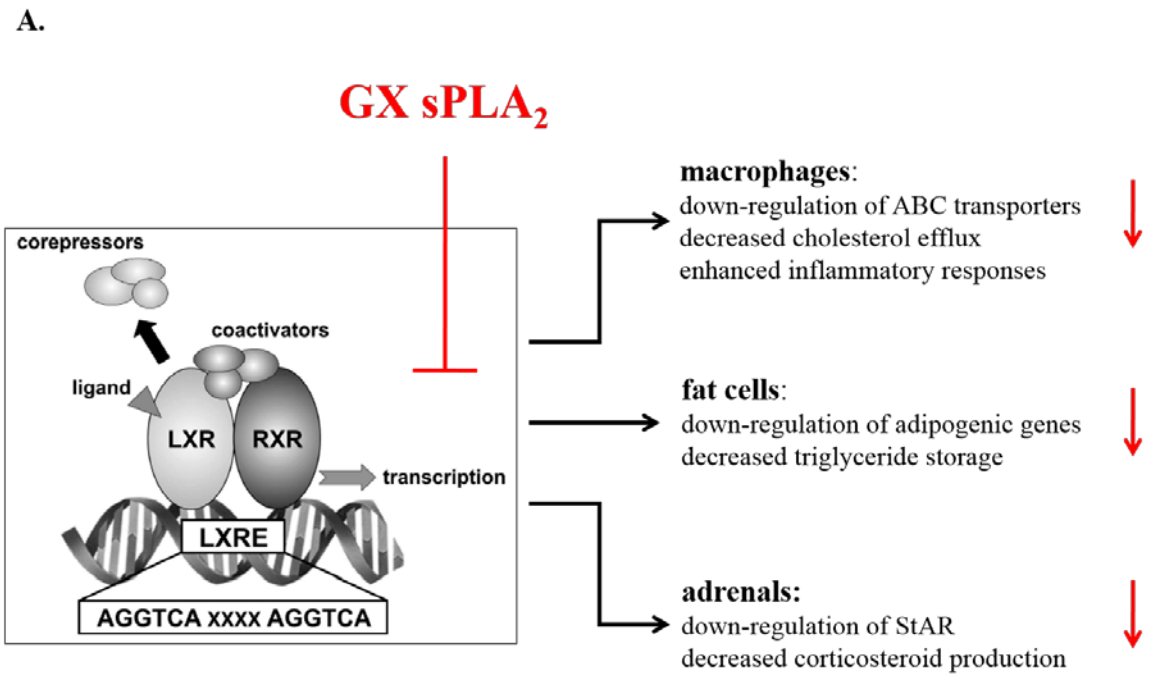

**Figure 1.3: (continued)**

**B.**

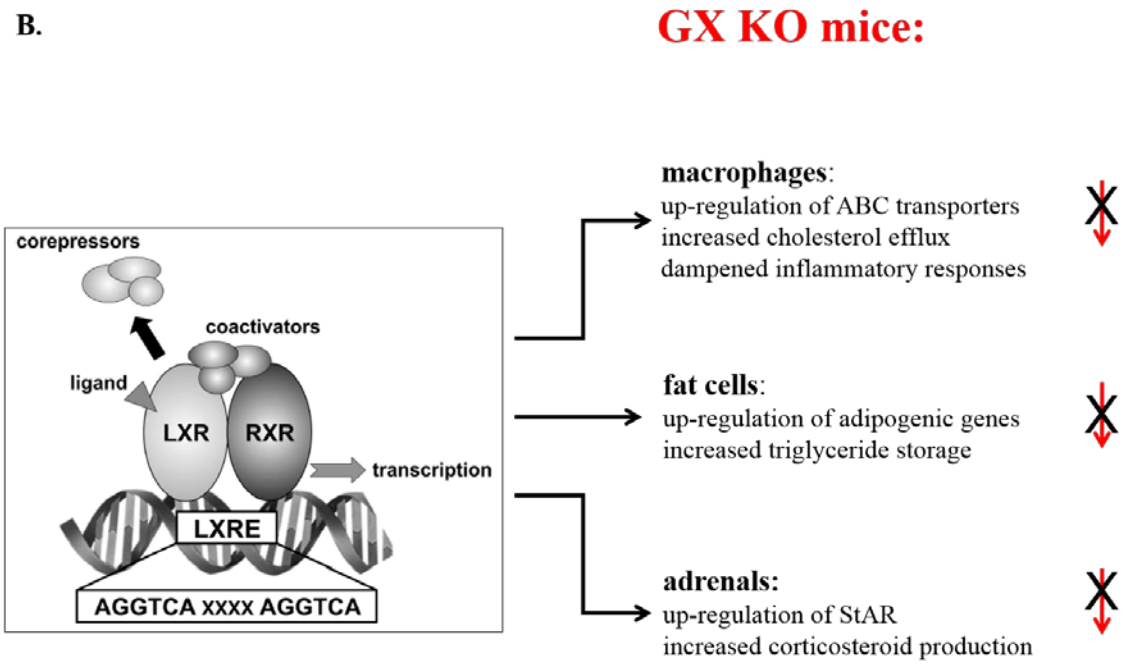

**Figure 1.4: Relative expression of ABCA1 and ABCG1 mRNAs in MPMs from WT and GX KO mice.**

Data are relative to WT MPM values; **P < 0.01 compared to WT MPMs. (Adapted from Shridas et al., JBC, 2010).

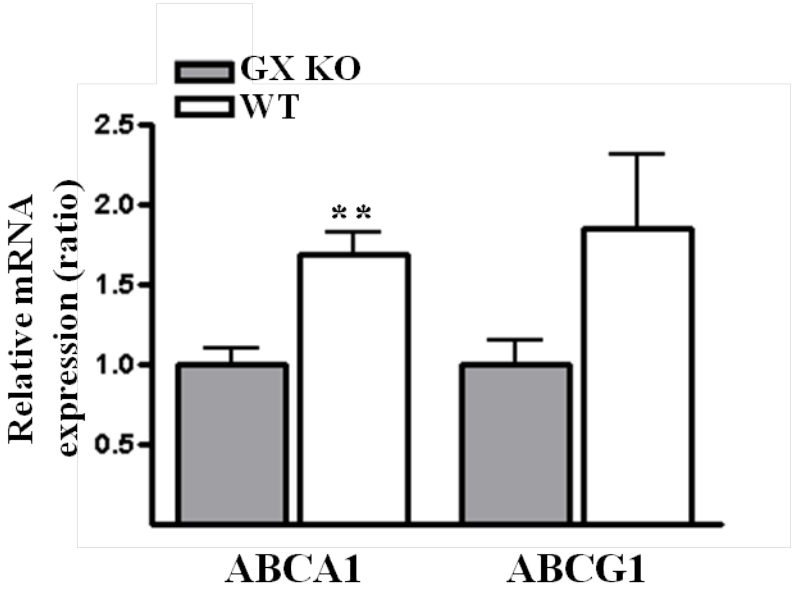

**Figure 1.5: GX KO mice have increased age-related weight gain compared to WT mice.**

A. Male C57BL/6 and GX KO mice in a C57BL/6 background were fed a normal rodent diet for 12 mo. B. Male C57BL/6 and GXKO littermates were singly housed at weaning, and body weights were determined weekly (n=4).*P<0.05 (Adapted from Li et al., FASEB J, 2010).

**A.**

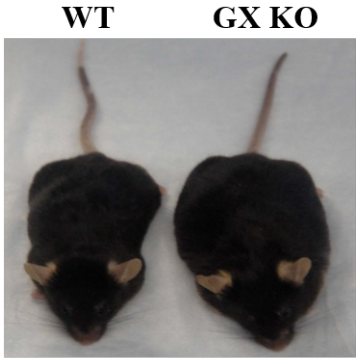


**B.**

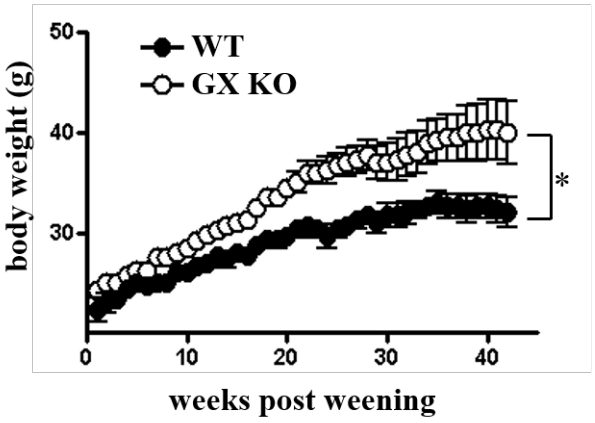

**Figure 1.6: GX KO mice have hypercorticosteronemia.**

Blood was collected from anesthetized 9-month-old WT (n = 5) and GX KO (n = 7) female mice by cardiac puncture. For ACTH treatments, 10-week-old mice received subcutaneous injections of 0.1 ml of saline or saline containing 4 units of ACTH at times 0, 12, and 24 h (n = 6).**P<0.01, ***P<0.01(adapted from Shridas et al., JBC, 2010).

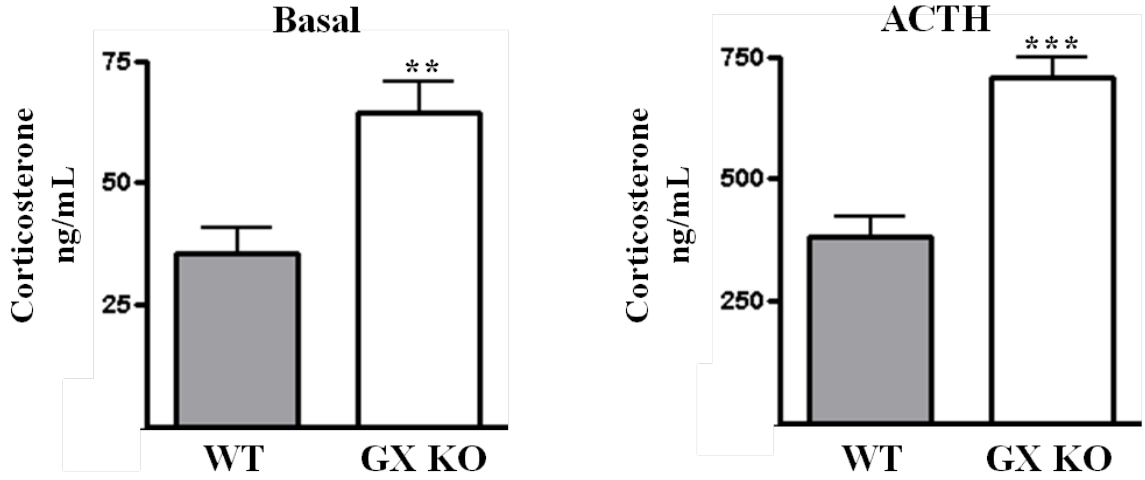

**Figure 1.7: GX $sPLA_2$ is cleaved by furin-like proprotein convertases.**

A. Schematic representation of GX $sPLA_2$. GX $sPLA_2$ is produced as a zymogen (pro-GX $sPLA_2$). B. The cleavage site within the prosegment contains a highly conserved dibasic motif, suggesting cleavage by furin-like proprotein convertases.

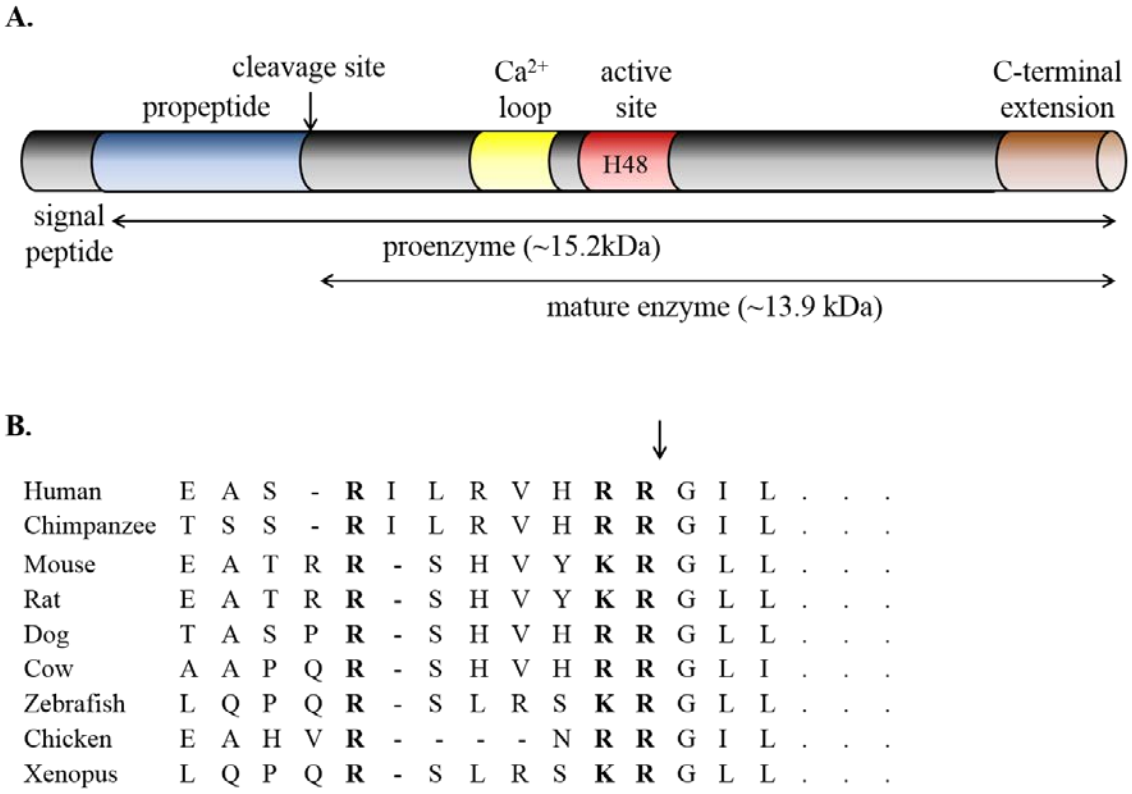

**Figure 1.8: Structure of Decanoyl-RVKR-cholomethylketone.**

Peptidyl chloroalkylketones containing the R-X-K/R-R motif irreversibly bind to the catalytic site of furin-like proprotein convertases (PCs), thereby inhibiting substrate processing[114].

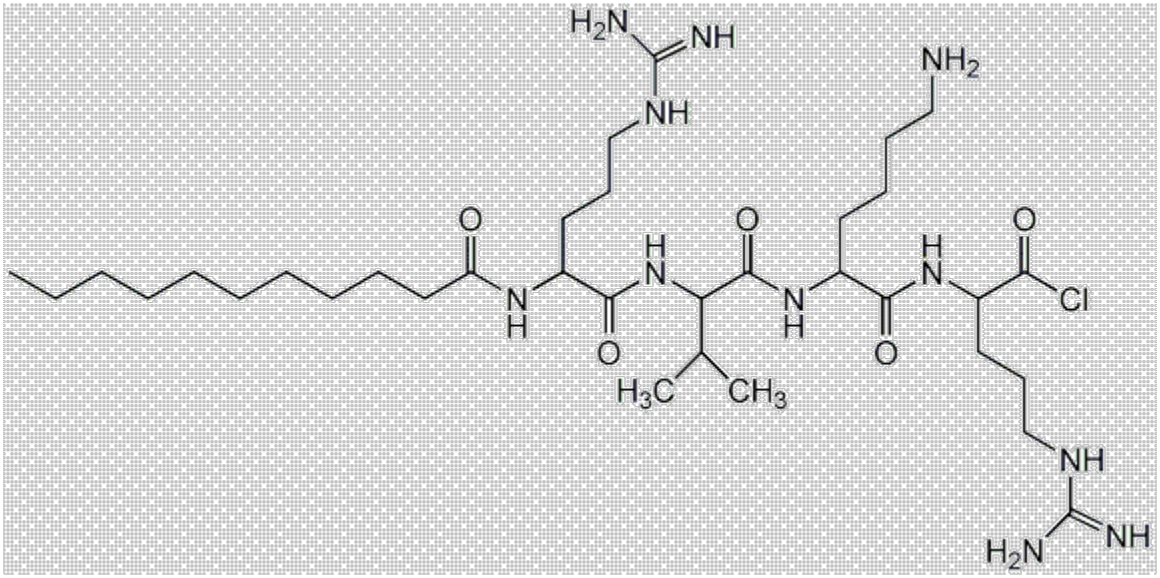

# Chapter Two

## Methods

### Mice

Targeted deletion of GX $sPLA_2$was carried out by InGenious Targeting Laboratory Inc. using embryonic stem cells derived from C57BL/6 mice. The targeting vector included a Neo cassette trapped inside exon 1, upstream of the translational start signal thereby replacing 564 bp of the GX $sPLA_2$ gene (Figure 2.1). Heterozygous breeding strategies were employed to produce male age-matched $GX^{+/+}$ (WT) and $GX^{-/-}$ (GX KO) mice. Mice were fed normal mouse chow diet ad libitum and were housed in an area on a 14-hour light/10-hour dark cycle. For some studies, 10-week old mice were assigned to either low fat diet (10% lard, D12450B, Research Diets) or high fat diet (60% lard, D12492, Research Diets) groups and maintained on diets for 16 weeks.

### Glucose Tolerance Tests

Mice were fasted for six hours at which point they were weighed. Baseline glucose values were then determined using a Contour glucose meter and test strips (Bayer HealthCare LLC) via tail vein prick with an 18 gauge 1 ½ inch needle. Mice were then given injections of a solution of 20% d-+-glucose (Sigma G7021) prepared in sterile phosphate buffered saline (PBS) intraperitoneally at a dose of either 1.5 g glucose per kg of body weight (0 and 4 weeks on diet) (i.e., 10 μl per gram of body weight) or 2 g glucose per kg body weight (8, 12, and 16 weeks on diet). Blood glucose measurements were then recorded 30, 60, 90, 120, and 180 minutes after glucose injection.

**Insulin Tolerance Tests**

Mice were fasted for six hours at which point were weighed. Baseline glucose values were then determined using the glucose meter via tail vein prick with an 18 gauge 1 ½ inch needle. Mice were then injected with Novolin R recombinant human insulin, (Novo Nordisk A/S) at a dose of 1 unit per kilogram of body weight. Blood glucose measurements were then recorded 30, 60, 90, 120, and 180 minutes after insulin injection.

**RNA extraction from adipose tissue**

Adipose tissue was excised and snap-frozen in liquid nitrogen until further processing. For RNA extraction, the RNeasy Lipid Tissue Kit (Qiagen) was used. To begin, approximately 100 mgs of frozen tissue was immediately added to 1mL of Qiazollysis reagent and placed on ice (1mL eppendorf tube). Lysis of adipose tissue was achieved using a hand homogenizer (VWR) for 15-30 seconds per sample. After a minute incubation 200 µL of chloroform was added to each sample at which point samples were vortexed for 10 seconds each. Samples were then centrifuged at 16,100 x g for 10 minutes at 4$^{o}$C. Upon centrifugation, the upper, acqueous layer was transferred into a fresh 1 mL eppendorf tube containing 600 µL of 70% ethanol. After mixing by briefly vortexing, up to 700 µL of sample was transferred to an RNeasy spin column placed in a 2mL collection tube. Sample was then centrifuged at 16,100 x g for 1 minute at 4$^{o}$C. Flow-through was discarded and the process was repeated as necessary until the entire sample had been transferred to the spin column. Following centrifugation 700 µL per sample of buffer RW1 was added to the spin column and samples were again centrifuged at 16,100 x g for 1 minute at 4$^{o}$C. The flow-through was discarded. 500 µL of buffer RPE

per sample was then added to the spin column and it was centrifuged at 16,100 x g for 1 minute at 4oC. After the flow through was discarded, the spin column containing the sample was centrifuged once more at 16,100 x g for 1 minute at 4$^{o}$C to remove any residual wash buffer. Spin column was then placed in a clean 1mL eppendorf tube at which point 40 µL of RNase free water was added to each spin column in order to elute the RNA. RNA concentrations were quantified using the NanoDrop Spectrophotometer (Thermo Scientific) and stored at -80$^{o}$C until further use.

**Immunofluorescent staining**

Adipose tissue was collected and fixed in 10% paraformaldehyde. 5 µM thick, paraffin embedded adipose tissue samples were mounted on glass slides. For deparaffinization, slides were immersed in xylene (3x for 5 minutes each), followed by immersion in progressively diluted ethanol solutions, 100% ethanol, 3x for $_{2}$ minutes each, 95% ethanol, 3x for 2 minutes each, and 70% ethanol, 3x for $_{2}$ minutes each, followed by a $_{2}$x rinse in PBS for 1 minute each. This was followed by a 30 minute heat-induced antigen retrieval (HIER) in which samples were immersed in 1x (DAKO) antigen retrieval buffer and placed in boiling water bath for 30 minutes. Upon completion samples were allowed to cool for at least 1 hour. Samples were then washed in PBS and immersed in a hydrogen peroxide solution (800 µL 30% w/w $H_2O_2$ in 50 mL PBS) for 10 minutes to quench endogenous peroxidases. The samples were then rinsed in PBS and incubated in TNB [180 mL dd$H_2O$ plus 20 mL of 10X TN buffer, (for 1L 10X TN buffer; 121.14 g Tris-HCl free base, 87.7 g NaCl, 800 mL, pH to 7.5 with 6N HCl) plus 1 g of Perkin Elmer blocking reagent (cat. # FP1020), warmed to 60$^{o}$C for 1 hour]. After 1 hour TNB was drained off and 250 µL of primary antibody diluted in TNB (1/100) was added

to samples. After overnight incubation in humidified container at 4$^{o}$C, primary antibody was drained off and samples were washed TNT buffer (160 ml of 10x TN, 16 mL of 10% Triton-X, dd$H_2O$ to 1600 mL), 3x for 5 minutes each. The samples were then incubated in secondary antibody diluted in TNB (1/1000) (Peroxidase AffiniPureF(ab')$_2$ Frag Goat Anti-Rat IgG, Jackson Laboratories 112-036-072) for 1 hour at room temperature. The secondary antibody was then drained off and sample was again washed in TNT buffer, 3x for 5 minutes each. A 1/50 dilution of TSA stock was prepared using amplification diluent from TSA, Plus Cyanine 3 System (Perkin Elmer). The samples were then incubated in TSA for 10 minutes at room temperature followed by a 3x wash cycle in TNT buffer (5 minutes each). After wash buffer was drained, mounting media was added, Anti-Fade Reagent containing DAPI (Invitrogen) and slide covers were added. The next day samples were analyzed using fluorescence microscopy.

**Phospholipase activity assay**

Conditioned media was harvested and assayed for phospholipase activity using a colorimetric assay as previously described by Wooton-Kee et al[115]. Briefly, using 1-palmitoyl-$_2$-oleoylphosphatidylglycerol (POPG) (Matreya) as substrate, mixed micelles were prepared by dissolving 7 mg of POPG in 0.2 mL mixture of 4.0% (w/v) Nonidet P-40 and 2.0% sodium deoxycholate to 37$^{o}$C, and then adding 1.8 ml of warm assay buffer (0.12 mol/liter Tris-HCl, pH 8, 12 mmol/liter $CaCl_2$, 0.1 mmol/liter EDTA). Enzymatic activity was assayed by adding 10µl of conditioned media 40µl of substrate solution. After incubating at 37$^{o}$C for 20 minutes, the amount of free fatty acids released was quantified using a NEFA-C kit (Wako Chemicals).

**sPLA$_2$ activity assay**

Media was collected and centrifuged at 16,100 x g for 5 minutes at 4$^o$C. Upon centrifugation media was transferred into fresh 1 mL eppendorf tube. sPLA$_2$ activity was measured using sPLA$_2$ assay kit (Cayman Chemical) according to the manufacturers' instructions. Briefly, 10 μL of clarified media was assayed for phospholipase activity using a 1, 2-dithio analog of diheptanoylphoosphatidylcholine. Upon hydrolysis of the thioester bond at the sn-2 position, free thiols were detected using 5, 5-dithio-bis-(2-nitrobenzoic acid) (DTNB). The plate was immediately placed in an xMARKmicroplate reader spectrophotometer (Bio-Rad) and absorbance was measured at 414 nM every minute for 20 minutes.

**Immunobotting**

Cells were washed using Delbecco's phosphate buffered saline (DPBS) and harvested using RIPA buffer (Sigma) supplemented with Complete Mini protease inhibitor cocktailtablets (Roche). Total cellular protein was quantifiedusingBicinchoninic acid (BCA) assay. For StAR protein expression analysis, 10μg of cell lysate was resolved by sodium dodecyl sulfate polyacrylamide electrophoresis (SDS-PAGE) (4% stacking/10% resolving gel) and transferred to a polyvinylidene fluoride (PVDF) membrane Immobilon-P (Millipore) for western blotting. Membranes were blocked in TBST ($_2$0mM Tris, 200mM NaCl, 0.5% Tween 20, pH 7.6) containing 5% nonfat mild for 1 hour. After blocking, membranes were washed with TBST followed by overnight incubation at 4$^o$C using an anti-StAR primary antibody (Santa Cruz, StAR FL-285) diluted in TBST containing 5% nonfat milk. Membranes were again washed with TBST and incubatedin HRP-conjugated secondary antibody in TBST containing 5% nonfat milk

for 2 hours at room temperature. Following a final wash in TBST, membranes were incubated for 2 minutes in enhanced chemiluminescence (ECL) (Amersham) and analyzed using autoradiography film. Quantification of bands was carried out using Image Station 440 (Kodak) and the Kodak ID 3.6 software. For GX $sPLA_2$ protein expression analysis, conditioned media was centrifuged at 16,100 x g for 5 minutes at room temperature and transferred to a fresh 1mL eppendorf tube. 20μL of conditioned media was resolved by SDS-PAGE (4% stacking/14% resolving gel) and processed as described above using an anti-FLAG antibody (Agilent, anti-FLAG M2).

**Reporter Assays**

Y1 BS1 adrenal cells were grown to approximately 75% confluence and then transfected with mouse 3X-FLAG-tagged GX $sPLA_2$ expression vector or the corresponding pcDNA3.0 control vector (0.4μg) along with pTK-3-LXRE-Luc reporter construct (0.4μg), mLXRα, (0.1μg), mRXR (0.1μg), renilla- luciferase (Promega, $0.0_2$μg), and furin or PCSK6 (0.4μg) (Origene) using Lipofectamine 2000 according to the manufacturer's protocol. Both the mLXR and the 3X-LXRE were gifts from Dr. Peter Tontonoz (UCLA). After 18 hours, cells were incubated in fresh media (high glucose DMEM (HyClone), supplemented with 10% heat-inactivated fetal bovine serum, 100 units/ml penicillin, and 100 μg/ml streptomycin), and either 0 or 1μM T0901317 for 24 hours. Cells were washed with DPBS and harvested in 1 x PLB buffer (Promega). Luminescence was measured using the Dual-Luciferase Reporter Assay System (Promega).

**Quantitative real time-PCR**

Cells were grown in $_2$4-well plates and total RNA was harvested using RNeasy Mini Kit (Qiagen) according to manufacturers' instructions. Briefly, cells were harvested in 350 µL RLT buffer containing 10 µL Beta-mercaptoethanol/mL of RLT. Sample was immediately added to 350 µL 70% ethanol and vortexed. Sample was transferred to RNeasy spin column and centrifuged at 16,100 x g for 1 minute at 4$^o$C. The flowthrough was discarded and 750 µL RW1 buffer was added to spin column followed by centrifuged at 16,100 x g for 1 minute at 4$^o$C. Flowthrough was again discarded and 500 µL of RPE buffer was added followed by centrifugation at 16,100 x g for 1 minute at 4$^o$C. This step was repeated a second time. Samples were then centrifuged at 16,100 x g for 2 minutes at 4$^o$C to remove any residual liquid. The spin column was transferred to a clean 1 mL eppendorf tube at which point 30 µL of RNase free $H_2O$ was added to spin column and samples were incubated at room temperature for 1 minute followed by 16,100 x g for 1 minute at 4$^o$C. RNA abundance was quantified using the NanoDrop Spectrophotometer (Thermo Scientific) and stored at -80oC until further use. Reverse transcription was carried out using the High Capacity cDNA Reverse Transcription Kit (Applied Biosystems). Quantitative real time-PCR was carried out using Power SYBR Green PCRMaster Mix (Applied Biosystems) using the following restrictions: 95$^o$C for 3 minutes; 95$^o$C for 10 seconds, 58$^o$ for 30 seconds, 72$^o$C for 30 seconds (40 cycles); 10$^o$C hold. Primer sequences specific for particular genes of interest are presented in Table 2.1.

**Gene silencing with small interfering RNA (siRNA)**

A set of ON-TARGET plus SMART pool siRNA (Thermo Scientific) synthetic oligonucleotides directed toward the mouse PCSK6 target sequences (5'-UAAACAAGCUUUCGAGUAU-3', 5'-GGUCAGAGAUGAACGUCCA-3', 5'-CGAGAUGCCUGGCGUCACA-3', and 5'-GAUGAGACCUUCUGCGCGA-3') and toward the mouse furin target sequences (5'-CGACAUCGGCAAACGGCUA-3', 5'-GAAGAAUCAUCCCGACCUA-3', 5'-GAAAGUGAGCCAUUCGUAU-3', and 5'-GCGCCACACAGUUCGGCAA-3'). The ON-TARGET plus Non-targeting pool (Thermo Scientific) was used as a control. The transfection of GX $sPLA_2$ 3x-FLAG stably expressing Y1 adrenal cells (Y1-GX) was achieved using Dharmafect 1 transfection reagent (Thermo Scientific) according to manufacturer's instructions.

**Expression of GX $sPLA_2$ in Y1 cells**

Murine Y1 adrenal cells were purchased from American Type Culture Collection (ATCC) and maintained in F-12K media (ATCC) supplemented with 2.5% non heat-inactivated fetal bovine serum (Invitrogen), 15% non heat-inactivated horse serum (Invitrogen), 100 units/mL penicillin, 100 µg/mL streptomycin. A C-terminal 3x FLAG-tagged mouse GX $sPLA_2$cDNA was developed by PCR using forward (5'-CTGAAGCTTATGCTGCTGCTACTG-3') and reverse (5'-ATGAATTCTCACTTGTCATCGTCGTCCTTGTAGTCGATATCGTGGTCCTTGTAGTCTCCATCGTGGTCCTTGTAGTAGTCATT-3') primers containing HindIII and EcoRI restriction sites, respectively, and a previously generated GX $sPLA_2$ fused to a single C-terminal FLAG-tag in pcDNA 3.1 (Invitrogen) as a template[55]. The PCR product was purified over a 1% agarose gel in 1x Tris-acetate buffer (TAE) (for 1 L of 50x, 242 g

Tris base 57.1 mL glacial acetic acid, and 0.5 M EDTA, pH 8.0) containing 0.02% ethidium bromide. PCR product was eluted from gel using QIAguick Gel Extraction Kit (Qiagen). Then both the GX $sPLA_2$cDNA and pcDNA 3.1 was incubated at room temperature for 4 hours with HindIII and EcorI endonucleases (New England Biolabs, NEB). The digestion product was again purified over a 1% agarose gel and purified using the Qiagen gel extraction kit. A ligation reaction was then carried out at room temperature for 10 minutes using T4 DNA ligase (NEB) and a molar ratio of GX $sPLA_2$cDNA/pcDNA 3.1 of 3/1. The ligation reaction mixture was then used to transform 5-alpha F'Iq competent e-coli cells (NEB) according to the manufacturer's instructions. The DNA sequence was confirmed in collaboration with Davis Sequencing. Y1 cells were then transfected with the C-terminal 3x FLAG-tagged GX $sPLA_2$ using Lipofectamine 2000 (Invitrogen) according to the manufacturer's instructions. Stable clones were selected for using 500µg/mL G418 (Invitrogen).

**Co-expression of GX $sPLA_2$ with furin and PCSK6**

Mouse cDNA clones for furin (accession # BC048234) and subtilisin/kexin type 6 (PCSK6) (accession # NM_011048.1) were purchased from Origene (catalog # MC202300 and MR215393, respectively). HEK 293 cells were maintained in DMEM/High Glucose (HyClone) supplemented with 10% heat-inactivated FBS (Invitrogen) and 100 units/mL penicillin, 100 µg/mL streptomycin. All experiments were carried out in 24 well plates grown to ~80% confluency at the time of transfection. 0.8 µg DNA total was transiently transfected using Lipofectamine $_2$000 (Invitrogen) according to the manufacturer's protocol. Briefly, using a ratio of 1 µg DNA/2.5 µLLipofectamine, 0.8 µg DNA/ well was diluted up to 50 µL with serum-free Opti-MEM (Invitrogen) and

incubated at room temperature for 5 minutes. At the same time 2 μL of Lipofectamine/well was diluted up to 50 μL with serum-free Opti-MEM and incubated a room temperature for 5 minutes. After 5 minute incubation period, 50 μL of diluted Lipofectamine was added to 50 μL of diluted DNA and incubated at room temperature for $_2$0 minutes to allow DNA-Lipofectamine complexes to form. After the 20 minute incubation period, 100 μL of DNA-Lipofectamine complexes was added to each well. HEK 293 cells were then incubated for 8 hours in transfection media. Cells were then incubated in fresh media for 24 hours. Upon harvest, cells were washed with 0.5 mL of ice-cold PBS. After aspirating off PBS, whole cell lysates were harvested in 100 μL RIPA lysis buffer (Sigma) and stored in -20$^o$C. The media was collected and centrifuged at 16,100 x g for 5 minutes at 4oC. After centrifugation, media was transferred to a fresh 1 mL eppendorf tube and stored at -20$^o$C until further processing.

**Progesterone Assay**

Media was collected and centrifuged at 16,100 x g for 5 minutes at 4$^o$C. Upon centrifugation media was transferred into fresh 1 mL eppendorf tube. Samples were stored at -80$^o$C until further processing. Progesterone in the media was measured using the Progesterone EIA kit (Cayman Chemicals) according to the manufacturer's instructions. Briefly, media samples were diluted in EIA buffer 1/25. It is a competition based assay in which progesterone competes with progesterone conjugated to an acteylcholinesterase (AChE) (progesterone tracer) for binding. AChE cleaves acetylcholine, exposing the free thiol which is then free to react with the detection reagent DTNB.

## Statistics

Statistical analysis between two groups was carried out using a two-tailed student's t-test. For comparison of more than two groups, statistical significance was determined using a 1-way analysis of variance (ANOVA) followed by Tukey's post-hoc analysis. For comparisons between multiple treatment groups, a 2-way ANOVA was used (example; diet and genotype). In the case of non-normally distributed data, a Mann-Whitney test was performed to determine significance between groups.

**Table 2.1: List of primers used for qRT-PCR analysis.**

| Genes | Forward | Reverse |
|---|---|---|
| 36b4 | 5'-AAG CGC GTC CTG GCA TTG TCT-3' | 5'-CCG CAG GGG CAG CAG TGG T-3' |
| 18s | 5'-CGG CTA CCA CAT CCA AGG AA-3' | 5'-GCT GGA ATT ACC GCG GCT-3' |
| TNFα | 5'-GGC AGG TCT ACT TTG GAG TCA TTG-3' | 5'-GTT AGA AGG ACA CAG ACT GG-3' |
| IL-1β | 5'-GTC ACA AGA AAC CAT GGC ACA T-3' | 5'-GCC CAT CAG AGG CAA GGA-3' |
| MCP-1 | 5'-TTC CTC CAC CAC CAT GCA G-3' | 5'-CCA GCC GGC AAC TGT GA-3' |
| IL-10 | 5'-CCA AGC CTT ATC GGA AAT GA-3' | 5'-TCT CAC CCA GGG AAT TCA AA-3' |
| IL-6 | 5'-CAA CGA TGA TGC ACT TGC AG-3' | 5'-GTA GCT ATG GTA CTC CAG AAG-3' |
| arginase-1 | 5'-TGG CTT TAA CCT TGG CTT GCT TCG-3' | 5'-AAG AAC AAG CCC TTG GGA GGA GAA-3' |
| MR | 5'-CCA CAG CAT TGA GGA CTT TG-3' | 5'-ACA GCT CAT CAT TTG GCT CA-3' |
| iNOS | 5'-GCA GCT GGG CTG TAC AAA-3' | 5'-AGC GTT TCG GGA TCT GAA T-3' |
| StAR | 5'-TTGGGCATACTCAACAACCA-3' | 5'-GAAACACCTTGCCCACATCT-3' |
| furin | 5'-TGA GCC ATT CGT ATG GCT ACG-3' | 5'-GGA CAC AGC TTT TCT GGT GCA-3' |
| PCSK1 | 5'-GGA TCT CTT CAA TGA TCC AAT GTG G-3' | 5'-CCT CAA TGG CAT CAG TTA CAA-3' |
| PCSK2 | 5'-GAG ACC CGT CTT CAC GAA TC-3' | 5'-GTT GAA CCA GTC ATC TGT GTA TCG-3' |
| PCSK5 | 5'-GGG CGG AGA GGC CTT GGA-3' | 5'-TTT GTC GGT CTG TGC TTT CCA C-3' |
| PCSK6 | 5'-GCA TAG AAA GGA ATC ACC CAG-3' | 5'-TGT AGC CAT CAC AGG AGC AG-3' |
| PCSK7 | 5'-CCC ACC CTG ATG AGG AGA ATG-3' | 5'-AAA GGC ATC CGT CCC TCC TCA-3' |
| F4/80 | 5'-CTT TGG CTA TGG CCT TCC AGT C-3' | 5'-GCA AGG AGG ACA GAG TTT ATC GTG-3' |

**Figure 2.1: Generation of GX sPLA$_2$ deficient mice.**

White boxes represent exons. Restriction enzyme sites are indicated. In this approach, the Neo cassette is trapped inside exon 1 before the ATG and replaces 564 bps of the gene Figure provided by InGenious Targeting Laboratory Inc.

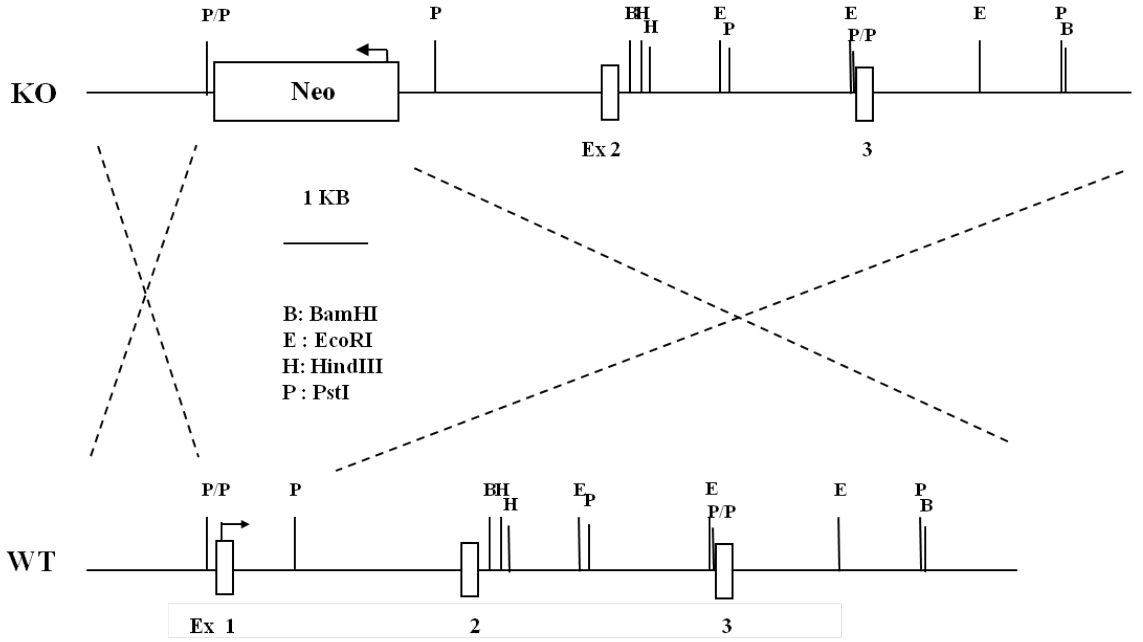

## Chapter Three

## GX sPLA$_2$ deficiency does not protect mice against high fat diet induced metabolic dysfunction and adipose tissue inflammation

### 3.1 Introduction

Diet induced obesity is associated with metabolic derangements including glucose intolerance and insulin resistance[116]. The rapid expansion of adipose tissue (AT) in response to diet induced obesity (DIO) is associated with the recruitment of adipose tissue macrophages (ATMs). It is now well established that AT infiltration by ATMs leads to glucose intolerance and peripheral insulin resistance[97]. However, the sequence of events contributing to the recruitment of inflammatory ATMs remains unclear.

It has been hypothesized by Cinti and colleagues that DIO leads to the acquisition of an AT phenotype characterized by necrotic-like adipocyte death[117]. In this model, the excessive accumulation of lipid into AT results in adipocyte hypertrophy and eventually, adipocyte cell death. The formation of crown-like structures (CLSs), sites of macrophage infiltration and inflammation, may then contribute to decreased insulin sensitivity. We have recently shown that when compared to wild type (WT) mice, GX sPLA$_2$ deficient mice (GX KO) have increased age-related weight gain[54]. The increased weight gain in GX KO mice is associated with increased adiposity and enlarged adipocytes. When stromal vascular fraction (SVF) cells are isolated from both GX KO and WT mice and differentiated into mature adipocytes, SVF cells from GX KO mice accumulate significantly more triglycerides than SVF cells from WT mice. This phenotype likely results from the derepression of liver X receptor (LXR) transcriptional activation of

lipogenic gene expression. Paradoxically, this increased adiposity in GX KO mice is associated with improved age-related glucose intolerance (Shridas et al., unpublished data). Therefore, GX KO mice may provide a unique model for understanding mechanisms involved in the recruitment of ATMs to dysfunctional AT.

The metabolic dysfunction associated with diet-induced obesity, including impaired glucose tolerance and decreased insulin sensitivity, may be attributed to macrophage derived AT inflammation[118,119]. Interestingly, when compared to control mice, GX KO mice have reduced plasma cytokine levels in response to i.p. injection of lipopolysaccharide (LPS)[43]. This phenotype is associated with blunted toll-like receptor 4 (TLR4) signaling in macrophages, presumably due to altered macrophage lipid raft cholesterol content. Peritoneal macrophages isolated from GX KO mice have increased expression of the cholesterol efflux transporters ATP-binding cassette A1 (ABCA1) and G1 (ABCG1); well-established LXR target genes. Moreover, GX KO macrophages demonstrate enhanced ApoA1 mediated cholesterol efflux capacity compared to WT mice. Nevertheless, the role of GX $sPLA_2$ in modulating HFD induced metabolic dysfunction and AT inflammation has yet to be investigated. Hence, we hypothesized that GX $sPLA_2$ deficiency would protect against HFD induced AT inflammation and metabolic dysfunction.

## 3.2 Results

### GX $sPLA_2$ deficiency has no effect on HFD induced adiposity.

We have previously reported that GX KO mice have increased age-related adiposity[54]. To determine if GX $sPLA_2$ deficiency alters body composition in response to

HFD, DIO was established in both WT and GX KO mice (Figure 3.1A). However, after 16 weeks of HFD feeding there was no apparent difference in the body weights or body composition between genotypes in either the low fat (LF) or high fat (HF) fed groups (Figure 3.1A, B).

**GX $sPLA_2$ deficiency does not alter plasma lipid profiles in response to HFD.**

To determine if GX $sPLA_2$ deficiency altered plasma lipid profiles of mice fed a HFD, we analyzed plasma total cholesterol, triglycerides, and free fatty acids. While plasma total cholesterol was significantly increased in both WT and GX KO mice fed a HFD, no significant difference between genotypes in either low fat or high fat fed groups was observed (Figure 3.2A). Furthermore, no differences in plasma triglycerides or plasma free fatty acids was observed in response to HFD in either genotype (Figure 3.2B, C).

**GX $sPLA_2$ deficiency partially protects against HFD induced glucose intolerance but not insulin resistance.**

In order evaluate the effect of GX $sPLA_2$ deficiency on the metabolic derangements associated with HFD feeding, glucose and insulin tolerance tests were performed at 4 week intervals. After 8 weeks of HFD feeding, WT but not GX KO mice demonstrated decreased glucose tolerance in response to i.p. glucose challenge as measured by the area under the curve (AUC) (Figure 3.3). Unexpectedly, after 12 weeks of HF feeding GX KO mice were no longer protected against HFD induced glucose intolerance when compared to WT mice, and this relationship held true through the remainder of the study (Figure 3.3). In order to evaluate alteration in insulin sensitivity in response to HFD feeding insulin tolerance tests were performed. Insulin resistance in

response to HDF feeding was not apparent until 16 weeks of feeding as assessed by the AUC (Figure 3.4). However, there were no apparent differences in insulin sensitivity between genotypes in either the LF or HF fed groups.

**HFD-induced adipocyte hypertrophy is not altered by GX sPLA$_2$ deficiency.**

The increase in fat mass in response to HFD (Figure 3.1A) was associated with enlarged adipocytes in both WT and GXKO mice (Figure 3.5A) and there were no apparent differences in adipocyte size between genotypes in either the LF or HF fed groups (Figure 3.5C). However, there did appear to be a trend toward larger adipocytes in GX KO mice fed a HFD (Figure 3.5B).

**GX sPLA$_2$ deficiency does not protect against HFD-induced ATM infiltration of AT.**

The expansion of AT in response to HFD leads to active AT remodeling and is associated with a depot dependent infiltration of inflammatory ATMs[97]. Hence, the presence of F4/80, a pan macrophage marker, was quantified in epididymal adipose tissue (eAT) by immunofluorescent staining. When compared to LF fed mice, an increase in ATM infiltration was seen in both WT and GX KO mice fed a HFD, but there was no difference in the diet dependent accumulation of ATMs between genotypes after 16 weeks of feeding (Figure 3.6B). Results from immunofluorescent staining were confirmed using qRT-PCR analysis (Figure 3.6A), clearly demonstrating a HFD dependent increase in F4/80 mRNA isolated from eAT in both WT and GX KO mice with no significant difference between genotypes.

**GX $sPLA_2$ deficiency does not protect against AT inflammation in response to HFD.**

The infiltration of ATMs in response to HFD is accompanied by the increased gene expression of inflammatory mediators which may play a causal role in the development of insulin resistance and type-2 diabetes[118]. Therefore, we analyzed expression levels of several of cytokines implicated in AT insulin resistance. When compared to LF fed mice, the expression levels several cytokines including tumor necrosis factor-α (TNF-α), interleukin-6 (IL-6), interleukin-10 (IL-10), interleukin-1β (IL-1β), and monocyte chemoattractant protein-1 (MCP-1), were increased in eAT isolated from both WT and GX KO mice fed a HFD (Figure 3.7).Nonetheless, GX $sPLA_2$ deficiency was unable to abrogate the increases in inflammatory cytokine expression in response to HFD[120].

**GX $sPLA_2$ deficiency does not alter the polarization of infiltrating ATMs in response to HFD.**

The AT expansion associated with obesity results in a phenotypic switch in the polarization of ATMs toward a more inflammatory profile. ATM polarization appears to be an important determinant in the development of glucose intolerance and insulin resistance in response to HFD[106,120,121]. Hence, we looked to see if deficiency in GX $sPLA_2$ altered the polarization of infiltrating ATMs. The M1 "classically activated" macrophages have increased gene expression of inflammatory mediators including TNF-α and inducible-nitric oxide synthase (iNOS)[120]. TNF-α, but not iNOS, expression was increased in the eAT in both WT and GX KO mice in response to HFD (Figure 3.8A). Unexpectedly, TNF-α was significantly increased in GX KO mice when compared to WT mice fed a HFD. When mannose receptor (MR) and arginase-1 (markers of "alternatively

activated" M2 macrophages) gene expression were analyzed in the eAT, a HFD dependent increase in MR was observed with no significant differences between genotypes (Figure 3.8B). The expression of arginase-1 was only increased in GX KO mice fed a HFD but results were confounded by extreme variability.

### 3.3 Discussion

Type-2 diabetes is a chronic inflammatory disease characterized by the dysregulation of hepatic glucose metabolism, decreased glucose uptake in insulin-sensitive tissue including skeletal muscle and AT, and pancreatic β-cell dysfunction. We recently reported that when compared to control mice, GX KO mice have increased age-related weight gain due to an increase in adiposity[54]. However, the increased adiposity in the GX KO mice was associated with improved age-related glucose intolerance. Additionally, GX $sPLA_2$ deficiency resulted in a marked improvement in pancreatic β-cell function as assessed by glucose-stimulated insulin secretion (GSIS) (Shridas et al., unpublished data). Notably, GX KO mice had diminished plasma cytokine levels in a model of sepsis, likely the result of attenuated macrophage mediated inflammatory responses[43]. In the present study we investigated the role of GX $sPLA_2$ in HFD induced metabolic dysfunction and AT inflammation. Here we report that mice deficient in GX $sPLA_2$ are only modestly protected from HFD induced metabolic dysfunction.

Body weights and percent fat mass were not significantly different between genotypes in either the LF or HF fed groups. This finding was unexpected given our previous data that GX KO mice had increased age-related weight gain and adiposity compared to control mice[54]. There are however conflicting reports regarding the effect of GX $sPLA_2$ deficiency on body weight and adiposity[122]. It should also be noted that when

we previously reported increased weight gain and adiposity that these mice were singly caged at weaning[54], potentially laying the foundation for inter-study variation in results. Additionally, these mice were fed normal rodent diet (Teklad Global 18% Protein Rodent Diet 2018S, 6.2% calories from fat, and absent of cholesterol) which has a very different dietary composition from the diets used in the current study in which mice were placed on low fat and high fat diets where 10% and 60% of the total calories were derived from fat respectively (Research Diets, D12450-B and D-12492).

DIO results in metabolic derangements including glucose intolerance and peripheral insulin resistance. Previous studies from our laboratory suggest that GX KO mice are protected from age-related glucose intolerance. Hence, we hypothesized that GX $sPLA_2$ deficiency would protect against HFD induced metabolic dysfunction. However the current findings suggest that GX $sPLA_2$ deficiency exerts very modest and transient protection against HFD induced glucose intolerance and insulin resistance. In adipocytes, the insulin-dependent uptake of glucose is achieved through the translocation of glucose transporter type-4 (GLUT4) from intracellular storage vesicles to the plasma membrane[123]. Notably, deletion of adipose GLUT4 resulted in an ~53% reduction in whole-body insulin-stimulated glucose uptake and leads to marked insulin resistance in both the liver and skeletal muscle[124]. Interestingly, activation of the LXR has been shown to improve glucose tolerance in a model of DIO. This affect was attributed to the LXR dependent increase in glucose transporter type-4 (GLUT4) expression in AT but not skeletal muscle[113]. Conversely, mice deficient in LXRβ were glucose intolerant due to diminished glucose-stimulated insulin secretion[125]. However, LXRβ deficiency also appears to protect mice from diet or age-related weight gain. One way in which GLUT4

gene expression is controlled in AT is through activation of the nuclear receptor LXR[113]. Interestingly, GLUT4 gene expression is not regulated by insulin in AT, whereas treatment of mice with insulin and the LXR agonist T0901317 synergistically increased AT GLUT4 expression in vivo[113]. AT insulin-resistance, either as the result of hyperinsulinemia or HFD feeding, led to decreased insulin-dependent GLUT4 translocation to the plasma membrane due to perturbations in the phosphatidylinositol 3-kinase (PI3K)/AKT signaling axis[126]. We have recently shown that GX $sPLA_2$ acts to negatively regulate LXR transcriptional activation in adipocytes[54]. Thus, it is feasible that any effects GX $sPLA_2$ deficiency had on LXR dependent GLUT4 gene expression in AT would be negated by the decrease in insulin sensitivity in response to HFD. However, recent studies from our lab also suggest that GX $sPLA_2$is capable of suppressing pancreatic insulin secretion, probably through the production of prostaglandin $E_2$ (Shridas et al., unpublished data), a known inhibitor of GSIS in pancreatic islet cells. This observation is consistent with the fact that when compared with WT mice, GX KO mice were partially protected from HFD induced glucose intolerance after 8weeks of feeding with no differences in insulin sensitivity between genotypes during this time (Table 2). These findings suggest that the beneficial effects of GX $sPLA_2$ deficiency on blood glucose levels after HFD feeding may be due to its role in regulating GSIS in the pancreas.

The recruitment of inflammatory ATMs into AT in response to HFD is linked to the development of metabolic abnormalities including glucose intolerance and insulin resistance. Indeed, the absence of ATM recruitment to dysfunctional AT in response to HFD normalizes insulin sensitivity and blood glucose levels[119,127]. We have recently

shown in a model of angiotensin II induced abdominal aortic aneurism (AAA) formation that GX $sPLA_2^{-/-}$/$apoE^{-/-}$ (GX DKO) mice have reduced expression of the pan macrophage marker F4/80in the abdominal aorta when compared to $apoE^{-/-}$ control mice[49]. Therefore we investigated the possibility that GX $sPLA_2$ deficiency may protect against ATM infiltration of AT in response to HFD. However, ATM content within the eAT of GX KO mice fed a HFD was not significantly different from that of HFD fed control mice. Notably, Wu et al.[128] showed that ATM content is unchanged with age, they went on to argue that adipocytes and not stromal cells derived from adipose tissue of aged mice are responsible for the increases in AT inflammatory cytokine expression. However, other studies have shown that while total macrophage content is unchanged in aged mice when compared to young, the ATM subtype found in the AT of aged mice is altered but not clearly distinguishable as either M1 or $M_2$ macrophages[105]. These findings suggest that, at least in mice, the mechanisms underlying AT inflammation and metabolic dysfunction associated with aging may be different from that of DIO. While GX $sPLA_2$deficiency clearly protects against age-related glucose intolerance, ATM content and polarity has not been assessed in aged-GX KO mice.

The increased expression of inflammatory cytokines in AT in response to DIO is a major contributor to AT insulin resistance. Several groups, including our own, have now demonstrated a role for GX $sPLA_2$ in potentiating the inflammatory response in vivo[43,129,130]. However, GX $sPLA_2$ deficiency did not protect mice from HFD-induced inflammatory cytokine production within the eAT. In fact, GX KO mice fed a HFD actually had significantly increased expression of TNF-α, compared to HFD fed control mice. However, this was also accompanied by a compensatory increase in IL-10

expression. This might be suggestive of increased macrophage infiltration in GX KO mice; however the F4/80 immunofluorescent staining and qRT-PCR data refute this possibility.

The increased cytokine expression in the eAT of GX KO mice was unexpected given that GX $sPLA_2$ deficiency in macrophages results in a reduced inflammatory response to LPS[43]. One possible explanation for the data is that GX KO mice fed a HFD have enhanced infiltration of lymphocytes into the eAT compared to control HFD fed mice. Flow cytometry studies by Penicaud et al. demonstrated that in mice, increased adiposity and in particular increased eAT mass was positively associated with enhanced T cell infiltration[131,132]. Visceral AT from obese humans is characterized by increased numbers of T and natural killer (NK) cells, likely accounting for the enhanced expression of IFNγ, and regulated upon activation, normal T-cell expressed and secreted (RANTES)[133]. Importantly, T helper cell type-1 (Th1) derived cytokines are important modulators macrophage polarity. In particular, the Th1 derived cytokine, IFNγ may act to promote a "classically activated" M1 macrophage phenotype[134]. IFNγ deficient mice have reduced AT inflammation and decreased infiltration of ATMs in response to diet-induced obesity, and this is associated with improved glucose tolerance compared to control mice[135]. Importantly, splenic CD4+ T cells isolated from GX DKO (GX $sPLA_2^{-/-}$ /$Ldlr^{-/-}$) mice have an enhanced proliferative capacity and an exaggerated Th1 phenotype compared to CD4+ T cells from control $Ldlr^{-/-}$ mice. Moreover, flow cytometry experiments demonstrated an ~35% increase in IFNγ+ CD4+ T cells within the GX DKO CD4+ T cell population as a whole. Thus, when compared to control mice, enhanced Th1

derived cytokine production in GX KO mice may contribute to AT inflammation and metabolic dysfunction in the context of diet-induced obesity.

A role for TLR4 in mediating DIO and insulin resistance has been previously reported[101,136]. Importantly, TLR4 deficiency has been shown to promote alternative activation of ATMs[104]. As previously mentioned, our lab reported that GX KO mice have reduced plasma inflammatory cytokine expression in response to LPS, likely due to blunted TLR4 signaling in macrophages. Lipid raft cholesterol content is known to influence TLR4 dependent inflammatory signaling[137,138]. It has recently been shown that increased gene expression of cholesterol efflux transporters ABCA1 and ABCG1can alter macrophage polarization toward $M_2$ alternatively activated macrophages[108]. Interestingly, peritoneal macrophages isolated from GX KO mice have increased expression of LXR target genes ABCA1 and ABCG1 when compared to macrophages from WT mice. Thus, we hypothesized that GX $sPLA_2$ deficiency may result in a shift toward less inflammatory M2 macrophages in the AT of mice fed a HFD. However, GX $sPLA_2$ deficiency did not predispose ATMs toward a less inflammatory M2 phenotype. It has been suggested that dietary fatty acids may act to inhibit LXR activation[139]. Accordingly, LXRα gene expression is decreased in the AT of obese Zucker rats[140]. To this extent, ABCA1 expression is decreased in monocyte-derived macrophages isolated from overweight and obese human subjects and this is associated with reduced cholesterol efflux capacity in these cells[141]. Thus, because the less-inflammatory phenotype seen in peritoneal macrophages isolated from GX KO mice likely hinges upon the LXR dependent efflux of intracellular cholesterol resulting in altered lipid raft lipid content[43],

it reasonable to speculate that in a model of DIO where LXR activity is potentially down-regulated, that the effect of GX $sPLA_2$ deficiency may in fact be negligible.

The sub-clinical, chronic low-grade inflammation associated with diet-induced obesity appears to be causally linked to the ensuing metabolic perturbations that follow, including glucose intolerance and insulin resistance. Infiltrating ATMs contribute significantly to AT inflammation in response to over-nutrition. ATMs of obese mice are predominately M1-like macrophages characterized by the up-regulation of inflammatory genes including TNFα and iNOS. However, ATMs of obese mice demonstrate remarkable plasticity such that M1-like macrophages with a distinctive $F4/80^{+}CD11b^{+}CD11c^{+}$ phenotype prevail, while a lesser $F4/80^{+}CD11b^{+}CD11c^{-}$ M2-like can also be found[142]. However, evidence in humans suggests that a spectrum of macrophage subtypes likely exists and cannot be clearly distinguished as either M1 or M2[143,144]. Indeed, a sub-population of ATMs has been identified in humans that express several cell surface markers typical of "alternatively activated" M2 macrophages, but are capable of producing high levels of inflammatory cytokines[143]. Thus, clearly any efforts to characterize distinct subpopulations of ATMs may be undermined but what has become increasingly recognized as a continuum of ATM phenotypes within the AT in response to obesity.

**Figure 3.1: WT and GX KO mice have increased adiposity in response to HFD feeding.**

A. Male GX KO mice and littermate control mice were fed both LF and HF diets for 16 weeks and weights were recorded every other week. B. Body composition was determined by echo-MRI every 4 weeks.

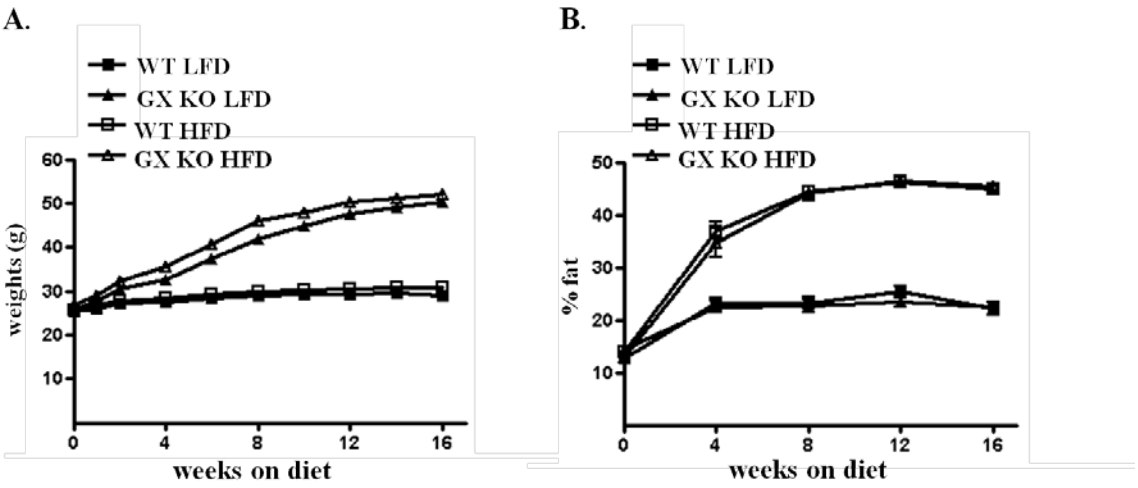

**Figure 3.2: Plasma lipid levels of WT and GX KO mice after 16 weeks on diet.**

Mouse plasma was collected via cardiac puncture and analyzed for A. total cholesterol, B. triglycerides, and C. free fatty acids. Overall effects of diet are indicated by *brackets*. Date represents means ± SEM. ***P<0.001

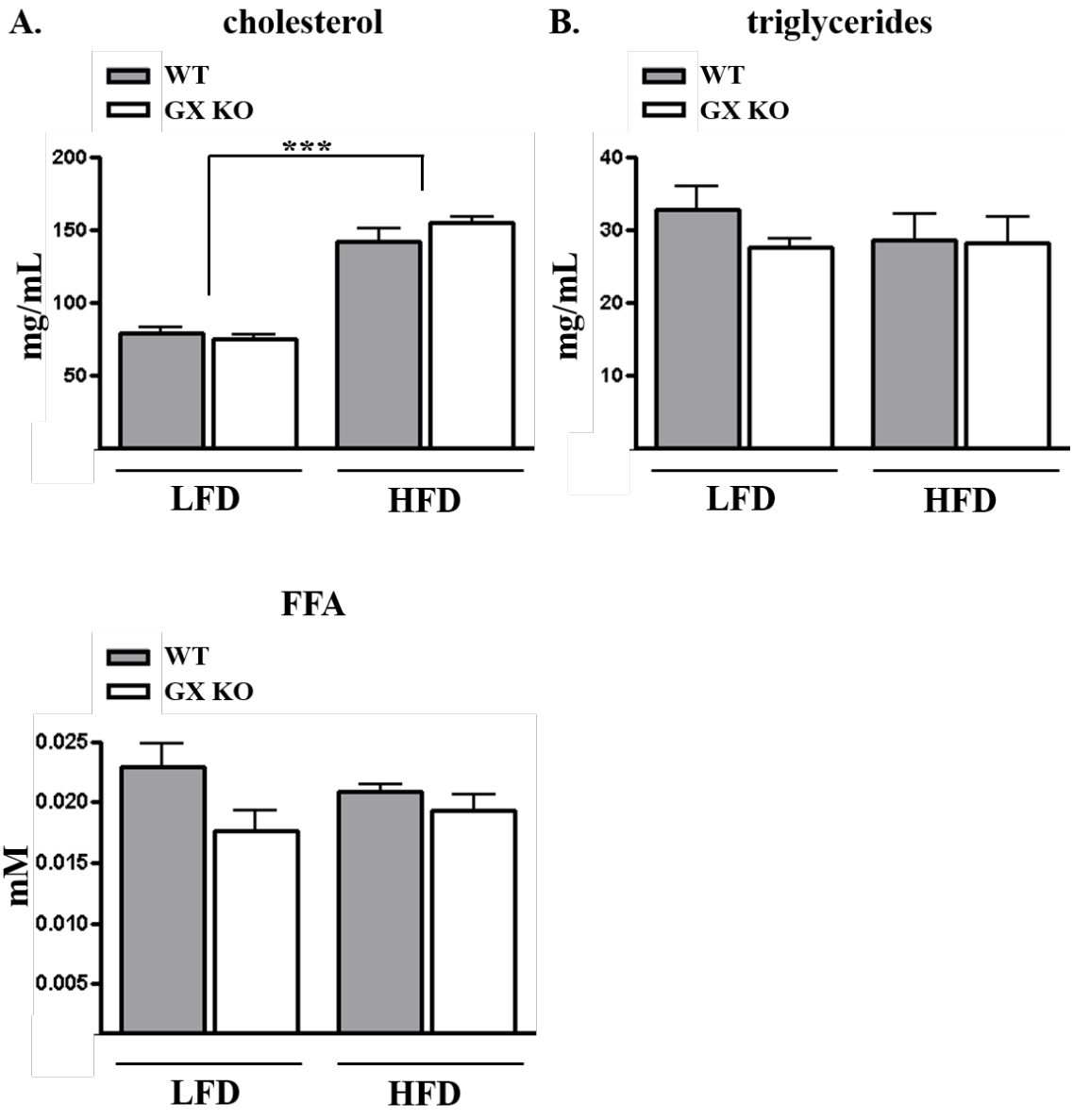

**Figure 3.3: GX KO mice are modestly protected against HFD-induced glucose intolerance.**

After mice were fasted for 6 hours, plasma glucose levels were measured before and after (every 30 minutes for 3 hours) intraperitoneal administration of either 1.5 g/kg glucose (weeks 0 and 4) or 2 g/kg glucose (weeks 8, 12 and 16). The data is represented as the area under the curve (AUC) in arbitrary units and is expressed as the mean ± SEM (n=5-6). Overall effects of diet are designated by *brackets*. Significant differences between genotypes within each diet are designated by horizontal *bars*. Data represent the mean ± SEM. * P< 0.05, ** P<0.01

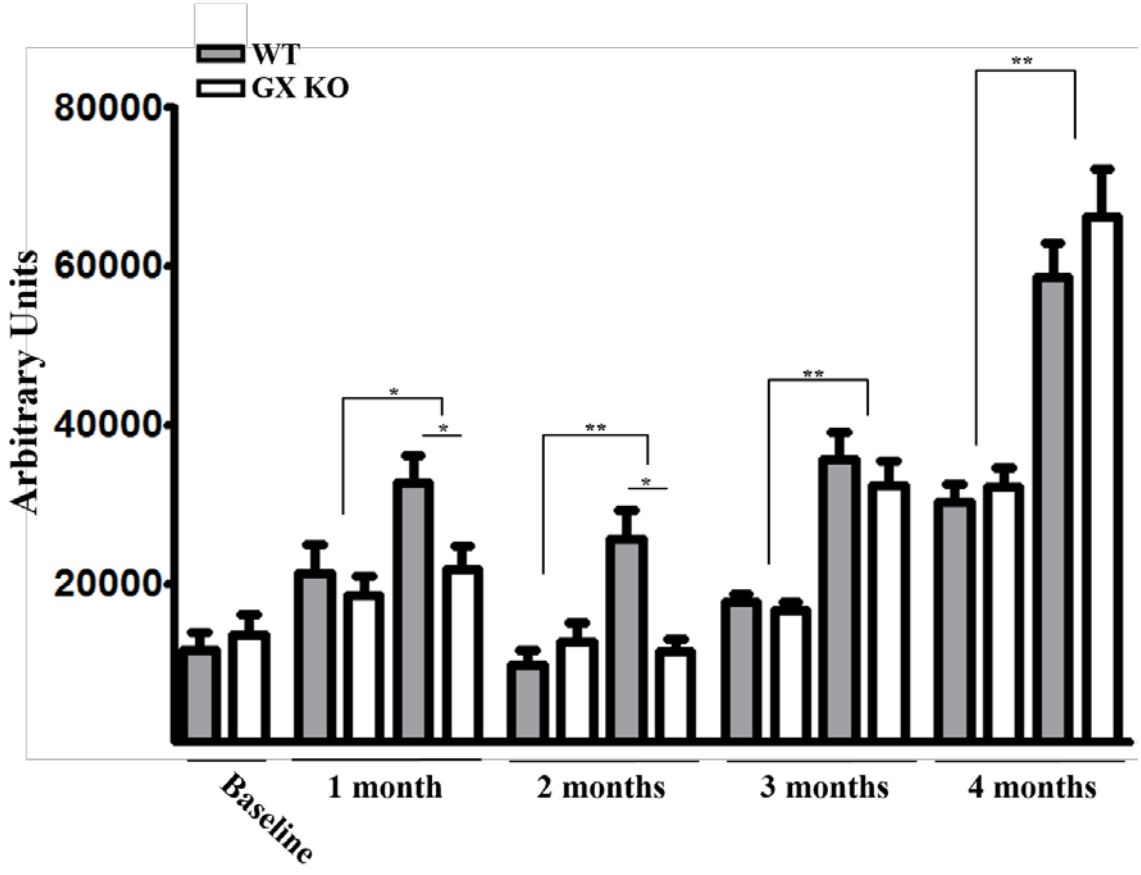

**Figure 3.4: GX KO mice are not protected against HFD-induced insulin resistance.**

After mice were fasted for 6 hours, plasma glucose levels were measured before and after (every 30 minutes for 3 hours) intraperitoneal administration of 1 u/kg insulin. Data represents the AUC in arbitrary units and is expressed as the mean ± SEM. Overall effects of diet are designated by *brackets*. Significant differences between genotypes within each diet are designated by *bars*. Significant differences between genotypes within each diet are designated by horizontal *bars*. Data represent the mean ± SEM. * P< 0.05, ** P<0.01

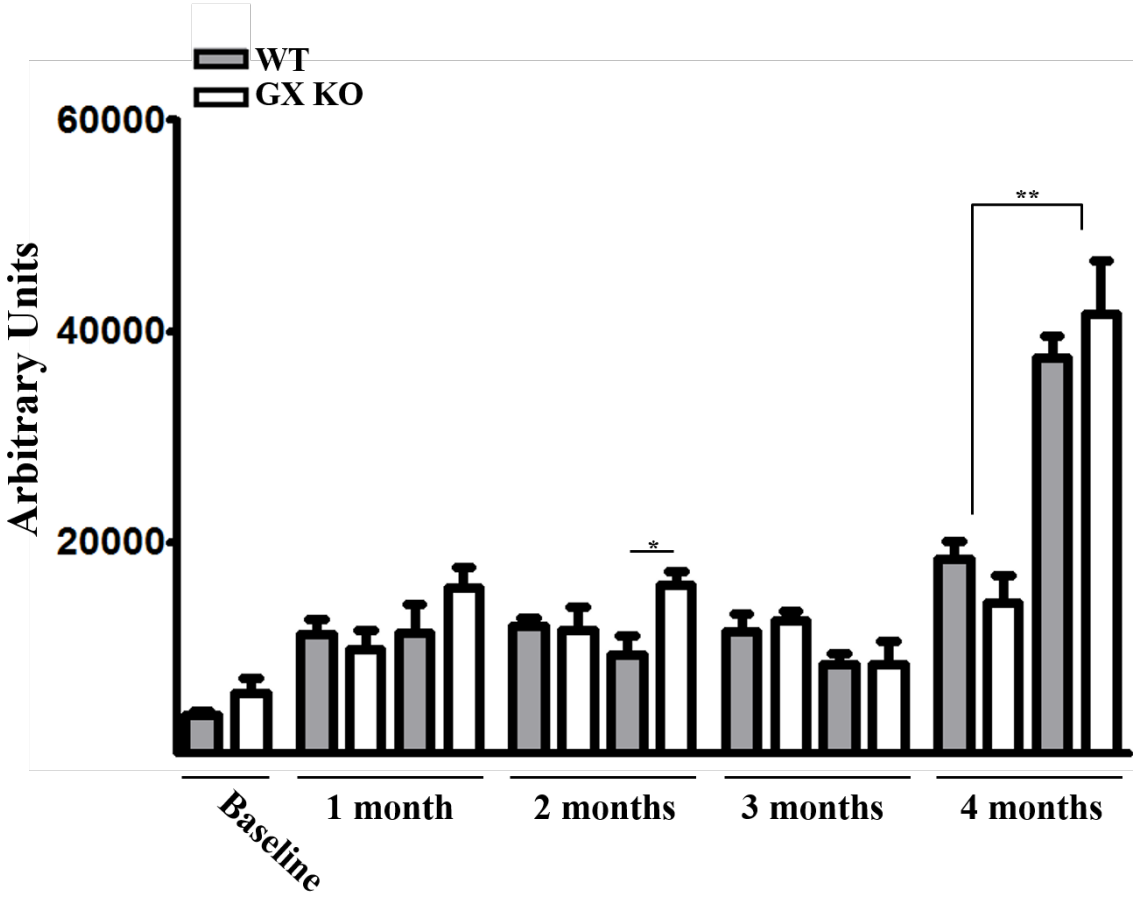

**Figure 3.5: HFD feeding results in increased adipocyte hypertrophy in both WT and GX KO mice.**

A. Paraffin embedded epididymal adipose tissue (eAT) was stained using hematoxylin and eosin. B. The frequency distribution of adipocyte cell surface area of HF fed mice was analyzed. Frequency distribution represents 3 randomly chosen eAT sections from 3 mice per group. C. The average adipocyte cell surface area from C. was determined.

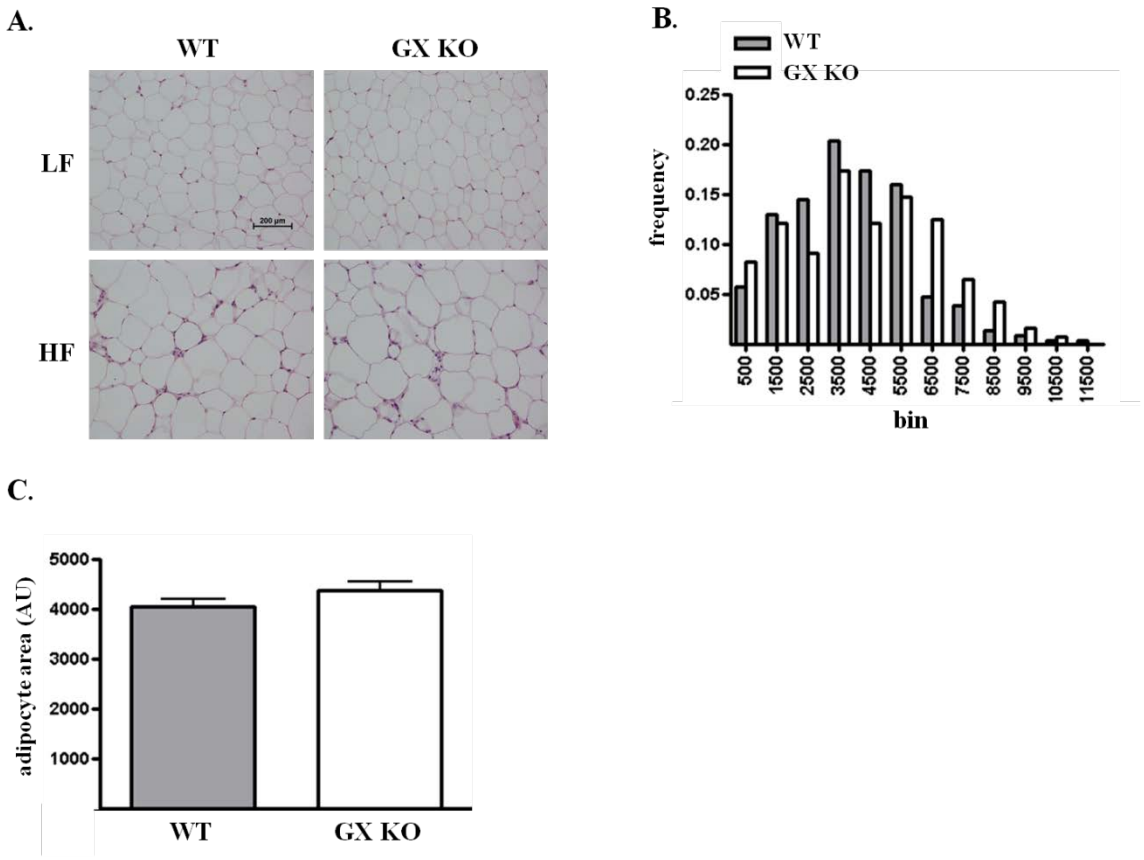

**Figure 3.6: GX KO mice are not protected against HFD-induced macrophage infiltration of AT.**

WT and GX KO mice were fed LF and HF diets for 16 weeks at which point epididymal adipose tissue (eAT) was harvested for further analysis. A. RNA was isolated from eAT and qRT-PCR was performed using primers specific for pan macrophage marker F4/80 (n=10-12). B. eAT was stained using an antibody specific for the pan-macrophage marker F4/80 and detected using immunofluorescence microscopy. Overall effects of diet are indicated by *brackets*. Date represents means ± SEM. ***p<0.001

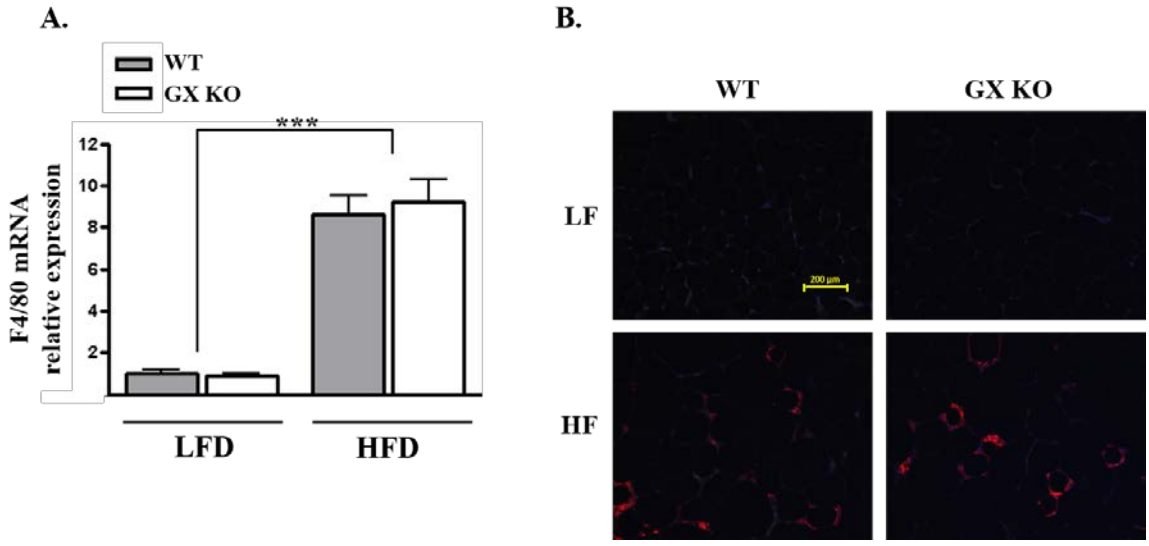

**Figure 3.7: GX KO mice are not protected against HFD-induced AT inflammation.**

qRT-PCR was performed on RNA isolated from the epididymal fat pads of mice using primers specific for genes IL-6, IL-10, MCP-1, IL-1β, and TNF-α. # P<0.05, ##P<0.01 indicates significant difference between diets within a given genotype. Overall effects of diet are designated by *brackets*. Significant differences between genotypes within each diet are designated by horizontal *bars*. Data represent the mean ± SEM. *P<0.05, **P<0.01, P<0.001

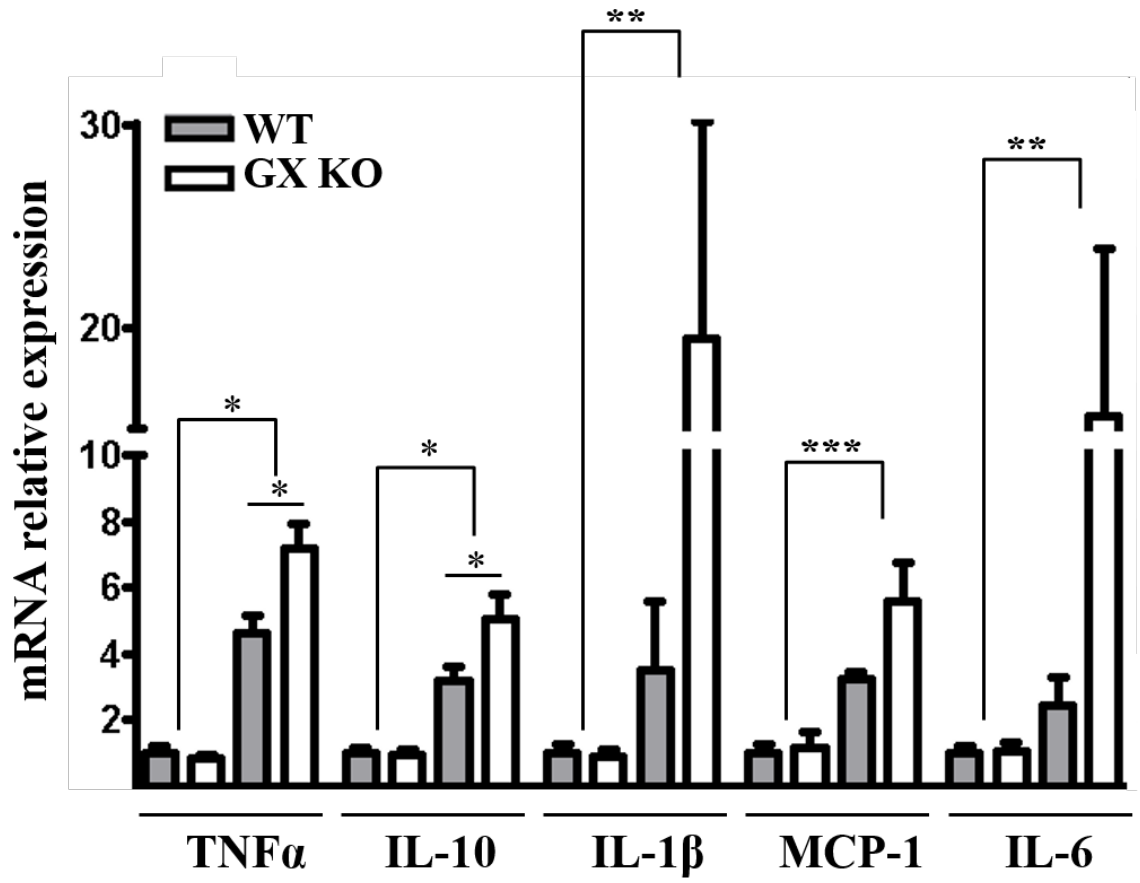

**Figure 3.8: GX sPLA2 deficiency does not alter the polarity of infiltrating ATMs.**

RNA was isolated from the epididymal fat pads after 16 weeks on diet and qRT-PCR was performed using primers specific for A. M1 (TNF-α, and iNOS) and B. M2 (MR, and arginase-1) macrophage markers (n=10-12). Overall effects of diet are designated by *brackets*. Significant differences between genotypes within each diet are designated by horizontal *bars*. Data represent the mean ± SEM. *P<0.05, ***P<0.001

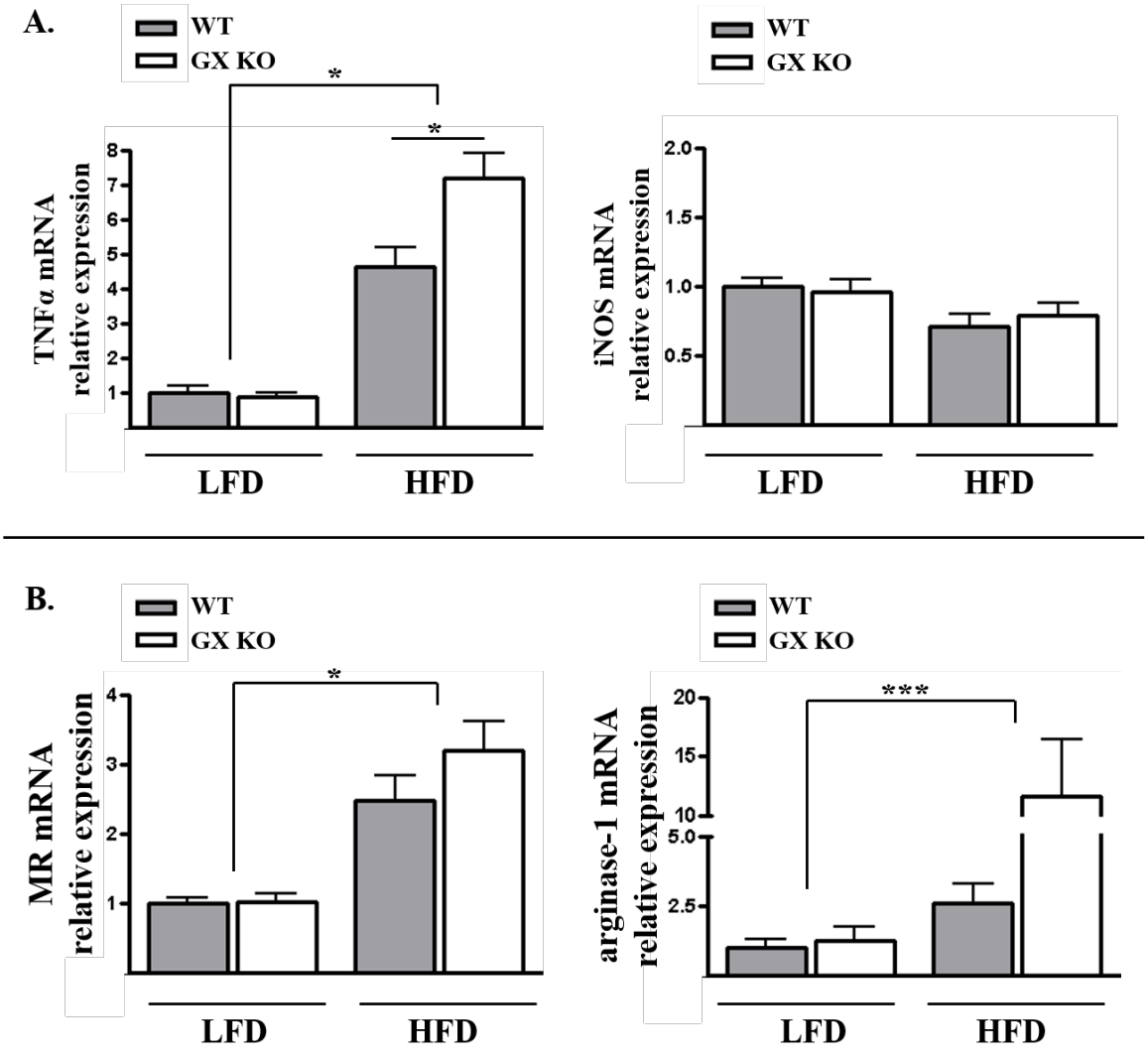

# Chapter 4

## Pro-GX $sPLA_2$ processing by furin-like proprotein convertases: Implications for the regulation of adrenal steroidogenesis

### 4.1 Introduction

The secreted phospholipase $A_2$ ($sPLA_2$) family of enzymes hydrolyzes membrane phospholipids at the sn-$_2$ position to liberate free fatty acids and lysophospholipids. The $sPLA_2$ family is characterized by their low molecular weight (~14-18 kDa), requirement for millimolar concentrations of $Ca^{2+}$, and utilization of a highly conserved catalytic histidine-asparagine dyad within their active sites. Eleven $sPLA_2$ members have been identified (group IB, IIA, IIC, IID, IIE, IIF, III, V, X, XIIA, and XIIB $PLA_2$-like protein that lacks catalytic activity) and placed into different groups based on the number and position of conserved cysteine residues that form disulfide bridges, generating a semi-rigid three-dimensional structure (reviewed in[1]). Members of the $sPLA_2$ family exhibit unique tissue distributions and disparate substrate specificities, reflecting their distinct roles in a range of physiological processes.

Among the $sPLA_2$s, Group X (GX) $sPLA_2$ has the most potent hydrolytic activity toward zwitterionic phospholipids including phosphatidylcholine (PtdCho)[38], the most abundant phospholipid in mammalian plasma membranes and lipoprotein particles. GX $sPLA_2$ has a wide tissue distribution, including the small intestine, testes, brain, pancreas, lung, thymus, spleen, peripheral blood leukocytes, among others[39,45]. Notably, GX $sPLA_2$ appears to preferentially hydrolyze arachidonate and linoleate at the sn-$_2$ position of PtdCho containing lipoproteins[45,46]. The predilection of GX $sPLA_2$ for arachidonate

has important consequences with respect to the generation of bioactive lipids. For example, GX $sPLA_2$ has been implicated in the production of eicosanoids including $PGE_2$, $PGD_2$, leukotriene B4, and cysteinyl leukotrienes (cysLTs) in a Th2 cytokine-driven mouse model of asthma[41].

The generation of C57BL/6 mice with targeted deletion of GX $sPLA_2$ (GX KO mice) has led to new insights into novel mechanisms by which GX $sPLA_2$ modulates physiological processes. Our laboratory reported that GX KO mice fed a normal rodent diet gain more weight and exhibit increased adiposity compared to wild-type mice[54]. We also determined that stromal vascular cells isolated from adipose tissue of GX KO mice accumulate significantly more triglyceride when induced to differentiate into adipocytes compared to cells from wild-type mice. Conversely, overexpression of GX $sPLA_2$ in OP9 pre-adipocytes resulted in a significant 50% reduction in triglyceride accumulation during differentiation into mature adipocytes, an effect that was associated with significantly reduced induction of adipogenic genes, including PPARγ, SREBP-1c, SCD1, and FAS. Activation of the liver X receptor (LXR), a nuclear receptor known to up-regulate adipogenic gene expression, was suppressed in OP9 cells when GX $sPLA_2$was overexpressed, leading us to conclude that GX $sPLA_2$ negatively regulates adipogenesis, possibly by suppressing LXR activation. We also determined that GX $sPLA_2$ suppresses LXR activation in macrophages, resulting in reduced expression of ATP-binding cassette transporters A1 (ABCA1) and G1 (ABCG1)[53]. Consequently, macrophages from GX KO mice exhibit increased cellular cholesterol efflux and decreased cellular cholesterol content. GX $sPLA_2$ is also expressed in adrenal cells, where it suppresses corticosteroid production through a mechanism that also appears to involve LXR. Compared to wild-

type mice, GX KO mice have significantly increased plasma corticosterone levels under both basal and adrenocorticotropic hormone (ACTH)-induced conditions. The expression of steroidogenic acute regulatory protein (StAR), the rate-limiting protein in corticosteroid production, is significantly increased in adrenal glands from GX KO mice compared to wild-type adrenal glands. Conversely, in the mouse adrenal Y1 cell line, overexpression of GX $sPLA_2$ suppresses StAR expression. Results from luciferase reporter assays indicated that GX $sPLA_2$ antagonizes StAR promoter activity and LXR-mediated StAR promoter activation in adrenal cells. In summary, results from gain-of-function and loss-of-function studies in multiple tissues indicate that GX $sPLA_2$ modulates cellular metabolism by negatively regulating LXR target gene expression.

Given the potent ability of GX $sPLA_2$ to hydrolyze cell membranes and generate bioactive lipid mediators, its hydrolytic activity is likely under tight regulation. GX $sPLA_2$ is one of only three $sPLA_2$s produced as an inactive pro-enzyme, such that cleavage of an N-terminal pro-segment is necessary for its enzymatic activity[45]. Studies in transgenic mice with constitutive GX $sPLA_2$ expression indicated that the inactive precursor is the predominant form expressed in most tissues under normal conditions[58]. However, enzymatically active GX $sPLA_2$ was detected in the transgenic mice in tissues with inflammatory granulation, suggesting that proteolytic activation may occur during inflammation. The N-terminal pro-segment of GX $sPLA_2$ comprises eleven amino acids ending in a dibasic motif, suggesting cleavage by member(s) of the furin-like proprotein convertase (PC) family. Recently, Jemel et al.[59] showed that in transfected human embryonic kidney (HEK 293) cells, the second residue within the dibasic doublet is necessary and sufficient for GX $sPLA_2$ processing and hydrolytic activity. Furthermore,

using a panel of non-specific protease inhibitors, the involvement of PCs in GX $sPLA_2$maturation and activation in 293 cells was confirmed. However, the identity of the individual PCs involved in GX $sPLA_2$ processing in physiologically relevant tissues remained to be investigated.

During the course of studying GX $sPLA_2$ in adrenal cells, we noted significantly increased phospholipase activity secreted by Y1 cells stably transfected with a GX $sPLA_2$ expression construct, and to a lesser extent, control-transfected Y1 cells, in response to ACTH treatment. We reasoned that this increase in secretion reflected post-transcriptional regulation of GX $sPLA_2$, since the promoter driving recombinant GX $sPLA_2$ expression in our cell system would not be expected to be regulated by ACTH[53]. Thus, mouse Y1 cells provided us a physiologically relevant model for understanding GX $sPLA_2$ regulation. In this study we establish that pro-GX $sPLA_2$ is proteolytically activated in Y1 adrenal cells by furin and PCSK6, two members of the PC family. We also provide evidence that PC-dependent proteolytic activation of pro-GX $sPLA_2$ is enhanced under ACTH-stimulated conditions, suggesting a novel mechanism for regulating adrenal steroidogenesis.

## 4.2 Results

### ACTH increases GX $sPLA_2$ proteolytic activation in Y1 adrenal cells.

To investigate mechanisms involved in regulating GX $sPLA_2$ activity in adrenal cells, we generated mouse Y1 cells stably expressing GX $sPLA_2$ fused to a C-terminal 3x FLAG sequence (Y1-GX). This chimeric construct allowed us to monitor GX $sPLA_2$ processing based on differences in the molecular weight of the inactive precursor, pro-

GX (~15.2 kDa) and the mature form of the enzyme, m-GX (~13.9 kDa). In accordance with our previous findings[55], ACTH treatment resulted in a modest but significant increase in the phospholipase activity secreted by control-transfected Y1 cells (Y1-C) (Figure 4.1A). The increased phospholipase activity in response to ACTH was highly significant in Y1-GX cells (Figure 4.1A). Associated with the increase in phospholipase activity in ACTH-treated Y1-GX cells was an increase in the ratio of m-GX:pro-GX $sPLA_2$ in response to ACTH stimulation (Figure 4.1B). In the case of untreated Y1-GX cells, the ratio of m-GX:pro-GX $sPLA_2$ present in the media was ~0.8:1. This contrasts to ACTH- treated cells, where the ratio of m-GX $sPLA_2$:pro-GX $sPLA_2$ was ~1.5:1. Thus, ACTH treatment resulted in an ~2-fold increase in the amount of m-GX $sPLA_2$ relative to pro-GX $sPLA_2$ present in the media. m-GX $sPLA_2$ was not detected in cell lysates of Y1-GX cells in either the absence or presence of ACTH (Figure 4.1C). Taken together, these results suggest that ACTH enhances the phospholipase activity secreted by Y1-GX cells, likely by increasing the proteolytic processing of pro-GX $sPLA_2$, and that pro-GX $sPLA_2$ is the major, if not exclusive, form detected intracellularly.

**GX $sPLA_2$ processing and activity are blocked by the furin-like proprotein convertase inhibitor RVKR.**

The family of furin-like proprotein convertases (PCs) has recently been implicated in the proteolytic activation of GX $sPLA_2$ in transfected HEK 293 cells[59]. To investigate the role of PCs in regulating GX $sPLA_2$proteolytic activation in mouse Y1 adrenal cells, $sPLA_2$ activity and pro-GX $sPLA_2$ processing was assessed in Y1-GX cells treated with the PC inhibitor, Dec-RVKR-cmk (RVKR). After overnight incubation, both pro- and m-GX $sPLA_2$ were detected in the media of vehicle-treated Y1-GX cells, and

ACTH treatment significantly increased the ratio of m-GX $sPLA_2$:pro-GX $sPLA_2$ secreted by Y1-GX cells (Figure 4.2A). However, the increased processing of pro-GX-$sPLA_2$ in response to ACTH treatment was almost completely abolished in the presence of RVKR. This decrease in processing was accompanied by a significant reduction in $sPLA_2$ activity secreted by the cells (Figure 4.2B). These results demonstrate a role for furin-like PCs in the proteolytic activation of GX $sPLA_2$ in Y1 adrenal cells under both basal and ACTH-stimulated conditions.

**Furin and PCSK6 expression is increased in Y1 cells treated with ACTH**.

To identify candidate PCs that may be responsible for regulating GX $sPLA_2$ activity in adrenal cells, we quantified mRNA abundance for each member of the PC family in both Y1-Cand Y1-GX cells under basal and ACTH-stimulated conditions. Among the six candidate convertases, only four were expressed at appreciable levels (Ct value <35): furin, PCSK5, PCSK6, and PCSK7 (Figure 4.3). Ct values for PC1 and $PC_2$ were >35 in both basal and ACTH-treated cells. Interestingly, both furin and PCSK6 mRNA abundance were significantly increased in response to overnight incubation with ACTH, consistent with the enhanced pro-GX $sPLA_2$ processing. Unexpectedly, furin, PCSK5, and PCSK6 were increased in response to GX $sPLA_2$ overexpression. Since furin and PCSK6 were up-regulated in response to ACTH, we further investigated the role of these PCs in regulating GX $sPLA_2$ processing in Y1 cells.

**Pro-GX $sPLA_2$ is proteolytically cleaved by furin and PCSK6.**

Previous reports characterizing the substrate specificity of PCs suggest some redundancy in functionality for some, but not all, targets (reviewed in[61]). In order to

assess whether pro-GX $sPLA_2$ is a substrate for furin and/or PCSK6 proteolytic activation, GX $sPLA_2$ was co-expressed with either furin or PCSK6 in HEK293 cells. The ratio of m-GX $sPLA_2$:pro-GX $sPLA_2$ in media from HEK293 cells expressing GX $sPLA_2$ alone was ~1:1(Figure 4.4A). Expression of either furin or PCSK6 resulted in an almost complete conversion of pro-GX $sPLA_2$ to the mature form, indicating that pro-GX $sPLA_2$ is a substrate for both PCs. m-GX $sPLA_2$ was not detected in whole-cell lysates, indicating that furin- and PCSK6-dependent pro-GX $sPLA_2$ processing occurs extracellularly in HEK 293 cells (Figure 4.4B).

**Both furin and PCSK6 contribute to pro-GX $sPLA_2$ processing in Y1 cells.**

In order to determine if furin and/or PCSK6 mediate GX $sPLA_2$proteolytic activation in adrenal cells, we employed small interfering RNAs (siRNAs) to suppress the expression of furin mRNA, PCSK6 mRNA, or both mRNAs. Both furin and PCSK6 expression was effectively blunted ~75% using this approach (Figure 4.5A, B). Neither knockdown of furin or PCSK6 alone was able to significantly inhibit processing of GX $sPLA_2$ secreted by Y1 cells (Figure 4.6A). However, knockdown of both furin and PCSK6 together resulted in a significant reduction in pro-GX $sPLA_2$ cleavage. As expected, ACTH treatment significantly increased the ratio of m-GX $sPLA_2$:pro-GX $sPLA_2$ in the media compared to vehicle-treated cells (Figure 4.6B). However, enhanced pro-GX $sPLA_2$ processing in response to ACTH was significantly decreased when furin and PCSK6 expression was suppressed. These findings strongly suggest that both furin and PCSK6 mediate GX $sPLA_2$ processing in Y1 adrenal cells, and ACTH-induced increases in GX $sPLA_2$ activity is at least partly due to up-regulation of these convertases.

**The suppression of LXR activation by GX $sPLA_2$ is enhanced when furin or PCSK6 are overexpressed.**

We previously reported that GX $sPLA_2$ inhibits LXR-mediated target gene activation through a mechanism that is dependent on its enzymatic activity[53]. Therefore, we investigated whether proteolytic activation of GX $sPLA_2$ by furin or PCSK6 enhances GX $sPLA_2$-dependent inhibition of LXR activation. As expected, GX $sPLA_2$ overexpression in HEK 293 cells suppressed the transcriptional activation of an LXR reporter construct under both basal and T0901317-treated conditions (Figure 4.7A, B). The inhibitory effect of GX $sPLA_2$ on LXR activation was augmented when either furin or PCSK6 was co-expressed, indicating that GX $sPLA_2$ processing by furin-like proprotein convertases may represent an important mechanism for regulating GX $sPLA_2$-mediated inhibition of LXR transcriptional activation.

**GX $sPLA_2$-mediated suppression of steroidogenesis requires furin-like proprotein convertase activity.**

StAR plays a critical function in adrenal corticoid synthesis by delivering cholesterol to steroidogenic enzymes located in the inner mitochondrial membrane. Given its key role in corticosteroid production, StAR mRNA expression is under both positive and negative control by a variety of transcription factors, including LXR[56]. Given our previous finding that GX $sPLA_2$ suppresses StAR expression in an LXR-dependent manner[55], it was of interest to investigate whether inhibiting PC activity impacted the ability of GX $sPLA_2$ to regulate StAR, and hence steroid production in adrenal cells. As we reported previously, GX $sPLA_2$ overexpression inhibited StAR protein expression in Y1 cells under both basal (Figure 4.8A) and ACTH-stimulated

conditions (Figure 4.8B). This inhibitory effect was abolished when cells were treated with RVKR at a dose that significantly reduced the amount of m-GX $sPLA_2$ and $sPLA_2$ activity secreted by the cells (Figure 4.8 and Figure 4.10). Collectively, these results indicate that furin-like proprotein convertases are required for GX $sPLA_2$-mediated StAR regulation.

We next assessed the effect of inhibiting PCs on steroid production in Y1-GX cells. Since Y1 cells do not express $_2$1-hydroxylase, the enzyme required for conversion of progesterone to corticosterone[145], progesterone levels in conditioned media were measured as an indicator of steroid production by these cells. As expected, treatment with increasing concentrations of RVKR resulted in a dose-dependent decrease in phospholipase activity secreted by Y1-GX cells (Figure 4.9A). Notably, progesterone production was reciprocally increased in response to increasing concentrations of RVKR (Figure 4.9B). In accordance with previous findings, GX $sPLA_2$ overexpression significantly decreased progesterone production by Y1 cells under both basal and ACTH-stimulated conditions (Figure 4.9C). Treatment with RVKR ablated the inhibitory effect of GX $sPLA_2$ on progesterone production, consistent with the conclusion that pro-GX $sPLA_2$ processing by PCs is necessary for GX $sPLA_2$ mediated suppression of steroidogenesis in Y1 cells.

### 4.3 Discussion

Furin-like PCs are calcium-dependent serine proteases that mediate the post-translational processing and activation of numerous molecules important for tissue and whole-body homeostasis, such as cell surface receptors, pro-hormones, growth factors, matrix metalloproteinases, and adhesion molecules (reviewed in[61]). Perturbations in PC

activity have been implicated in multiple pathological conditions, including various endocrinopathies, infectious diseases, cancer, and Alzheimer's disease, reflecting their fundamental role in diverse physiological processes. Here we identify pro-GX $sPLA_2$ as a previously unrecognized substrate for two members of the PC family, furin and PCSK6, and provide evidence that proteolytic activation of pro-GX $sPLA_2$ by PCs represents a novel mechanism for regulating glucocorticoid production in adrenal cells.

The initial observation that prompted our study was the finding that phospholipase activity secreted by Y1-GX cells, and to a lesser extent Y1-C cells, was significantly increased when cells were stimulated by ACTH[55]. We speculated that the increase in $sPLA_2$ activity was due to enhanced conversion of both endogenous and ectopically expressed pro-GX $sPLA_2$ to m-GX $sPLA_2$ in ACTH-treated cells. A recent study by Jemel et al. provided strong evidence that pro-GX $sPLA_2$ is proteolytically activated by a furin-like PC, although the identity of the specific PC(s) was not determined[59]. In an initial screening by RT-PCR we determined that four members of the PC family are expressed in Y1 adrenal cells, furin, PCSK5, PCSK6, and PCSK7. We conclude that both furin and PCSK6 play a major role in pro-GX $sPLA_2$ processing in adrenal cells based on the following findings: 1) furin and PCSK6 mRNA abundance were both significantly induced by ACTH in Y1 adrenal cells; 2) pro-GX $sPLA_2$ processing and activation were blocked in ACTH-treated Y1 cells by the PC inhibitor RVKR; 3) co-transfection of pro-GX $sPLA_2$ with either furin or PCSK6 significantly enhanced pro-GX $sPLA_2$ processing in HEK 293 cells; and 4) pro-GX $sPLA_2$ processing in adrenal cells was effectively blocked when the expression of both furin and PCSK6 was suppressed.

Analysis of PC cleavage preferences and substrate specificities reveals considerable overlap among several members of the PC family[146]. However, caution should be taken when attempting to draw conclusions from studies using short unfolded peptides as substrates. Redundancy in furin substrate cleavage specificity has been described in the liver using an interferon-inducible Mx-Cre/loxP furin deficient mouse model[147]. Both soluble furin and PCSK6 are able to cleave pro-Nodal while bound to its co-receptor at the cell surface[148,149]. However, unique furin substrates including the iron regulatory protein, pro-hepcidin, and pro-bone morphogenic protein 10 (pro-BMP10) in the developing heart, have also been described[150,151]. Our data that suppression of both furin and PCSK6 by siRNA-mediated gene silencing is required in order to effectively block pro-GX $sPLA_2$ processing provides direct evidence for redundancy, at least in Y1 adrenal cells.

In the current study, we only detected m-GX $sPLA_2$ in the media, while only pro-GX $sPLA_2$ could be found in cell lysates. Furin is thought to process substrates in the trans-Golgi network, at the cell surface, and in endosomes; whereas PCSK6 dependent processing is believed to take place in the extracellular matrix. Notably, furin has been shown to process endogenously produced substrates exclusively at the cell surface. Pro-ADAMTS9 was shown to be processed by furin at the cell surface before being secreted into the media[152]. Importantly, no evidence for mature-ADAMTS9 could be found in the cell lysates. Our findings are in contrast to a previous report that utilized cell-permeable and cell-impermeable inhibitors to define the cellular location of pro-GX $sPLA_2$ processing. In this study, the authors concluded that that pro-GX $sPLA_2$ processing takes place both before and after secretion[59]. This conclusion was supported by the finding that

exogenously added pro-GX $sPLA_2$ did not hydrolyze cell membranes. The reason for the discrepancy between these two findings is unclear; however, the possibility exists that PC dependent processing of pro-GX $sPLA_2$ occurs coincident with secretion.

The present study confirms previous findings from our laboratory documenting the role of GX $sPLA_2$ in modulating adrenal steroidogenesis[55]. GX KO mice have increased plasma corticosterone levels under both basal and ACTH-induced stress conditions[55]. This phenotype is due at least partly to a direct effect of GX $sPLA_2$ in the adrenal gland, since primary adrenal cells isolated from GX KO mice produce higher levels of glucocorticoids in response to ACTH compared to cells from wild-type mice[55]. We determined that GX $sPLA_2$-mediated suppression of progesterone production in Y1 adrenal cells is dependent on its hydrolytic activity, as evidenced by the fact that GX $sPLA_2$, but not a catalytically inactive mutant lacking the active-site histidine residue, suppressed basal and ACTH-induced progesterone production in Y1 cells. Our finding that treatment with the PC inhibitor, RVKR, abolished GX $sPLA_2$-dependent suppression of progesterone production under both basal and ACTH-stimulated conditions is consistent with previous observations that removal of the N-terminal pro-segment is necessary for GX $sPLA_2$ hydrolytic activity[39]. Importantly, the derepression of progesterone production in Y1-GX cells treated with RVKR was associated with both decreased pro-GX $sPLA_2$ processing and $sPLA_2$ activity in conditioned media from these cells. Furthermore, RVKR resulted in significantly reduced $sPLA_2$ activity secreted by Y1-C cells (data not shown), suggesting that upon processing, endogenous GX $sPLA_2$ contributes significantly to the phospholipase activity secreted by Y1 adrenal cells. Taken together, these data indicate that PCs proteolytically activate pro-GX $sPLA_2$,

which in turn acts to suppress glucocorticoid production in adrenal cells. Although the mechanism has not been completely delineated, GX $sPLA_2$ appears to negatively regulate adrenal glucocorticoid production through transcriptional suppression of StAR, most likely by reducing the activation of LXR[55]. StAR represents the rate-limiting protein in steroid hormone production, and many of the factors known to regulate steroidogenesis including LXR have their effect by targeting StAR[153,154]. Results from the current study demonstrate that suppression of LXR reporter activation by GX $sPLA_2$ is enhanced in the presence of either furin or PCSK6, and that inhibition of pro-GX $sPLA_2$ processing by RVKR restores StAR protein expression in Y1-GX cells to levels comparable to Y1-C cells. Together, these findings suggest that processing of pro-GX $sPLA_2$ by PCs is necessary for GX $sPLA_2$-dependent suppression of LXR target gene activation.

The body has evolved a complex regulatory network for finely tuning adrenal steroid production. Pituitary-derived ACTH stimulates the adrenals to produce glucocorticoids, which feedback on both the anterior pituitary and the hypothalamus to inhibit ACTH and corticotropin releasing hormone (CRH), respectively. Here we provide evidence for a negative feedback-loop in adrenal cells whereby ACTH increases PC expression, resulting in conversion of pro-GX $sPLA_2$ to m-GX $sPLA_2$, which in turn acts to suppress glucocorticoid production. What remains to be determined are the mechanism(s) responsible for turning off the activity of GX $sPLA_2$. One potential pathway is the M-type $sPLA_2$-receptor ($sPLA_2$-R), which has been implicated in the lysosomal degradation of GX $sPLA_2$. Chinese hamster ovary (CHO) cells overexpressing the $sPLA_2$-R rapidly degraded GX $sPLA_2$, resulting in a marked reduction in $PGE_2$ production compared to non-$sPLA_2$ receptor expressing cells [36]. A soluble form of the

$sPLA_2$-R has been identified in mouse plasma that binds and inactivates GX $sPLA_2$. The in vitro incubation of GX $sPLA_2$ with plasma from wild-type mice but not $sPLA_2$-R deficient mice decreases phospholipase activity[37]. We determined that the $sPLA_2$-R is expressed in mouse adrenal glands and Y1 cells[55]. Interestingly, silencing $sPLA_2$-R expression in YI-GX cells resulted in significantly reduced progesterone production, consistent with the possibility that the $sPLA_2$-R internalizes and/or inactivates GX $sPLA_2$, thereby reducing the magnitude of GX $sPLA_2$'s suppressive effect[55].

Understanding the tissue-specific regulation of pro-GX $sPLA_2$ processing will provide novel insights into the regulatory mechanisms governing physiological processes in which GX $sPLA_2$ is thought to play a role. In addition to adrenal cells, studies in our lab documented that GX $sPLA_2$ negatively regulates LXR target gene expression in macrophages and adipocytes, with significant consequences with respect to macrophage cholesterol efflux capacity[53], macrophage-mediated inflammatory responses[43], and adipocyte lipogenesis[54]. Given that both furin and PCSK6 are ubiquitously expressed[61], it is tempting to speculate that these PCs are the predominant proteases involved in the conversion of pro-GX $sPLA_2$ to m-GX $sPLA_2$ in multiple cell types. Interestingly, furin mRNA expression and $sPLA_2$ activity is significantly increased in J774 macrophages stably expressing GX $sPLA_2$ when treated with lipopolysaccharide (unpublished data). Clearly, further studies are needed in order to solidify the roles of individual PCs in modulating GX $sPLA_2$ activity in different tissues.

**Figure 4.1:**

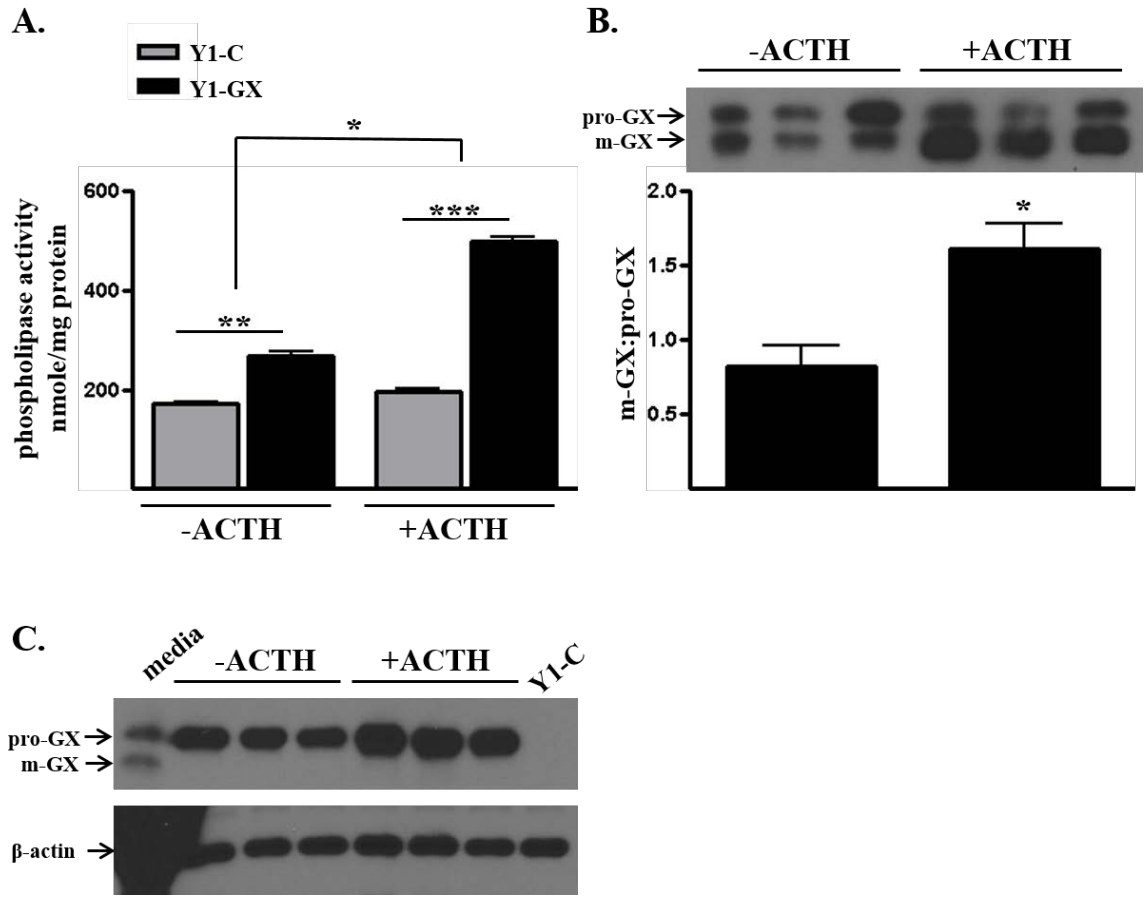
A.
Y1-C
Y1-GX
phospholipase activity
nmole/mg protein
600
400
200
*
**
***
-ACTH
+ACTH
B.
-ACTH
+ACTH
pro-GX
m-GX
m-GX:pro-GX
2.0
1.5
1.0
0.5
*
C.
media
-ACTH
+ACTH
Y1-C
pro-GX
m-GX
β-actin

**Figure 4.1 (continued): ACTH increases pro-GX $sPLA_2$ processing and phospholipase activity secreted by Y1 adrenal cells.**

Y1 adrenal cells were stably transfected with either a control expression vector (Y1-C) or a vector expressing 3X FLAG-tagged GX $sPLA_2$ (Y1-GX) and then incubated with 0 or 100nM ACTH for $_2$0 hrs. A. Phospholipase activity in conditioned media was measured (n=6). B. Conditioned media (20μL) was immunoblotted using an anti-FLAG antibody (top); results from densitometric analyses are shown below (n=3). Data is expressed as the ratio of m-GX $sPLA_2$:pro-GX $sPLA_2$ in the media. C. Whole-cell lysates (10μg protein) were immunoblotted using anti-FLAG antibody (top) and anti-β-actin (bottom). For comparison, conditioned media from vehicle-treated Y1-GX cells ("media") and lysates from Y1-C cells (Y1-C) were also analyzed. Data are means ± SEM and are representative of three independent experiments. * $P<0.05$, ** $P<0.01$, *** $P<0.001$

**Figure 4.2: Pro-GX $sPLA_2$ processing and activity are blocked by the furin-like proprotein convertase inhibitor RVKR.**

A. Y1-GX cells were incubated with 0 or 100nM ACTH in the presence or absence of 25 μM RVKR for 20 hrs, at which time media was collected for immunoblotting with anti-FLAG (top); results from densitometric analyses are shown below. Data are expressed as the ratio of m-GX $sPLA_2$:pro-GX $sPLA_2$ in the media. B. $sPLA_2$ activity in the media was quantified. Data are means ± SEM and are representative of three independent experiments. ** P<0.01, *** P<0.001

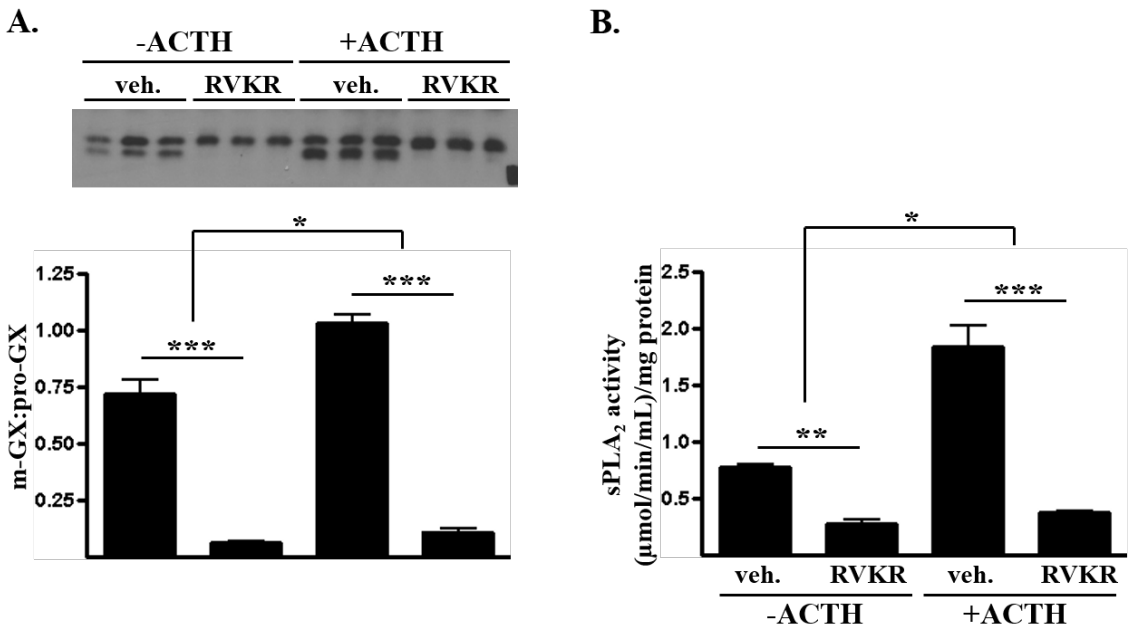

**Figure 4.3: ACTH increases furin and PCSK6 gene expression in adrenal cells.**

Both Y1-C and Y1-GX cells were incubated for 16 hr with either 0 or 100nM ACTH, and furin-like proprotein convertase gene expression was quantified by qRT-PCR (n=3). Data are means ± SEM and are representative of two independent experiments. *P<0.05

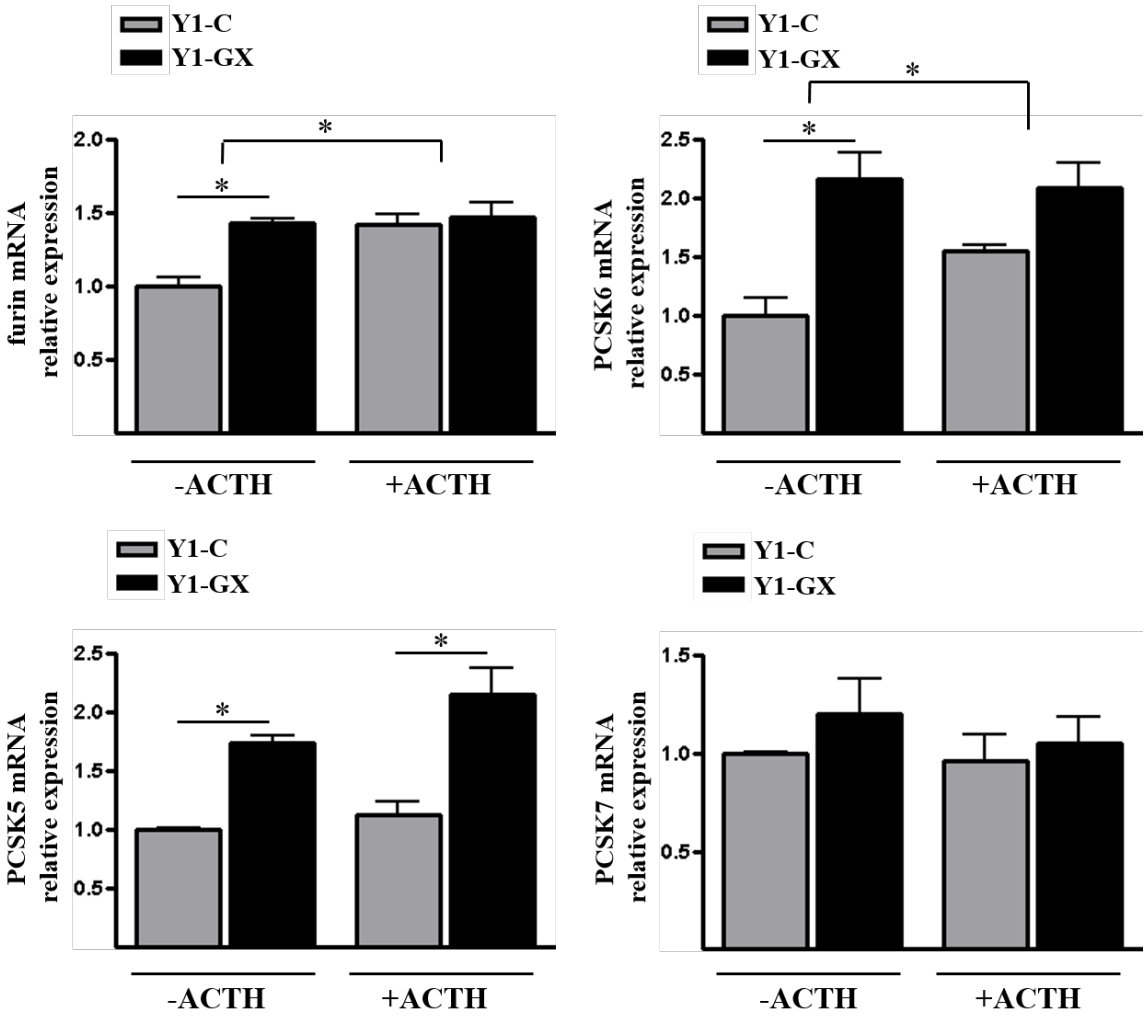

**Figure 4.4: Pro-GX $sPLA_2$ is proteolytically cleaved by furin and PCSK6.**

HEK293 cells were transiently co-transfected with 3X FLAG-tagged GX $sPLA_2$ and either a control vector (GX-C) or a vector encoding furin (GX-F) or PCSK6 (GX-P). Cells were then incubated in fresh media for 24 hrs. A. Conditioned media was immunoblotted using anti-FLAG antibody (top); results from densitometric analyses are shown below. Data are expressed as the ratio of m-GX $sPLA_2$:pro-GX $sPLA_2$ in the media. B. Whole-cell lysates (10μg protein) were immunoblotted using anti-FLAG antibody (top) and anti-β-actin (bottom). Data are means ± SEM and are representative of two independent experiments. *** P<0.001

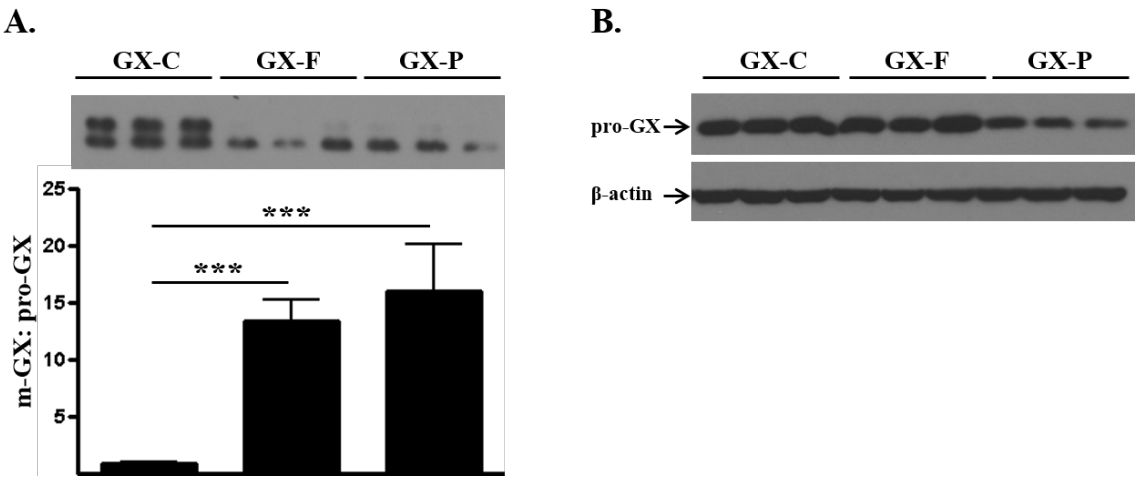

**Figure 4.5: Small interfering-RNA mediated knockdown of furin and PCSK6.**

Y1-GX cells were transiently transfected with either control siRNA (scr) or siRNA targeting furin (F-si), PCSK6 (P-si), or both siRNAs (F/P-si). Furin (left) and PCSK6 (right) mRNAs were quantified by qRT-PCR. Data are means ± SEM. (n=3). *** P<0.001

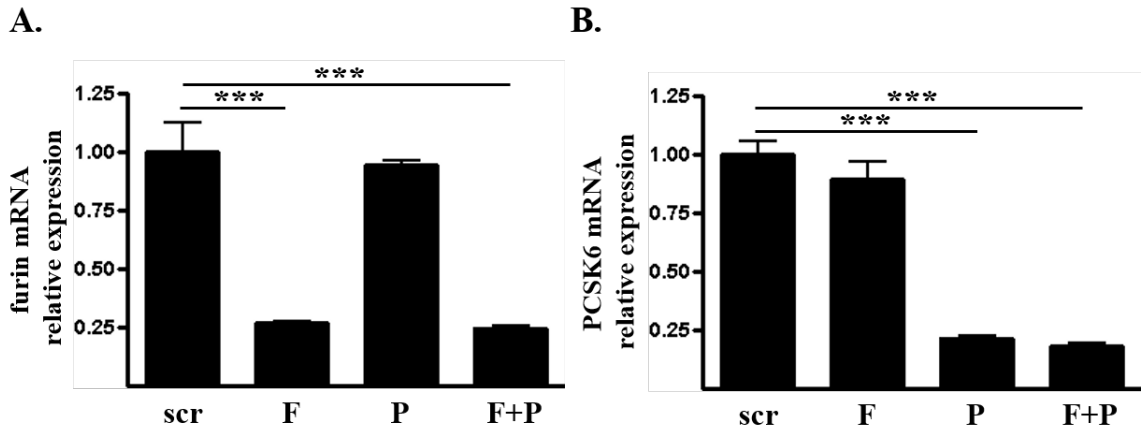

**Figure 4.6: Pro-GX $sPLA_2$ processing in mouse Y1 adrenal cells is dependent on furin and PCSK6 gene expression.**

A. Y1-GX cells were transiently transfected with either control siRNA (scr) or siRNA targeting furin (F-si), PCSK6 (P-si) or both siRNAs (F/P-si). B. Y1-GX cells transiently transfected with either control siRNA (scr) or siRNA targeting both furin and PCSK6 (F/P-si). Cells were then incubated in fresh media containing either 0 or 100nM ACTH for 20 hr. Data (means ± SEM) are expressed as the ratio of m-GX $sPLA_2$:pro-GX $sPLA_2$ in the media, and are representative of two independent experiments. * $P<0.05$, ** $P<0.01$

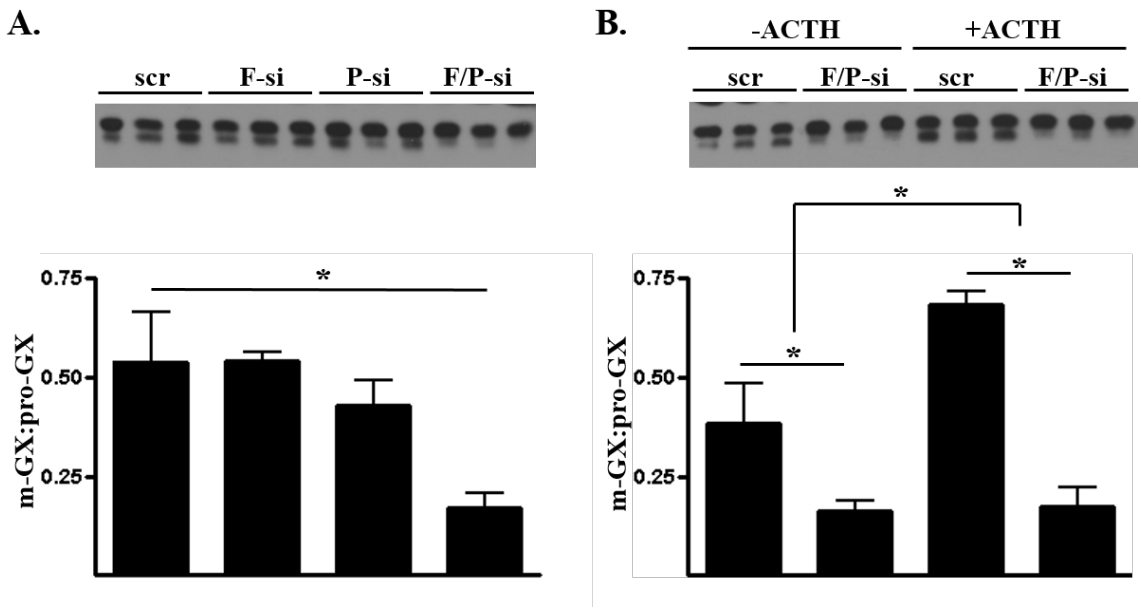

**Figure 4.7: Pro-GX $sPLA_2$ processing by furin or PCSK6 enhances GX $sPLA_2$-dependent inhibition of LXR-mediated gene activation.**

HEK 293 cells were transiently co-transfected with ptk-3X LXRE-luc reporter construct and vectors encoding mLXRα, mRXR, renilla-luciferase and either a control vector (293-C) or a vector encoding GX $sPLA_2$ in the absence (293-GX) or presence of A. furin (293-GX+F) or B. PCSK6 (293-GX+P). Cells were then incubated in media containing either 0 or 1μM T0901317 for 24 hours prior to measurements of luciferase activity. Data are means ± SEM (n=4) and are representative of two independent experiments. * P<0.05, *** P<0.001

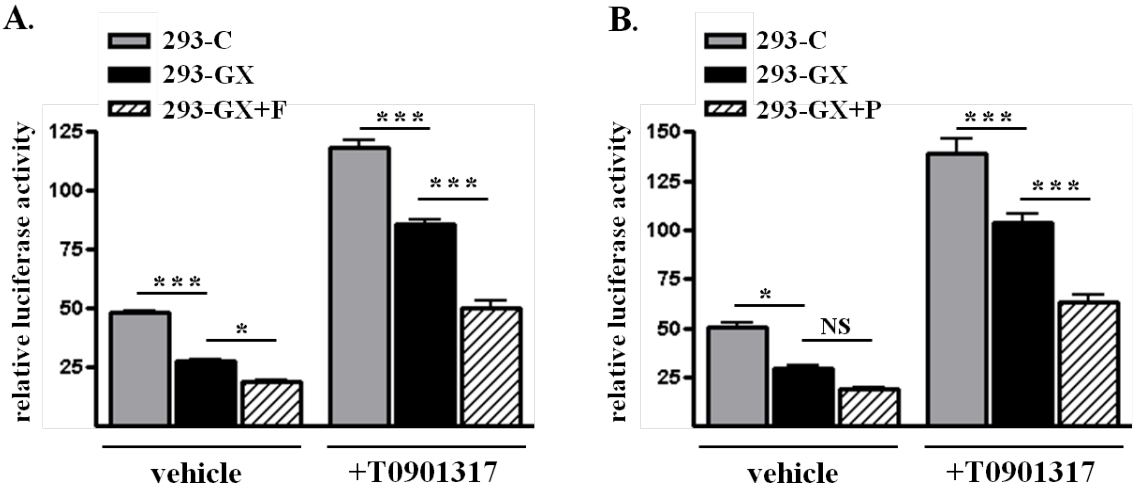

**Figure 4.8: Inhibition of StAR protein expression by GX-sPLA$_2$ is abolished by RVKR.**

Y1 cells were transiently transfected with either a control vector (Y1-C) or a vector encoding 3X-FLAG tagged GX sPLA$_2$ (Y1-GX). Cells were then incubated in media containing 0 or 100nM ACTH and either DMSO vehicle or 25μM RVKR for 18 hours. Immunoblot analysis of total cell lysates was performed using antibodies specific for StAR and β-actin. A. StAR and β-actin expression in Y1-C cells (lanes 1-4), Y1-GX cells (lanes 5-8), and Y1-GX cells treated with RVKR (lanes 9-12) in the absence of ACTH (top). Results from densitometric analyses (bottom) are expressed as the ratio of StAR:β-actin. B. StAR and β-actin expression in Y1-C cells (lanes 1-4), Y1-GX cells (lanes 5-8), and Y1-GX cells treated with RVKR (lanes 9-12) in the presence of 100 nM ACTH (top). Results from densitometric analyses (bottom) are expressed as the ratio of StAR:β-actin. Data are means ± SEM (n=3-4). * P<0.05

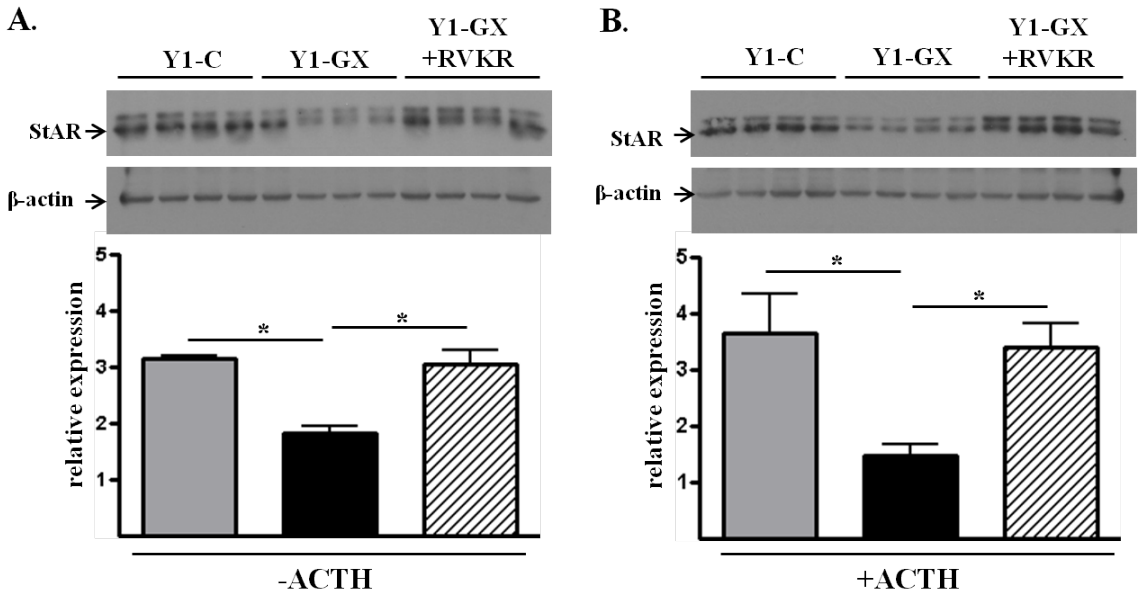

**Figure 4.9: GX $sPLA_2$-mediated inhibition of progesterone production by adrenal cells requires furin-like proprotein convertase activity.**

Y1 cells were transiently transfected with 3X-FLAG tagged GX $sPLA_2$. Cells were then incubated with the indicated concentrations of RVKR for 20 hours. A. $sPLA_2$ activity and B. progesterone levels were assayed in the media. C. Y1 cells were transiently transfected with either a control vector (Y1-C) or a vector encoding 3X-FLAG tagged GX $sPLA_2$ (Y1-GX). Cells were then incubated in media containing 0 or 100nM ACTH and either DMSO vehicle or 25μM RVKR for 20 hours. The concentration of progesterone in the media was measured and expressed relative to total cellular protein. Data are means ± SEM and are representative of two independent experiments (n=6). *** P<0.001

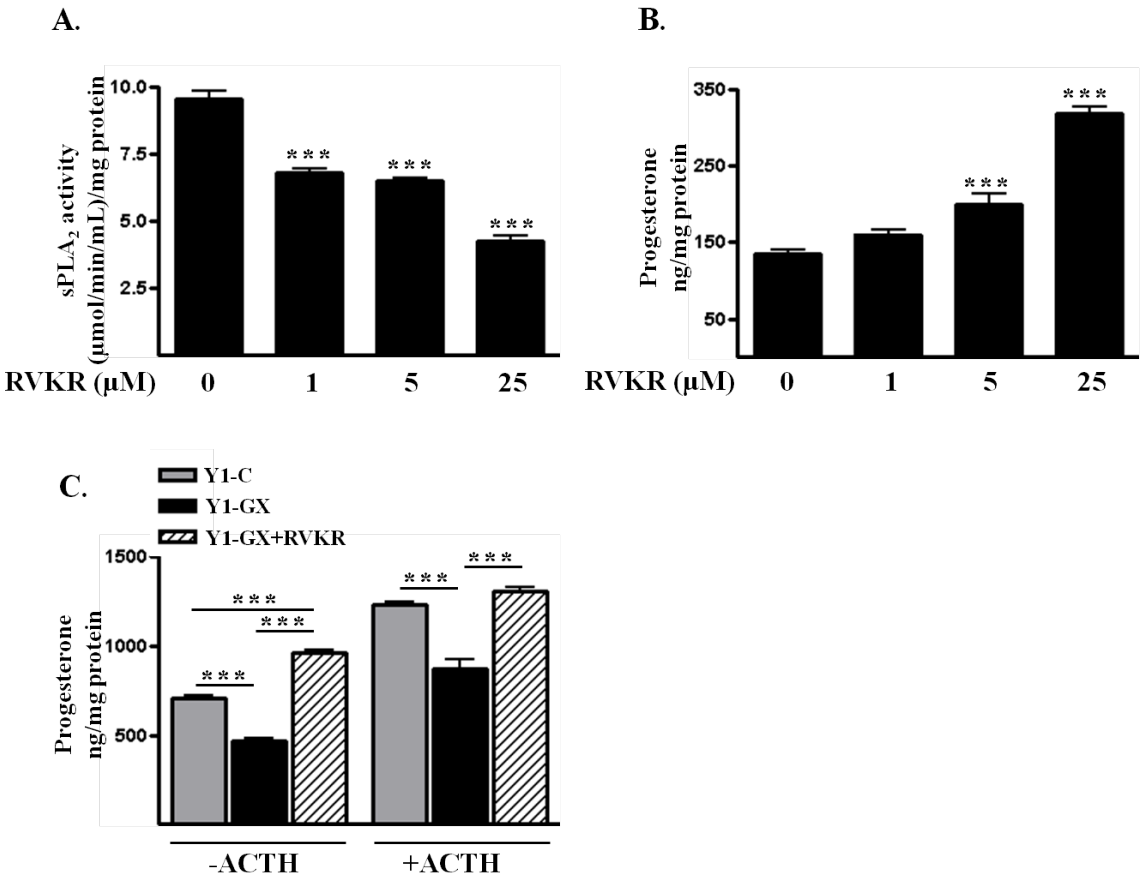

**Figure 4.10: The PC inhibitor RVKR significantly reduces phospholipase activity and m-GX $sPLA_2$ secreted by Y1 cells.**

Y1 cells were transiently transfected with either a control vector (Y1-C) or a vector encoding 3X-FLAG tagged GX $sPLA_2$ (Y1-GX). Cells were then incubated in media containing 0 or 100nM ACTH in the presence or absence of 25μM RVKR for 20 hours. A. $sPLA_2$ activity in the media was quantified and normalized to total cell protein. B. Conditioned media was immunoblotted with anti-FLAG antibody (top); results from densitometric analyses are shown below. Data are means ± SEM and are representative of three independent experiments (n=3). * P<0.05, ** P<0.01, ***P<0.01

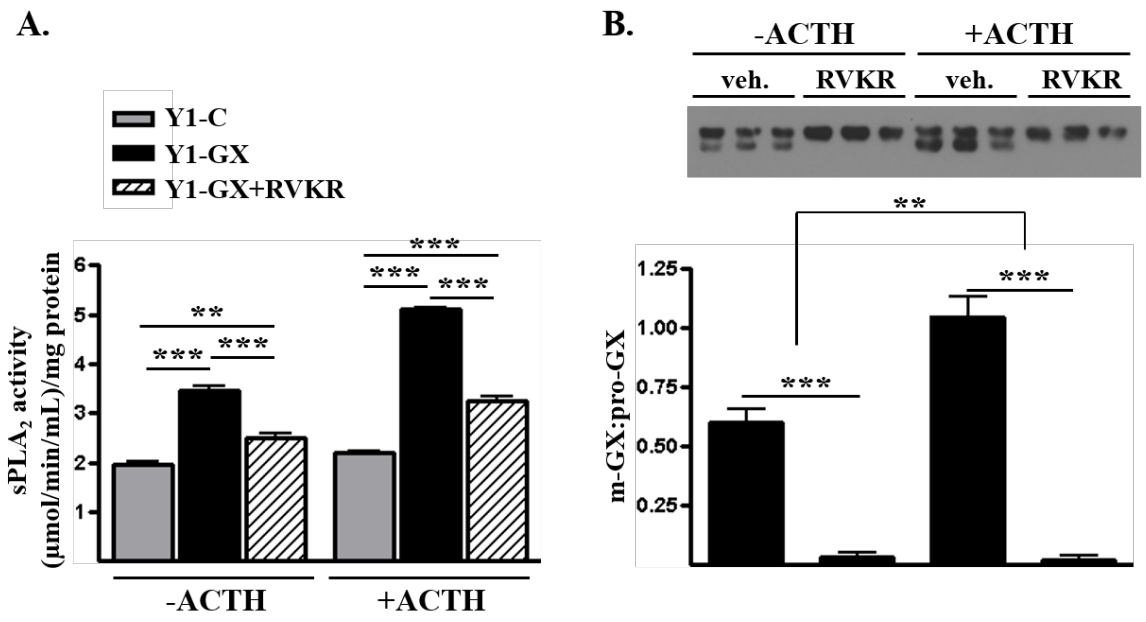

# Chapter 5

## Conclusions and future directions

### 5.1 Introduction

The phospholipase $A_2$ ($PLA_2$) family of enzymes consists of the cytosolic-$PLA_2$s, the $Ca^{2+}$- independent $PLA_2$s ($iPLA_2$s), the platelet-activating factor (PAF) acetyl hydrolases, and the small molecular weight secreted $PLA_2$s ($sPLA_2$s). All members within this family hydrolyze the sn-$_2$ ester bond of glycerophospholipids liberating free fatty acids and lysophospholipids. Products generated from the hydrolysis of biological membranes provide an almost limitless number of bioactive lipid mediators with a diverse array of physiological functions. Thus, members of the $PLA_2$ family have evolved unique substrate preferences based on their differences in biochemical structure, sub-cellular localization, and $Ca^{2+}$ dependence. GX $sPLA_2$ is the most potent $sPLA_2$ toward phosphatidylcholine, the most abundant phospholipid in mammalian cell membranes. GX $sPLA_2$ has a wide tissue distribution represented in the diverse array of biological processes it is known to mediate. As we continue to develop our understanding of the function and regulation of GX $sPLA_2$, it will likely provide valuable insight into the important physiological processes in which it is known to play a role.

### 5.2 GX $sPLA_2$ and AT inflammation and metabolic dysfunction

The onset of obesity is characterized by the rapid expansion of adipose tissue (AT) depots, and subsequently, active AT remodeling. The remodeling of AT, defined as AT hypertrophy and hyperplasia, is associated with the recruitment of inflammatory adipose tissue macrophages (ATMs). The infiltration of ATMs appears to be causally

linked to the development of metabolic abnormalities including glucose intolerance and insulin resistance. We have previously demonstrated that GX KO mice have increased age-related weight gain, and this was due to an increase in overall adiposity[54]. Despite the increased fat mass, GX KO mice were protected from age-related glucose intolerance (Shridas et al., unpublished data). Importantly, findings from our lab also indicated that macrophage mediated inflammatory responses are blunted in GX KO mice[43]. However, the role of GX $sPLA_2$ in diet-induced obesity (DIO) had not been investigated. Hence, we endeavored to determine the role of GX $sPLA_2$ in promoting macrophage mediated AT inflammation and metabolic dysfunction in a model of DIO. The current findings suggest that GX KO mice are only modestly protected from high fat diet (HFD) induced glucose intolerance. Moreover, GX KO mice were not protected from HFD induced insulin resistance. Most unexpectedly, markers of ATM infiltration and AT inflammation were unchanged in GX KO mice when compared to control mice. These findings suggest that whole-body GX $sPLA_2$ deficiency has a negligible effect on HFD induced AT inflammation and metabolic dysregulation.

### 5.2.1 Macrophage GX $sPLA_2$ and AT inflammation

The acquisition of C57BL/6 mice with a floxed GX $sPLA_2$ allele may provide novel insight into the role of GX $sPLA_2$ in promoting high fat diet (HFD)-induced metabolic dysfunction. Previous studies from our lab have defined a role for GX $sPLA_2$ in modulating macrophage inflammatory responses by altering lipid raft cholesterol content, resulting in blunted toll-like receptor (TLR) signaling[43]. Indeed, peritoneal macrophages isolated from GX KO mice have enhanced apoA1 mediated cholesterol efflux capacity, probably due to the increased expression of the liver X receptor (LXR)

target genes, ATP-binding cassette transporter A1 (ABCA1) and G1 (ABCG1)[53]. When bone marrow-derived macrophages from ABCA1 deficient mice were stimulated with lipolysaccharide (LPS), they secreted less IL-10 and had enhanced inflammatory cytokine production compared to wild type (WT) macrophages, reminiscent of alternatively activated macrophages[108]. Thus, given the phenotype seen in GX KO macrophages, it would stand to reason that GX KO mice fed a HFD would be protected against HFD-induced ATM infiltration and AT inflammation. However, there were no differences in ATM infiltration or markers of AT inflammation GX KO and WT mice. Therefore, the question remains, why doesn't GX $sPLA_2$ deficiency result in decreased ATM accumulation or reduced AT inflammation in response to HFD?

### 5.2.2 GX $sPLA_2$ and the regulation of adipogenesis

GX $sPLA_2$ is produced by adipocytes, albeit to a lesser extent than macrophages[54]. However, our group has previously demonstrated that aged GX KO mice had enlarged fat cells compared to WT mice[54]. In vitro studies suggested that this phenotype could be attributed to GX $sPLA_2$s ability to suppress LXR target gene expression, namely, SREBP-1c, DGAT1, FAS, and SCD-1. During obesity, the rapid expansion of AT is associated with adipocyte hypertrophy and hyperplasia. It has been suggested that the angiogenic response to rapidly expanding AT may be inadequate, and local hypoxia within the AT may contribute to AT inflammation during the early stages of disease[155]. Using expression levels of hypoxia inducible factor-1α (HIF-1α) as a surrogate marker, AT hypoxia has been demonstrated in models of genetic and diet induced obese mouse models[156,157]. AT hypoxia is accompanied be the expression several inflammatory cytokines including TNF-α, IL-1β, IL-6, PAI-1, and TGF-β among

others[156,158]. Furthermore, in vitro studies indicate that hypoxia may act to inhibit preadipocyte differentiation thus tipping the scale from a hyperplastic AT phenotype to one dominated predominately by hypertrophy[159,160]. It is unclear whether increased adipocyte cell mass in GX KO mice contributes to local hypoxia within the AT, thus potentiating the inflammatory response. Thus, is the blunted inflammatory macrophage inflammatory response in GX KO macrophages masked by the increased hypertrophy in GX KO adipocytes (Figure 5.1)? It would be of interest to learn if the adipocyte-specific deletion of GX $sPLA_2$ would negatively impact metabolic function and AT inflammation in either aged of high fat fed mice. Conversely, would the macrophage-specific deletion of GX $sPLA_2$ protect mice from HFD-induced AT inflammation and metabolic dysregulation in the absence of any effects on adipocyte function?

### 5.2.3 Adrenal GX $sPLA_2$ and metabolic dysfunction

GX KO mice have increased plasma corticosterone levels under both basal and ACTH-induced stress conditions[55]. This phenotype was likely due the derepression of the steroidogenic acute regulatory protein (StAR), a known LXR target gene[56]. While the impact of hypercorticosteronemia on metabolic function in GX KO mice has not been defined, there is reason to believe that it could introduce confounding factors when attempting to interpret the role of macrophage-derived GX $sPLA_2$ in high fat diet induced metabolic dysfunction and AT inflammation. There is now evidence to suggest that hyperglucocorticoidism may contribute to the pathophysiology of the metabolic syndrome. Indeed, increased secretion of GCs in patients suffering from Cushing's syndrome leads to central obesity, hyperglycemia, hyperlipidemia, glucose intolerance, and hypertension[87]. GCs have been shown to cause insulin resistance in skeletal muscle

but act to augment insulin signaling in subcutaneous fat depots[161]. In the liver, GC's promote gluconeogenesis resulting in enhanced hepatic glucose output[93,94]. Thus, adrenal GX $sPLA_2$ deficiency may be contributing to what is becoming recognized as a particularly convoluted metabolic phenotype. Therefore, the question remains, does adrenal GX $sPLA_2$ deficiency promote glucoregulatory imbalances independent of its effects in other tissues?

### 5.3 The GX $sPLA_2$ regulatory network

Previous work from our lab has demonstrated the role for GX $sPLA_2$ in the regulation of glucocorticoid production in the adrenals. GX KO mice exhibited hypercorticosteronemia under both basal and ACTH-stimulated conditions. In vitro studies attributed this affect to GX $sPLA_2$s ability to negatively regulate the liver X receptor (LXR) transcriptional activation of StAR, the rate-limiting protein involved in glucocorticoid production. Therefore, understanding how GX $sPLA_2$ is being regulated in the adrenals may provide valuable insight into the mechanisms governing adrenal steroidogenesis. In this study, we identified pro-GX $sPLA_2$ as a novel substrate for PC mediated proteolysis in Y1 adrenal cells. We also demonstrated that proteolytic activation of pro-GX $sPLA_2$ by PCs was necessary for GX $sPLA_2$ dependent suppression of StAR, and subsequently, glucocorticoid production (Figure 5.2). These studies have set the stage for further investigation into the complex regulatory network surrounding GX $sPLA_2$,not only in the adrenals but in other tissues where GX $sPLA_2$ has been shown to play an important physiological role[43,49,53-55].

### 5.3.1 ACTH dependent regulation of PCs in the adrenals

In the current study, we defined a role for furin and PCSK6 in the ACTH-induced proteolytic activation of pro-GX $sPLA_2$ in Y1 adrenal cells. ACTH treatment of Y1 cells resulted in enhanced furin and PCSK6 gene expression. However, the regulatory mechanisms underlying the ACTH-dependent activation of furin and PCSK6 remain undefined. ACTH stimulation of G-protein coupled receptors (GPCRs) predominately results in the Gαs mediated production of cAMP and the subsequent activation of PKA. The Janus-kinase signal transducer (JAK2) has recently been implicated in ACTH/cAMP induced steroidogenesis[80]. Under either basal or ACTH-stimulated conditions, the JAK2 dependent phosphorylation of the cAMP response element binding protein (CREB) prevented its proteosomal degradation, leading to increased transcriptional activation of StAR[80]. In adrenocortical cells, stimulation with either angiotensin II or magnonol resulted in the JAK2 dependent transcriptional activation of StAR, mediated in part through a MAPK/ERK1/2 pathway[162,163]. Notably, JAK/STAT signaling has been implicated in the regulation of furin gene expression and release of soluble-BAFF (a member of the TNF ligand superfamily) in stimulated gangliosides[164]. In HepG2 cells, transforming growth factor-β1 (TGF-β1) stimulation resulted in the ERK1/2 dependent increase in furin promoter activation and mRNA expression[165]. Similarly, ERK1/2 was involved in the enhanced furin expression in response to transferrin receptor activation[166]. Most notably, in Y1 adrenal cells, ACTH stimulation resulted in the increased phosphorylation of ERK1/2 and subsequently enhanced ERK1/2/MAPK activity[167]. The transcriptional regulation of PCSK6 is much less clearly defined, however sequence analysis of the 5' flanking region identified several potential binding sites for

transcription factors including SP-1, AP-1, AP-2, PEA3, Ets-1, GHF-1, basic helix-loop-helix (bHLH) proteins, and most notably CREB[168]. Therefore, ACTH stimulation of Y1 cells may result in a multifaceted response leading to the activation of both cAMP-dependent and independent (MAPK/ERK1/2) pathways, ultimately resulting in the CREB mediated up-regulation of PCs involved in the proteolytic cleavage of pro-GX $sPLA_2$ (Figure 5.3).

In the current study, we were able to show the up-regulation of PCSK6 mRNA in response to ACTH treatment of Y1 cells. However, the increase in mRNA abundance was relatively modest, and thus we cannot rule out the possibility that PCSK6 activity is also regulated post-translationally through the removal of its prosegment. PCs are produced as inactive precursors requiring two sequential cleavages of their prosegments in the endoplasmic reticulum and then in the trans-Golgi network. However, in Y1 adrenal cells, PCSK5A has been shown to retain its prosegment at the plasma membrane[65]. However, treatment with either ACTH or 8-bromo-cyclic AMP results in the decreased detection of the prosegment at the cell surface and increased PCSK5A proteolytic activity as evidenced by the enhanced processing of PCSK5 substrates, Lefty, ADAMTS-4 endothelial lipase, and PCSK9. PCSK5A binds heparin sulfate proteoglycans (HSPGs) on the cell surface through interaction with its cysteine-rich domain (CRD)[65]. This interaction is thought to impart substrate specificity and facilitate the removal of the prosegment. Intriguingly, PCSK6 also interacts with HSPGs via its CRD and thus may be regulated in a similar fashion[65]. Therefore, the post-translational regulation of PCSK6 may be yet another mechanism accounting for the enhanced pro-GX $sPLA_2$ processing in response to ACTH (Figure 5.3).

### 5.3.2 Regulation of PCs in other tissues

We have previously defined a role for GX $sPLA_2$ in modulating macrophage inflammatory responses. The overexpression of GX $sPLA_2$ results in augmented lipid raft cholesterol content and enhanced TLR4 mediated responses to LPS. However, it is unclear how GX $sPLA_2$ is regulated in macrophages. Among the PC family members, furin and PCSK6 are among the most widely expressed[61] and may therefore be responsible for pro-GX $sPLA_2$ cleavage in tissues other than the adrenals. Preliminary data from our lab suggests that the phospholipase activity secreted into the media by J774 macrophages stably expressing GX $sPLA_2$ (J774-GX) is increased in response to LPS (Zahoor et al., unpublished data). Importantly, LPS treatment of J774-GX macrophages also results in enhanced furin gene expression (Zahoor et al., unpublished data). However, the intracellular mechanisms underlying the up-regulation of furin in response to TLR4 activation are unknown. In bone marrow derived granulocytes, the TLR4 dependent shedding of TNF-receptor requires both p38 MAPK and furin[169]. The treatment of fibroblasts with tumor necrosis factor-α (TNF-α) results in increased furin activity and pro-MT1-MMP processing[170]. Using the human monocyte THP-1 cell line, it has been shown that PMA-induced macrophage differentiation is characterized by increased expression of furin and PCSK5, and enhanced pro-MT1-MMP processing[171]. Importantly, PMA-induced THP-1 differentiation resulted in the rapid, transient activation of MAPK signaling (ERK1/2, p38, JNK)[172-174]. Thus, MAPK signaling represents one potential mechanism underlying the regulation of PCs in macrophages and perhaps other relevant tissues where GX $sPLA_2$ is known to play a role.

### 5.3.3 GX $sPLA_2$-dependent up-regulation of PCs

There is now evidence to suggest that PC substrates may enhance PC expression, in what would constitute a feed-forward loop. Furin has been identified as the predominant transforming growth factor-β (TGF- β) converting PC[175]. Interestingly, in $HepG_2$ cells, TGF-β receptor stimulation led to the cooperative up-regulation of both Smad signaling and p42/p44 MAPK pathways, resulting in increased nuclear translocation of Smad2 and furin gene transactivation[165]. Data from our lab suggests that Y1 adrenal cells stably expressing GX $sPLA_2$ (Y1-GX cells) have significantly increased expression of select PCs, most notably, furin, PCSK6 and PCSK5, when compared to control transfected Y1 cells (Y1-C). Thus, PC up-regulation in response to enhanced GX $sPLA_2$ expression may represent a mechanism ensuring adequate PCs are available to proteolytically activate pro-GX $sPLA_2$. While the mechanisms governing the GX $sPLA_2$ dependent up-regulation of PCs is unclear, there is evidence to suggest that eicosanoids derived from membrane hydrolysis may play a role. Indeed, the cysteinyl leukotriene D4 (CysLTD4) enhanced furin expression in HEK 293 cells expressing the CysLT1-receptor[176]. Importantly, incubation of eosinophils with recombinant GX $sPLA_2$ resulted in the production of CysLTs[177].

### 5.3.4 Post-transcriptional regulation of GX $sPLA_2$

Results from our lab suggest that ectopically-expressed GX $sPLA_2$ mRNA abundance is increased in response to ACTH in Y1 cells. This finding likely indicates an increase in mRNA stability due to the fact that the CMV promoter-driven GX $sPLA_2$ is unlikely to be transcriptionally regulated by ACTH-stimulation. Intriguingly, within the 3'untranslated region (3'UTR) of GX $sPLA_2$ there exists a highly conserved target

sequence for miR-19a (Figure 5.4). Recently, the dysregulation of miR-19a has been described in chronic inflammatory diseases including ulcerative colitis (UC)[178]. Moreover, the 3'UTR of TNF-α was recently identified as a miR-19a target[179]. miR-19a expression levels were significantly reduced in the colons of both humans with ulcerative colitis (UC), and in dextran sodium sulfate (DSS) induced UC in rodent models[178]. Most notably, the decreased miR-19a levels are associated with significantly increased TNF- α in both human and rodent colon tissues. GX $sPLA_2$ has been implicated in several chronic inflammatory diseases including asthma, rheumatoid arthritis, and atherosclerosis to name a few[40,129,180]. Thus, it is tempting to speculate that miR-19a may represent a novel mechanism by which GX $sPLA_2$ mRNA stability can be altered.

### 5.3.5 GX $sPLA_2$ deactivation

The potency with which GX $sPLA_2$ hydrolyzes phosphatidylcholine infers there must be tightly controlled mechanisms regulating both the proteolytic activation of pro-GX $sPLA_2$ and perhaps of equal importance, the de-activation of mature-GX $sPLA_2$ (m-GX $sPLA_2$). There is evidence to suggest that GX $sPLA_2$ acts as a ligand for the $sPLA_2$ receptor ($sPLA_2$-R) in Chinese hamster ovary (CHO) cells[36]. Furthermore, GX $sPLA_2$ binding to the $sPLA_2$-R leads to increased GX $sPLA_2$ degradation and diminished $PGE_2$ production[36]. Notably, studies from our lab indicate $sPLA_2$-R silencing in Y1 cells stably expressing GX $sPLA_2$ leads to decreased progesterone levels[55]. Thus, it is feasible to speculate that in the absence of $sPLA_2$-R expression in Y1 cells more GX $sPLA_2$ is available to suppress progesterone production. Alternatively, a soluble form of the $sPLA_2$-R has been detected in mouse plasma where it binds and inactivates GX $sPLA_2$[37]. Indeed, in vitro incubation of GX $sPLA_2$ with plasma from wild type, but not $sPLA_2$-R

deficient mice, inhibits phospholipase activity[37]. Inhibitor studies in $sPLA_2$-R expressing CHO cells revealed a role for matrix metalloproteinase's (MMP's) in the proteolytic cleavage and release of membrane-bound $sPLA_2$-R[37]. However, the identity of the individual MMPs involved is unknown. Studies from our lab suggest that GX $sPLA_2$ may increase the expression of MMPs in the abdominal aorta of mice receiving subcutaneous infusion of angiotensin-II (ang-II)[49]. Taken together, the MMP dependent release of soluble $sPLA_2$-R from membranes could constitute a negative-feedback loop for limiting GX $sPLA_2$ hydrolytic activity.

### 5.3.6 GX $sPLA_2$ dependent suppression of LXR

GX $sPLA_2$ dependent hydrolysis of membrane phospholipids results in the release of free fatty acids, most notably arachidonic acid (AA) and lysophosphatidylcholine (LysoPtdCho) Previous work by our lab has defined a role for GX $sPLA_2$ as a negative regulator of liver X receptor (LXR) target gene expression[43,53-55]. In J774 macrophages, GX $sPLA_2$ hydrolytic activity is required for suppression if the LXR target genes, ATP-binding cassette A1 (ABCA1) and G1 (ABCG1). Importantly, the effect of GX $sPLA_2$ on ABCA1 and ABCG1 can be mimicked with treatment of J774 macrophages with AA but not LysoPtdCho. However, indomethacin, a non-selective cyclooxygenase-1/2 inhibitor, has no effect on GX $sPLA_2$ dependent inhibition of LXR target gene expression. Thus, GX $sPLA_2$ mediated inhibition of LXR transcriptional activity does not appear to be dependent on the production of prostanoids. To date, the mechanism by which GX $sPLA_2$ negatively regulates LXR activation has not been defined.

One possible mechanism by which GX $sPLA_2$ may inhibit LXR is through its inhibitory phosphorylation. The protein kinase A (PKA) dependent phosphorylation of

LXR at serine 198[181], which is embedded in a consensus MAPK phosphorylation sequence[182]. The phosphorylation of LXR prevents heterodimerization with retinoid X receptor (RXR) and recruitment of co-activator SCR-1, while enhancing recruitment of the co-repressor NcoR-1.Notably, in MA-10 mouse leydig cells, epoxygenase derived AA metabolites activated the cAMP/PKA signaling axis[183]. Similarly, PMA treatment results in the protein kinase C (PKC) dependent phosphorylation of LXR in HepG2 cells, leading to diminished SREBP-1c expression[182]. A route to PKC activation has been demonstrated in the ACTH dependent stimulation of GPCRs, resulting in the phospholipase C (PLC) dependent elevation of intracellular free $Ca^{2+}$[184]. The PLC-mediated hydrolysis of phosphatidylinositol 4,5-bisphosphate ($PIP_2$) produces two second messengers: inositol 1,4,5-trisphosphate (IP3),which releases $Ca^{2+}$ from intracellular stores, and diacylglycerol (DAG), which activates protein kinase C (PKC). In the presence of phosphatidylserine and $Ca^{2+}$, DAG activation of PKC triggers a kinase cascade mediated by Raf, MEK, and MAPKs[185]. In HEK293 cells, treatment with low levels of AA (<0.5μM) results in increased membrane targeting of PKC from the cytosol[186], likely facilitating PKC activation. In a model of oxidative stress induced inflammation, GV and GIIA $sPLA_2$ regulates the $cPLA_2\alpha$ dependent release of AA leading to the downstream activation of PKC and ERK1/2[187]. In low-density lipoprotein receptor-related protein 1 (LRP1) deficient smooth muscle cells (SMCs) the phosphorylation and subsequent activation of $cPLA_2\alpha$ was increased, and this was associated with decreased ABCA1 expression[188]. Notably, a $cPLA_2\alpha$ inhibitor restores ABCA1 expression in LRP1 deficient SMCs[188]. Thus, the GX $sPLA_2$ dependent

activation of PKC and downstream effectors including ERK1/2/MAPKs may lead to the inhibitory phosphorylation of LXR (Figure 5.5).

### 5.4 Concluding remarks

In conclusion, the tissue-specific deletion of GX $sPLA_2$ may provide valuable insight into its role in HFD-induced metabolic dysfunction that was otherwise confounded by the whole-body knockout. Indeed, it may further our understanding of not only the macrophage-adipocyte crosstalk in the context of DIO, but may shed new light on the role of the adrenals in the metabolic derangements associated with DIO.

The ability of GX $sPLA_2$ to potently hydrolyze membrane phospholipids has necessitated the evolution of a complex regulatory network to govern its hydrolytic activity. We have identified pro-GX $sPLA_2$ as a novel substrate for PCs in the adrenals. Moreover, we have identified a previously uncharacterized mechanism involved in the regulation of adrenal steroidogenesis. These findings have brought new questions to light. How are PCs being regulated in the adrenals? What PCs are involved in pro-GX $sPLA_2$ processing in other tissues? What are the intermediates involved in GX $sPLA_2$ dependent suppression of LXR transcriptional activity? As we continue to uncover the regulatory mechanisms surrounding GX $sPLA_2$s activation, these findings will provide important insight into the complex physiological processes in which GX $sPLA_2$ has been shown to play a role.

**Figure 5.1: GX $sPLA_2$ deficiency in adipocytes AND macrophages may cause opposing actions on DIO phenotype.**

GX KO in adipocyte results in increased adipocyte hypertrophy, potentially leading to more hypoxia, inflammatory cytokine production, and ATM recruitment. However, GX KO macrophages may be less responsive due to blunted TLR4 signaling. Thus, the absence of GX $sPLA_2$ in both adipocytes and macrophages may cancel each other out with respect to the metabolic phenotype in a model of DIO.

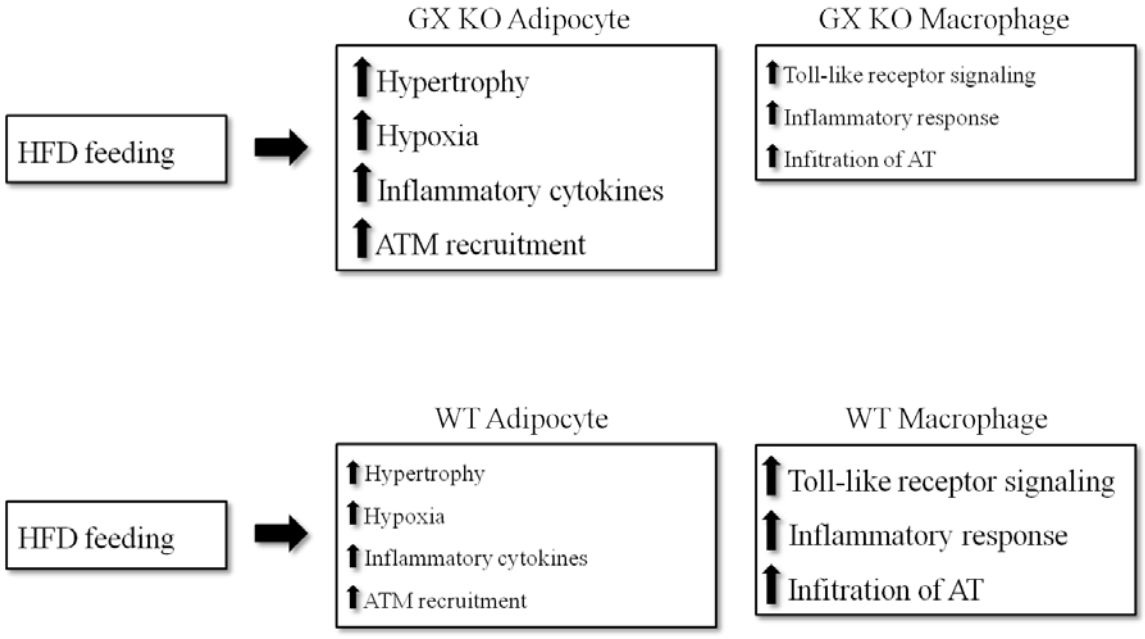

**Figure 5.2: ACTH enhances pro-GX $sPLA_2$ processing in Y1 adrenal cells.**

ACTH stimulation of GPCRs results in the enhanced expression of PCs, furin and PCSK6, possibly through the cAMP-dependent activation of the CREB. Furin and PCSK6 are subsequently processed through the trans-Golgi network and secreted. Activation of PCs results in enhanced pro-GX $sPLA_2$ processing and $sPLA_2$ activity, leading to increased production of AA. AA metabolites then go on to inhibit LXR target gene expression, namely StAR. The decreased expression of StAR results in diminished GC production.

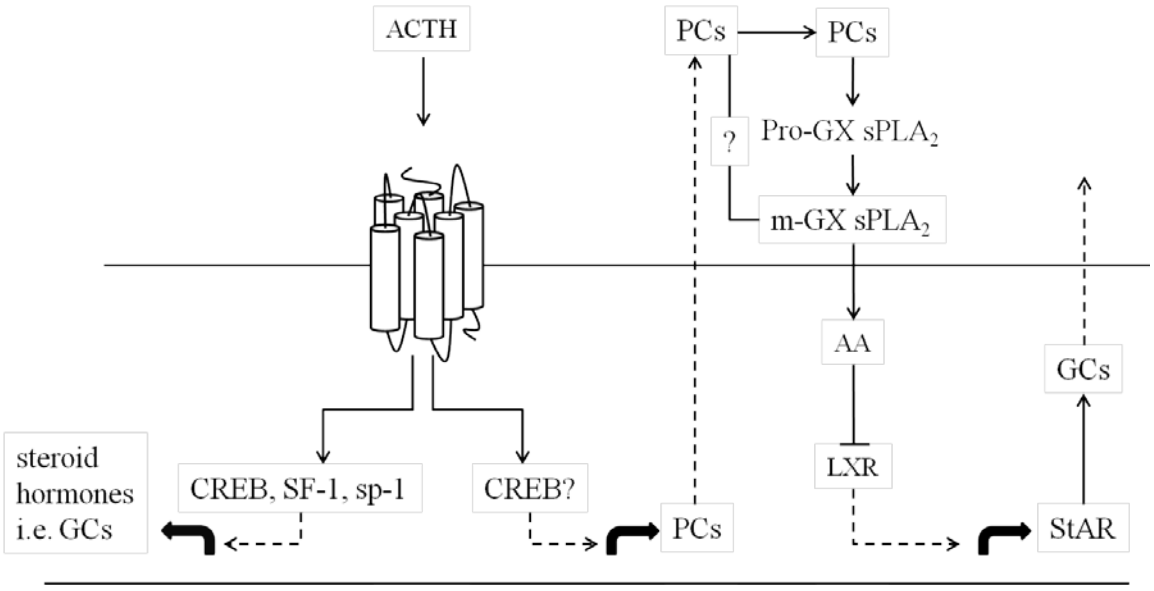

**Figure 5.3: Proposed mechanism for the ACTH dependent increase in PC expression in Y1 cells.**

ACTH stimulation of GPCRs results in the activation of cAMP dependent and independent (ERK1/2/MAPK) pathways. In the presence of JAK2, PKA and ERK1/2 converge to activate the CREB. CREB proceeds to increase the expression of PCs, furin and PCSK6.

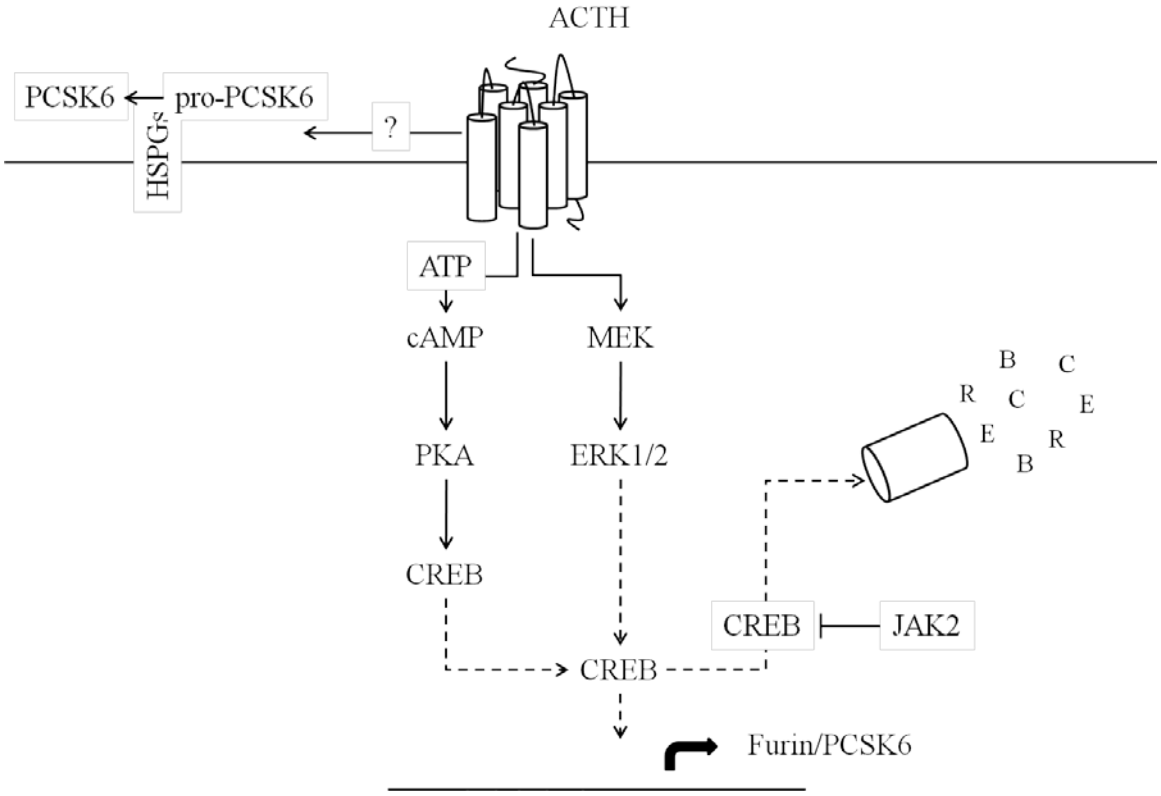

**Figure 5.4: Conserved miR-19a target sequence in the 3'untranslated region (3'UTR) of GX sPLA$_2$ (Pla$_2$g10).**

Highly conservedmiR-19a target sequence found in the 3'UTR of A. human GX sPLA$_2$, B. mouse GX sPLA$_2$, and C. rat GX sPLA$_2$.

**Figure 5.5: Proposed mechanism for GX $sPLA_2$ dependent suppression of LXR.**

The activation of GX $sPLA_2$ results in the $cPLA_2\alpha$ dependent and independent production of AA. AA potentiates the GPCR dependent activation of PLC, resulting in enhanced intracellular free $Ca^{2+}$ and PKC activation. PKC acts to suppress LXR/RXR heterodimerization associated with the recruitment of corepressors including NcoR-1 and the dissociation of coactivators such as SRC-1. Alternatively, AA may potentiate GPCR mediated activation of PKA, likewise suppressing LXR transcriptional activation.

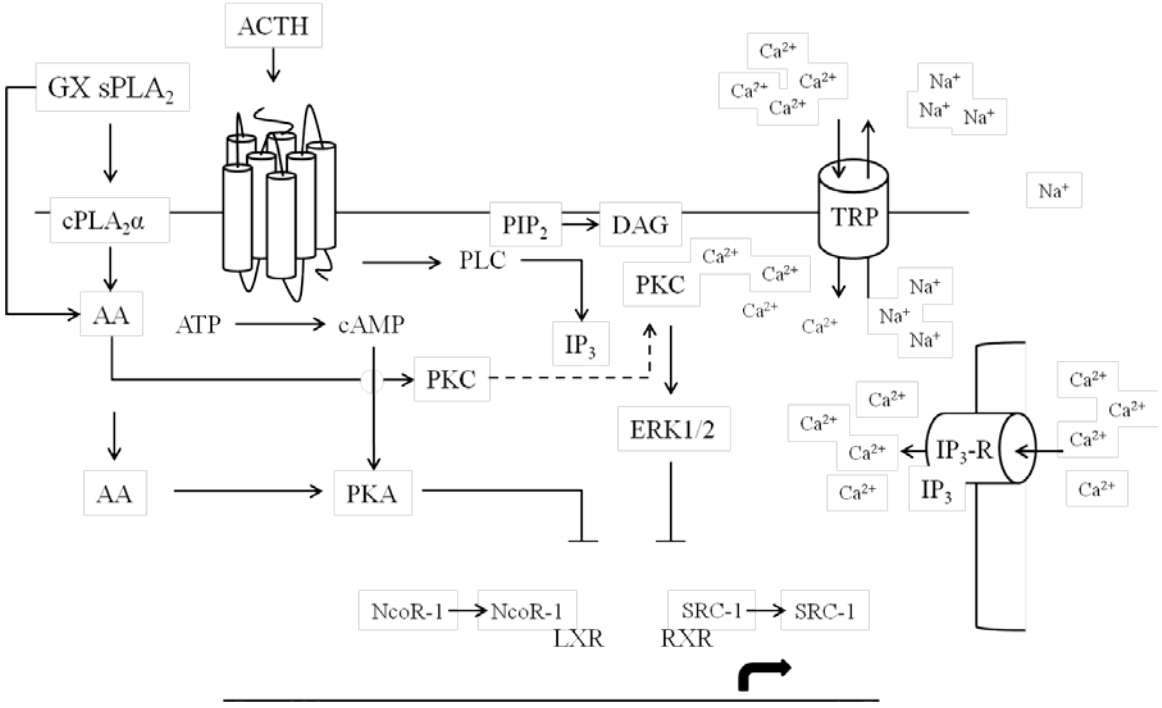

## References


1. Boyanovsky BB, Webb NR. Biology of secretory phospholipase A2. Cardiovascular drugs and therapy / sponsored by the International Society of Cardiovascular Pharmacotherapy 2009;23:61-72.
2. Qu XD, Lehrer RI. Secretory phospholipase A2 is the principal bactericide for staphylococci and other gram-positive bacteria in human tears. Infection and immunity 1998;66:2791-7.
3. Bezzine S, Bollinger JG, Singer AG, Veatch SL, Keller SL, Gelb MH. On the binding preference of human groups IIA and X phospholipases A2 for membranes with anionic phospholipids. The Journal of biological chemistry 2002;277:48523-34.
4. Bayburt T, Yu BZ, Lin HK, Browning J, Jain MK, Gelb MH. Human nonpancreatic secreted phospholipase A2: interfacial parameters, substrate specificities, and competitive inhibitors. Biochemistry 1993;32:573-82.
5. Murakami M, Koduri RS, Enomoto A, et al. Distinct arachidonate-releasing functions of mammalian secreted phospholipase A2s in human embryonic kidney 293 and rat mastocytoma RBL-2H3 cells through heparan sulfate shuttling and external plasma membrane mechanisms. The Journal of biological chemistry 2001;276:10083-96.
6. Bezzine S, Koduri RS, Valentin E, et al. Exogenously added human group X secreted phospholipase A(2) but not the group IB, IIA, and V enzymes efficiently release arachidonic acid from adherent mammalian cells. The Journal of biological chemistry 2000;275:3179-91.
7. Baker SF, Othman R, Wilton DC. Tryptophan-containing mutant of human (group IIa) secreted phospholipase A2 has a dramatically increased ability to hydrolyze phosphatidylcholine vesicles and cell membranes. Biochemistry 1998;37:13203-11.
8. Murakami M, Shimbara S, Kambe T, et al. The functions of five distinct mammalian phospholipase A2S in regulating arachidonic acid release. Type IIa and type V secretory phospholipase A2S are functionally redundant and act in concert with cytosolic phospholipase A2. The Journal of biological chemistry 1998;273:14411-23.
9. Murakami M, Masuda S, Shimbara S, et al. Cellular arachidonate-releasing function of novel classes of secretory phospholipase A2s (groups III and XII). The Journal of biological chemistry 2003;278:10657-67.
10. Kikawada E, Bonventre JV, Arm JP. Group V secretory PLA2 regulates TLR2-dependent eicosanoid generation in mouse mast cells through amplification of ERK and cPLA2alpha activation. Blood 2007;110:561-7.
11. Saiga A, Uozumi N, Ono T, et al. Group X secretory phospholipase A2 can induce arachidonic acid release and eicosanoid production without activation of cytosolic phospholipase A2 alpha. Prostaglandins & other lipid mediators 2005;75:79-89.
12. de Haas GH, Postema NM, Nieuwenhuizen W, van Deenen LL. Purification and properties of an anionic zymogen of phospholipase A from porcine pancreas. Biochimica et biophysica acta 1968;159:118-29.
13. Huggins KW, Boileau AC, Hui DY. Protection against diet-induced obesity and obesity- related insulin resistance in Group 1B PLA2-deficient mice. American journal of physiology Endocrinology and metabolism 2002;283:E994-E1001.

14. Labonte ED, Kirby RJ, Schildmeyer NM, Cannon AM, Huggins KW, Hui DY. Group 1B phospholipase A2-mediated lysophospholipid absorption directly contributes to postprandial hyperglycemia. Diabetes 2006;55:935-41.
15. Pruzanski W, Vadas P, Browning J. Secretory non-pancreatic group II phospholipase A2: role in physiologic and inflammatory processes. Journal of lipid mediators 1993;8:161-7.
16. Saegusa J, Akakura N, Wu CY, et al. Pro-inflammatory secretory phospholipase A2 type IIA binds to integrins alphavbeta3 and alpha4beta1 and induces proliferation of monocytic cells in an integrin-dependent manner. The Journal of biological chemistry 2008;283:26107-15.
17. Ye L, Dickerson T, Kaur H, et al. Identification of inhibitors against interaction between pro-inflammatory sPLA2-IIA protein and integrin alphavbeta3. Bioorganic & medicinal chemistry letters 2013;23:340-5.
18. Guidet B, Piot O, Masliah J, et al. Secretory non-pancreatic phopholipase A2 in severe sepsis: relation to endotoxin, cytokines and thromboxane B2. Infection 1996;24:103-8.
19. Liu MS, Liu CH, Wu G, Zhou Y. Antisense inhibition of secretory and cytosolic phospholipase A2 reduces the mortality in rats with sepsis*. Crit Care Med 2012;40:2132-40.
20. Hamaguchi K, Kuwata H, Yoshihara K, et al. Induction of distinct sets of secretory phospholipase A(2) in rodents during inflammation. Biochimica et biophysica acta 2003;1635:37-47.
21. Abraham E, Naum C, Bandi V, et al. Efficacy and safety of LY315920Na/S-5920, a selective inhibitor of 14-kDa group IIA secretory phospholipase A2, in patients with suspected sepsis and organ failure. Crit Care Med 2003;31:718-28.
22. Zeiher BG, Steingrub J, Laterre PF, Dmitrienko A, Fukiishi Y, Abraham E. LY315920NA/S-5920, a selective inhibitor of group IIA secretory phospholipase A2, fails to improve clinical outcome for patients with severe sepsis. Crit Care Med 2005;33:1741-8.
23. Bradley JD, Dmitrienko AA, Kivitz AJ, et al. A randomized, double-blinded, placebo-controlled clinical trial of LY333013, a selective inhibitor of group II secretory phospholipase A2, in the treatment of rheumatoid arthritis. J Rheumatol 2005;32:417-23.
24. Boyanovsky BB, van der Westhuyzen DR, Webb NR. Group V secretory phospholipase A2-modified low density lipoprotein promotes foam cell formation by a SR-A- and CD36-independent process that involves cellular proteoglycans. The Journal of biological chemistry 2005;280:32746-52.
25. Bostrom MA, Boyanovsky BB, Jordan CT, et al. Group v secretory phospholipase A2 promotes atherosclerosis: evidence from genetically altered mice. Arterioscler Thromb Vasc Biol 2007;27:600-6.
26. O'Donoghue ML, Mallat Z, Morrow DA, et al. Prognostic utility of secretory phospholipase A(2) in patients with stable coronary artery disease. Clin Chem 2011;57:1311-7.
27. Koenig W, Vossen CY, Mallat Z, Brenner H, Benessiano J, Rothenbacher D. Association between type II secretory phospholipase A2 plasma concentrations and activity and cardiovascular events in patients with coronary heart disease. Eur Heart J 2009;30:2742-8.

28. von Allmen CE, Schmitz N, Bauer M, et al. Secretory phospholipase A2-IID is an effector molecule of CD4+CD25+ regulatory T cells. Proceedings of the National Academy of Sciences of the United States of America 2009;106:11673-8.
29. Koduri RS, Gronroos JO, Laine VJ, et al. Bactericidal properties of human and murine groups I, II, V, X, and XII secreted phospholipases A(2). The Journal of biological chemistry 2002;277:5849-57.
30. Weinrauch Y, Elsbach P, Madsen LM, Foreman A, Weiss J. The potent anti-Staphylococcus aureus activity of a sterile rabbit inflammatory fluid is due to a 14-kD phospholipase A2. The Journal of clinical investigation 1996;97:250-7.
31. Weinrauch Y, Abad C, Liang NS, Lowry SF, Weiss J. Mobilization of potent plasma bactericidal activity during systemic bacterial challenge. Role of group IIA phospholipase A2. The Journal of clinical investigation 1998;102:633-8.
32. Harwig SS, Tan L, Qu XD, Cho Y, Eisenhauer PB, Lehrer RI. Bactericidal properties of murine intestinal phospholipase A2. The Journal of clinical investigation 1995;95:603-10.
33. Lambeau G, Barhanin J, Schweitz H, Qar J, Lazdunski M. Identification and properties of very high affinity brain membrane-binding sites for a neurotoxic phospholipase from the taipan venom. The Journal of biological chemistry 1989;264:11503-10.
34. Lambeau G, Schmid-Alliana A, Lazdunski M, Barhanin J. Identification and purification of a very high affinity binding protein for toxic phospholipases A2 in skeletal muscle. The Journal of biological chemistry 1990;265:9526-32.
35. Hanasaki K, Arita H. Phospholipase A2 receptor: a regulator of biological functions of secretory phospholipase A2. Prostaglandins & other lipid mediators 2002;68-69:71-82.
36. Yokota Y, Notoya M, Higashino K, et al. Clearance of group X secretory phospholipase A(2) via mouse phospholipase A(2) receptor. FEBS letters 2001;509:250-4.
37. Higashino Ki K, Yokota Y, Ono T, Kamitani S, Arita H, Hanasaki K. Identification of a soluble form phospholipase A2 receptor as a circulating endogenous inhibitor for secretory phospholipase A2. The Journal of biological chemistry 2002;277:13583-8.
38. Singer AG, Ghomashchi F, Le Calvez C, et al. Interfacial kinetic and binding properties of the complete set of human and mouse groups I, II, V, X, and XII secreted phospholipases A2. The Journal of biological chemistry 2002;277:48535-49.
39. Cupillard L, Koumanov K, Mattei MG, Lazdunski M, Lambeau G. Cloning, chromosomal mapping, and expression of a novel human secretory phospholipase A2. The Journal of biological chemistry 1997;272:15745-52.
40. Karabina SA, Brocheriou I, Le Naour G, et al. Atherogenic properties of LDL particles modified by human group X secreted phospholipase A2 on human endothelial cell function. FASEB journal : official publication of the Federation of American Societies for Experimental Biology 2006;20:2547-9.
41. Henderson WR, Jr., Chi EY, Bollinger JG, et al. Importance of group X-secreted phospholipase A2 in allergen-induced airway inflammation and remodeling in a mouse asthma model. The Journal of experimental medicine 2007;204:865-77.

42. Fujioka D, Saito Y, Kobayashi T, et al. Reduction in myocardial ischemia/reperfusion injury in group X secretory phospholipase A2-deficient mice. Circulation 2008;117:2977-85.
43. Shridas P, Bailey WM, Talbott KR, Oslund RC, Gelb MH, Webb NR. Group X secretory phospholipase A2 enhances TLR4 signaling in macrophages. J Immunol 2011;187:482-9.
44. Ricciotti E, FitzGerald GA. Prostaglandins and inflammation. Arterioscler Thromb Vasc Biol 2011;31:986-1000.
45. Morioka Y, Saiga A, Yokota Y, et al. Mouse group X secretory phospholipase A2 induces a potent release of arachidonic acid from spleen cells and acts as a ligand for the phospholipase A2 receptor. Archives of biochemistry and biophysics 2000;381:31-42.
46. Pruzanski W, Lambeau L, Lazdunsky M, Cho W, Kopilov J, Kuksis A. Differential hydrolysis of molecular species of lipoprotein phosphatidylcholine by groups IIA, V and X secretory phospholipases A2. Biochimica et biophysica acta 2005;1736:38-50.
47. Hallstrand TS, Lai Y, Henderson WR, Jr., Altemeier WA, Gelb MH. Epithelial regulation of eicosanoid production in asthma. Pulmonary pharmacology & therapeutics 2012;25:432-7.
48. Watanabe K, Fujioka D, Saito Y, et al. Group X secretory PLA2 in neutrophils plays a pathogenic role in abdominal aortic aneurysms in mice. American journal of physiology Heart and circulatory physiology 2012;302:H95-104.
49. Zack M, Boyanovsky BB, Shridas P, et al. Group X secretory phospholipase A(2) augments angiotensin II-induced inflammatory responses and abdominal aortic aneurysm formation in apoE-deficient mice. Atherosclerosis 2011;214:58-64.
50. Quinn MT, Parthasarathy S, Steinberg D. Lysophosphatidylcholine: a chemotactic factor for human monocytes and its potential role in atherogenesis. Proceedings of the National Academy of Sciences of the United States of America 1988;85:2805-9.
51. Ishimoto Y, Yamada K, Yamamoto S, Ono T, Notoya M, Hanasaki K. Group V and X secretory phospholipase A(2)s-induced modification of high-density lipoprotein linked to the reduction of its antiatherogenic functions. Biochimica et biophysica acta 2003;1642:129-38.
52. Ait-Oufella H, Herbin O, Lahoute C, et al. Group X secreted phospholipase A2 limits the development of atherosclerosis in LDL receptor-null mice. Arterioscler Thromb Vasc Biol 2013;33:466-73.
53. Shridas P, Bailey WM, Gizard F, et al. Group X secretory phospholipase A2 negatively regulates ABCA1 and ABCG1 expression and cholesterol efflux in macrophages. Arterioscler Thromb Vasc Biol 2010;30:2014-21.
54. Li X, Shridas P, Forrest K, Bailey W, Webb NR. Group X secretory phospholipase A2 negatively regulates adipogenesis in murine models. FASEB journal : official publication of the Federation of American Societies for Experimental Biology 2010;24:4313-24.
55. Shridas P, Bailey WM, Boyanovsky BB, Oslund RC, Gelb MH, Webb NR. Group X secretory phospholipase A2 regulates the expression of steroidogenic acute regulatory protein (StAR) in mouse adrenal glands. The Journal of biological chemistry 2010;285:20031-9.

56. Cummins CL, Volle DH, Zhang Y, et al. Liver X receptors regulate adrenal cholesterol balance. The Journal of clinical investigation 2006;116:1902-12.
57. Hallstrand TS, Lai Y, Altemeier WA, et al. Regulation and function of epithelial secreted phospholipase A2 group X in asthma. American journal of respiratory and critical care medicine 2013;188:42-50.
58. Ohtsuki M, Taketomi Y, Arata S, et al. Transgenic expression of group V, but not group X, secreted phospholipase A2 in mice leads to neonatal lethality because of lung dysfunction. The Journal of biological chemistry 2006;281:36420-33.
59. Jemel I, Ii H, Oslund RC, et al. Group X secreted phospholipase A2 proenzyme is matured by a furin-like proprotein convertase and releases arachidonic acid inside of human HEK293 cells. The Journal of biological chemistry 2011;286:36509-21.
60. Mounier CM, Ghomashchi F, Lindsay MR, et al. Arachidonic acid release from mammalian cells transfected with human groups IIA and X secreted phospholipase A(2) occurs predominantly during the secretory process and with the involvement of cytosolic phospholipase A(2)-alpha. The Journal of biological chemistry 2004;279:25024-38.
61. Artenstein AW, Opal SM. Proprotein convertases in health and disease. The New England journal of medicine 2011;365:2507-18.
62. Leduc R, Molloy SS, Thorne BA, Thomas G. Activation of human furin precursor processing endoprotease occurs by an intramolecular autoproteolytic cleavage. The Journal of biological chemistry 1992;267:14304-8.
63. Anderson ED, VanSlyke JK, Thulin CD, Jean F, Thomas G. Activation of the furin endoprotease is a multiple-step process: requirements for acidification and internal propeptide cleavage. The EMBO journal 1997;16:1508-18.
64. Molloy SS, Thomas L, VanSlyke JK, Stenberg PE, Thomas G. Intracellular trafficking and activation of the furin proprotein convertase: localization to the TGN and recycling from the cell surface. The EMBO journal 1994;13:18-33.
65. Mayer G, Hamelin J, Asselin MC, et al. The regulated cell surface zymogen activation of the proprotein convertase PC5A directs the processing of its secretory substrates. The Journal of biological chemistry 2008;283:2373-84.
66. Henrich S, Cameron A, Bourenkov GP, et al. The crystal structure of the proprotein processing proteinase furin explains its stringent specificity. Nature structural biology 2003;10:520-6.
67. Henrich S, Lindberg I, Bode W, Than ME. Proprotein convertase models based on the crystal structures of furin and kexin: explanation of their specificity. Journal of molecular biology 2005;345:211-27.
68. Chiron MF, Fryling CM, FitzGerald DJ. Cleavage of pseudomonas exotoxin and diphtheria toxin by a furin-like enzyme prepared from beef liver. The Journal of biological chemistry 1994;269:18167-76.
69. Nour N, Mayer G, Mort JS, et al. The cysteine-rich domain of the secreted proprotein convertases PC5A and PACE4 functions as a cell surface anchor and interacts with tissue inhibitors of metalloproteinases. Molecular biology of the cell 2005;16:5215-26.
70. Zhu X, Zhou A, Dey A, et al. Disruption of PC1/3 expression in mice causes dwarfism and multiple neuroendocrine peptide processing defects. Proceedings of the National Academy of Sciences of the United States of America 2002;99:10293-8.

71. Lloyd DJ, Bohan S, Gekakis N. Obesity, hyperphagia and increased metabolic efficiency in Pc1 mutant mice. Human molecular genetics 2006;15:1884-93.
72. Jackson RS, Creemers JW, Ohagi S, et al. Obesity and impaired prohormone processing associated with mutations in the human prohormone convertase 1 gene. Nature genetics 1997;16:303-6.
73. Furuta M, Yano H, Zhou A, et al. Defective prohormone processing and altered pancreatic islet morphology in mice lacking active SPC2. Proceedings of the National Academy of Sciences of the United States of America 1997;94:6646-51.
74. Rigotti A, Edelman ER, Seifert P, et al. Regulation by adrenocorticotropic hormone of the in vivo expression of scavenger receptor class B type I (SR-BI), a high density lipoprotein receptor, in steroidogenic cells of the murine adrenal gland. The Journal of biological chemistry 1996;271:33545-9.
75. Shen WJ, Patel S, Natu V, et al. Interaction of hormone-sensitive lipase with steroidogenic acute regulatory protein: facilitation of cholesterol transfer in adrenal. The Journal of biological chemistry 2003;278:43870-6.
76. Stocco DM. Intramitochondrial cholesterol transfer. Biochimica et biophysica acta 2000;1486:184-97.
77. Christenson LK, Strauss JF, 3rd. Steroidogenic acute regulatory protein (StAR) and the intramitochondrial translocation of cholesterol. Biochimica et biophysica acta 2000;1529:175-87.
78. Caron KM, Soo SC, Wetsel WC, Stocco DM, Clark BJ, Parker KL. Targeted disruption of the mouse gene encoding steroidogenic acute regulatory protein provides insights into congenital lipoid adrenal hyperplasia. Proceedings of the National Academy of Sciences of the United States of America 1997;94:11540-5.
79. Artemenko IP, Zhao D, Hales DB, Hales KH, Jefcoate CR. Mitochondrial processing of newly synthesized steroidogenic acute regulatory protein (StAR), but not total StAR, mediates cholesterol transfer to cytochrome P450 side chain cleavage enzyme in adrenal cells. The Journal of biological chemistry 2001;276:46583-96.
80. Lefrancois-Martinez AM, Blondet-Trichard A, Binart N, et al. Transcriptional control of adrenal steroidogenesis: novel connection between Janus kinase (JAK) 2 protein and protein kinase A (PKA) through stabilization of cAMP response element-binding protein (CREB) transcription factor. The Journal of biological chemistry 2011;286:32976-85.
81. Ronco AM, Moraga PF, Llanos MN. Arachidonic acid release from rat Leydig cells: the involvement of G protein, phospholipase A2 and regulation of cAMP production. The Journal of endocrinology 2002;172:95-104.
82. Maloberti P, Mele PG, Neuman I, et al. Regulation of arachidonic acid release in steroidogenesis: role of a new acyl-CoA thioestrase (ARTISt). Endocrine research 2000;26:653-62.
83. Maloberti P, Castilla R, Castillo F, et al. Silencing the expression of mitochondrial acyl-CoA thioesterase I and acyl-CoA synthetase 4 inhibits hormone-induced steroidogenesis. The FEBS journal 2005;272:1804-14.
84. Wang X, Dyson MT, Jo Y, Stocco DM. Inhibition of cyclooxygenase-2 activity enhances steroidogenesis and steroidogenic acute regulatory gene expression in MA-10 mouse Leydig cells. Endocrinology 2003;144:3368-75.

85. Shea-Eaton W, Sandhoff TW, Lopez D, Hales DB, McLean MP. Transcriptional repression of the rat steroidogenic acute regulatory (StAR) protein gene by the AP-1 family member c-Fos. Mol Cell Endocrinol 2002;188:161-70.
86. Yamazaki T, Higuchi K, Kominami S, Takemori S. 15-lipoxygenase metabolite(s) of arachidonic acid mediates adrenocorticotropin action in bovine adrenal steroidogenesis. Endocrinology 1996;137:2670-5.
87. Arnaldi G, Angeli A, Atkinson AB, et al. Diagnosis and complications of Cushing's syndrome: a consensus statement. J Clin Endocrinol Metab 2003;88:5593-602.
88. Diamant S, Shafrir E. Modulation of the activity of insulin-dependent enzymes of lipogenesis by glucocorticoids. European journal of biochemistry / FEBS 1975;53:541-6.
89. Wang CN, McLeod RS, Yao Z, Brindley DN. Effects of dexamethasone on the synthesis, degradation, and secretion of apolipoprotein B in cultured rat hepatocytes. Arterioscler Thromb Vasc Biol 1995;15:1481-91.
90. Itoh S, Igarashi M, Tsukada Y, Ichinoe A. Nonalcoholic fatty liver with alcoholic hyalin after long-term glucocorticoid therapy. Acta hepato-gastroenterologica 1977;24:415-8.
91. Nanki T, Koike R, Miyasaka N. Subacute severe steatohepatitis during prednisolone therapy for systemic lupus erythematosis. The American journal of gastroenterology 1999;94:3379.
92. Samuel VT, Liu ZX, Qu X, et al. Mechanism of hepatic insulin resistance in non-alcoholic fatty liver disease. The Journal of biological chemistry 2004;279:32345-53.
93. Friedman JE, Yun JS, Patel YM, McGrane MM, Hanson RW. Glucocorticoids regulate the induction of phosphoenolpyruvate carboxykinase (GTP) gene transcription during diabetes. The Journal of biological chemistry 1993;268:12952-7.
94. Argaud D, Zhang Q, Pan W, Maitra S, Pilkis SJ, Lange AJ. Regulation of rat liver glucose-6-phosphatase gene expression in different nutritional and hormonal states: gene structure and 5'-flanking sequence. Diabetes 1996;45:1563-71.
95. Tsuji A, Sakurai K, Kiyokage E, et al. Secretory proprotein convertases PACE4 and PC6A are heparin-binding proteins which are localized in the extracellular matrix. Potential role of PACE4 in the activation of proproteins in the extracellular matrix. Biochimica et biophysica acta 2003;1645:95-104.
96. Anderson ED, Molloy SS, Jean F, Fei H, Shimamura S, Thomas G. The ordered and compartment-specfific autoproteolytic removal of the furin intramolecular chaperone is required for enzyme activation. The Journal of biological chemistry 2002;277:12879-90.
97. Strissel KJ, Stancheva Z, Miyoshi H, et al. Adipocyte death, adipose tissue remodeling, and obesity complications. Diabetes 2007;56:2910-8.
98. Kanda H, Tateya S, Tamori Y, et al. MCP-1 contributes to macrophage infiltration into adipose tissue, insulin resistance, and hepatic steatosis in obesity. The Journal of clinical investigation 2006;116:1494-505.
99. Weisberg SP, Hunter D, Huber R, et al. CCR2 modulates inflammatory and metabolic effects of high-fat feeding. The Journal of clinical investigation 2006;116:115-24.
100. Suganami T, Yuan X, Shimoda Y, et al. Activating transcription factor 3 constitutes a negative feedback mechanism that attenuates saturated Fatty acid/toll-like

receptor 4 signaling and macrophage activation in obese adipose tissue. Circulation research 2009;105:25-32.
101. Saberi M, Woods NB, de Luca C, et al. Hematopoietic cell-specific deletion of toll-like receptor 4 ameliorates hepatic and adipose tissue insulin resistance in high-fat-fed mice. Cell metabolism 2009;10:419-29.
102. Michelsen KS, Doherty TM, Shah PK, Arditi M. TLR signaling: an emerging bridge from innate immunity to atherogenesis. J Immunol 2004;173:5901-7.
103. Zhu X, Owen JS, Wilson MD, et al. Macrophage ABCA1 reduces MyD88-dependent Toll-like receptor trafficking to lipid rafts by reduction of lipid raft cholesterol. Journal of lipid research 2010;51:3196-206.
104. Orr JS, Puglisi MJ, Ellacott KL, Lumeng CN, Wasserman DH, Hasty AH. Toll-like receptor 4 deficiency promotes the alternative activation of adipose tissue macrophages. Diabetes 2012;61:2718-27.
105. Lumeng CN, Liu J, Geletka L, et al. Aging is associated with an increase in T cells and inflammatory macrophages in visceral adipose tissue. J Immunol 2011;187:6208-16.
106. Odegaard JI, Ricardo-Gonzalez RR, Goforth MH, et al. Macrophage-specific PPARgamma controls alternative activation and improves insulin resistance. Nature 2007;447:1116-20.
107. Seo JB, Moon HM, Kim WS, et al. Activated liver X receptors stimulate adipocyte differentiation through induction of peroxisome proliferator-activated receptor gamma expression. Molecular and cellular biology 2004;24:3430-44.
108. Ma L, Dong F, Zaid M, Kumar A, Zha X. ABCA1 protein enhances Toll-like receptor 4 (TLR4)-stimulated interleukin-10 (IL-10) secretion through protein kinase A (PKA) activation. The Journal of biological chemistry 2012;287:40502-12.
109. Primeau V, Coderre L, Karelis AD, et al. Characterizing the profile of obese patients who are metabolically healthy. Int J Obes (Lond) 2011;35:971-81.
110. Tarcin O, Bajaj M, Akalin S. Insulin resistance, adipocyte biology, and thiazolidinediones: a review. Metabolic syndrome and related disorders 2007;5:103-15.
111. Kim JY, van de Wall E, Laplante M, et al. Obesity-associated improvements in metabolic profile through expansion of adipose tissue. The Journal of clinical investigation 2007;117:2621-37.
112. Johnson JA, Trasino SE, Ferrante AW, Jr., Vasselli JR. Prolonged decrease of adipocyte size after rosiglitazone treatment in high- and low-fat-fed rats. Obesity (Silver Spring) 2007;15:2653-63.
113. Laffitte BA, Chao LC, Li J, et al. Activation of liver X receptor improves glucose tolerance through coordinate regulation of glucose metabolism in liver and adipose tissue. Proceedings of the National Academy of Sciences of the United States of America 2003;100:5419-24.
114. Stieneke-Grober A, Vey M, Angliker H, et al. Influenza virus hemagglutinin with multibasic cleavage site is activated by furin, a subtilisin-like endoprotease. The EMBO journal 1992;11:2407-14.
115. Wooton-Kee CR, Boyanovsky BB, Nasser MS, de Villiers WJ, Webb NR. Group V sPLA2 hydrolysis of low-density lipoprotein results in spontaneous particle aggregation and promotes macrophage foam cell formation. Arterioscler Thromb Vasc Biol 2004;24:762-7.

116. Shoelson SE, Herrero L, Naaz A. Obesity, inflammation, and insulin resistance. Gastroenterology 2007;132:2169-80.
117. Cinti S, Mitchell G, Barbatelli G, et al. Adipocyte death defines macrophage localization and function in adipose tissue of obese mice and humans. Journal of lipid research 2005;46:2347-55.
118. Hotamisligil GS, Shargill NS, Spiegelman BM. Adipose expression of tumor necrosis factor-alpha: direct role in obesity-linked insulin resistance. Science 1993;259:87-91.
119. Patsouris D, Li PP, Thapar D, Chapman J, Olefsky JM, Neels JG. Ablation of CD11c-positive cells normalizes insulin sensitivity in obese insulin resistant animals. Cell metabolism 2008;8:301-9.
120. Lumeng CN, Bodzin JL, Saltiel AR. Obesity induces a phenotypic switch in adipose tissue macrophage polarization. The Journal of clinical investigation 2007;117:175-84.
121. Lumeng CN, DelProposto JB, Westcott DJ, Saltiel AR. Phenotypic switching of adipose tissue macrophages with obesity is generated by spatiotemporal differences in macrophage subtypes. Diabetes 2008;57:3239-46.
122. Sato H, Isogai Y, Masuda S, et al. Physiological roles of group X-secreted phospholipase A2 in reproduction, gastrointestinal phospholipid digestion, and neuronal function. The Journal of biological chemistry 2011;286:11632-48.
123. Simpson F, Whitehead JP, James DE. GLUT4--at the cross roads between membrane trafficking and signal transduction. Traffic 2001;2:2-11.
124. Abel ED, Peroni O, Kim JK, et al. Adipose-selective targeting of the GLUT4 gene impairs insulin action in muscle and liver. Nature 2001;409:729-33.
125. Gerin I, Dolinsky VW, Shackman JG, et al. LXRbeta is required for adipocyte growth, glucose homeostasis, and beta cell function. The Journal of biological chemistry 2005;280:23024-31.
126. Gonzalez E, Flier E, Molle D, Accili D, McGraw TE. Hyperinsulinemia leads to uncoupled insulin regulation of the GLUT4 glucose transporter and the FoxO1 transcription factor. Proceedings of the National Academy of Sciences of the United States of America 2011;108:10162-7.
127. Ito A, Suganami T, Yamauchi A, et al. Role of CC chemokine receptor 2 in bone marrow cells in the recruitment of macrophages into obese adipose tissue. The Journal of biological chemistry 2008;283:35715-23.
128. Wu D, Ren Z, Pae M, et al. Aging up-regulates expression of inflammatory mediators in mouse adipose tissue. J Immunol 2007;179:4829-39.
129. Henderson WR, Jr., Oslund RC, Bollinger JG, et al. Blockade of human group X secreted phospholipase A2 (GX-sPLA2)-induced airway inflammation and hyperresponsiveness in a mouse asthma model by a selective GX-sPLA2 inhibitor. The Journal of biological chemistry 2011;286:28049-55.
130. Atout R, Karabina SA, Dollet S, et al. Human group X secreted phospholipase A2 induces dendritic cell maturation through lipoprotein-dependent and -independent mechanisms. Atherosclerosis 2012;222:367-74.
131. Caspar-Bauguil S, Cousin B, Galinier A, et al. Adipose tissues as an ancestral immune organ: site-specific change in obesity. FEBS letters 2005;579:3487-92.

132. Caspar-Bauguil S, Cousin B, Andre M, et al. Weight-dependent changes of immune system in adipose tissue: importance of leptin. Experimental cell research 2006;312:2195-202.
133. Wu H, Ghosh S, Perrard XD, et al. T-cell accumulation and regulated on activation, normal T cell expressed and secreted upregulation in adipose tissue in obesity. Circulation 2007;115:1029-38.
134. Dalton DK, Pitts-Meek S, Keshav S, Figari IS, Bradley A, Stewart TA. Multiple defects of immune cell function in mice with disrupted interferon-gamma genes. Science 1993;259:1739-42.
135. Rocha VZ, Folco EJ, Sukhova G, et al. Interferon-gamma, a Th1 cytokine, regulates fat inflammation: a role for adaptive immunity in obesity. Circulation research 2008;103:467-76.
136. Davis JE, Gabler NK, Walker-Daniels J, Spurlock ME. Tlr-4 deficiency selectively protects against obesity induced by diets high in saturated fat. Obesity (Silver Spring) 2008;16:1248-55.
137. Koseki M, Hirano K, Masuda D, et al. Increased lipid rafts and accelerated lipopolysaccharide-induced tumor necrosis factor-alpha secretion in Abca1-deficient macrophages. Journal of lipid research 2007;48:299-306.
138. Olsson S, Sundler R. The role of lipid rafts in LPS-induced signaling in a macrophage cell line. Molecular immunology 2006;43:607-12.
139. de Vogel-van den Bosch HM, de Wit NJ, Hooiveld GJ, et al. A cholesterol-free, high-fat diet suppresses gene expression of cholesterol transporters in murine small intestine. Am J Physiol Gastrointest Liver Physiol 2008;294:G1171-80.
140. Juvet LK, Andresen SM, Schuster GU, et al. On the role of liver X receptors in lipid accumulation in adipocytes. Mol Endocrinol 2003;17:172-82.
141. Xu M, Zhou H, Wang J, Li C, Yu Y. The expression of ATP-binding cassette transporter A1 in Chinese overweight and obese patients. Int J Obes (Lond) 2009;33:851-6.
142. Nguyen MT, Favelyukis S, Nguyen AK, et al. A subpopulation of macrophages infiltrates hypertrophic adipose tissue and is activated by free fatty acids via Toll-like receptors 2 and 4 and JNK-dependent pathways. The Journal of biological chemistry 2007;282:35279-92.
143. Zeyda M, Farmer D, Todoric J, et al. Human adipose tissue macrophages are of an anti-inflammatory phenotype but capable of excessive pro-inflammatory mediator production. Int J Obes (Lond) 2007;31:1420-8.
144. Bourlier V, Zakaroff-Girard A, Miranville A, et al. Remodeling phenotype of human subcutaneous adipose tissue macrophages. Circulation 2008;117:806-15.
145. Parker KL, Chaplin DD, Wong M, Seidman JG, Smith JA, Schimmer BP. Expression of murine 21-hydroxylase in mouse adrenal glands and in transfected Y1 adrenocortical tumor cells. Proceedings of the National Academy of Sciences of the United States of America 1985;82:7860-4.
146. Remacle AG, Shiryaev SA, Oh ES, et al. Substrate cleavage analysis of furin and related proprotein convertases. A comparative study. The Journal of biological chemistry 2008;283:20897-906.
147. Roebroek AJ, Taylor NA, Louagie E, et al. Limited redundancy of the proprotein convertase furin in mouse liver. The Journal of biological chemistry 2004;279:53442-50.

148. Mesnard D, Donnison M, Fuerer C, Pfeffer PL, Constam DB. The microenvironment patterns the pluripotent mouse epiblast through paracrine Furin and Pace4 proteolytic activities. Genes & development 2011;25:1871-80.
149. Blanchet MH, Le Good JA, Mesnard D, et al. Cripto recruits Furin and PACE4 and controls Nodal trafficking during proteolytic maturation. The EMBO journal 2008;27:2580-91.
150. Guillemot J, Canuel M, Essalmani R, Prat A, Seidah NG. Implication of the proprotein convertases in iron homeostasis: proprotein convertase 7 sheds human transferrin receptor 1 and furin activates hepcidin. Hepatology 2013;57:2514-24.
151. Susan-Resiga D, Essalmani R, Hamelin J, et al. Furin is the major processing enzyme of the cardiac-specific growth factor bone morphogenetic protein 10. The Journal of biological chemistry 2011;286:22785-94.
152. Koo BH, Longpre JM, Somerville RP, Alexander JP, Leduc R, Apte SS. Cell-surface processing of pro-ADAMTS9 by furin. The Journal of biological chemistry 2006;281:12485-94.
153. Cherradi N, Capponi AM, Gaillard RC, Pralong FP. Decreased expression of steroidogenic acute regulatory protein: a novel mechanism participating in the leptin-induced inhibition of glucocorticoid biosynthesis. Endocrinology 2001;142:3302-8.
154. Fon WP, Li PH. Dexamethasone-induced suppression of steroidogenic acute regulatory protein gene expression in mouse Y-1 adrenocortical cells is associated with reduced histone H3 acetylation. Endocrine 2007;32:155-65.
155. Trayhurn P, Wang B, Wood IS. Hypoxia in adipose tissue: a basis for the dysregulation of tissue function in obesity? The British journal of nutrition 2008;100:227-35.
156. Ye J, Gao Z, Yin J, He Q. Hypoxia is a potential risk factor for chronic inflammation and adiponectin reduction in adipose tissue of ob/ob and dietary obese mice. American journal of physiology Endocrinology and metabolism 2007;293:E1118-28.
157. Rausch ME, Weisberg S, Vardhana P, Tortoriello DV. Obesity in C57BL/6J mice is characterized by adipose tissue hypoxia and cytotoxic T-cell infiltration. Int J Obes (Lond) 2008;32:451-63.
158. Hosogai N, Fukuhara A, Oshima K, et al. Adipose tissue hypoxia in obesity and its impact on adipocytokine dysregulation. Diabetes 2007;56:901-11.
159. Carriere A, Carmona MC, Fernandez Y, et al. Mitochondrial reactive oxygen species control the transcription factor CHOP-10/GADD153 and adipocyte differentiation: a mechanism for hypoxia-dependent effect. The Journal of biological chemistry 2004;279:40462-9.
160. Lin Q, Lee YJ, Yun Z. Differentiation arrest by hypoxia. The Journal of biological chemistry 2006;281:30678-83.
161. Gathercole LL, Bujalska IJ, Stewart PM, Tomlinson JW. Glucocorticoid modulation of insulin signaling in human subcutaneous adipose tissue. J Clin Endocrinol Metab 2007;92:4332-9.
162. Li J, Feltzer RE, Dawson KL, Hudson EA, Clark BJ. Janus kinase 2 and calcium are required for angiotensin II-dependent activation of steroidogenic acute regulatory protein transcription in H295R human adrenocortical cells. The Journal of biological chemistry 2003;278:52355-62.

163. Chen YC, Chang MF, Chen Y, Wang SM. Signaling pathways of magnolol-induced adrenal steroidogensis. FEBS letters 2005;579:4337-43.
164. Kim KS, Park JY, Jou I, Park SM. Functional implication of BAFF synthesis and release in gangliosides-stimulated microglia. Journal of leukocyte biology 2009;86:349-59.
165. Blanchette F, Rivard N, Rudd P, Grondin F, Attisano L, Dubois CM. Cross-talk between the p42/p44 MAP kinase and Smad pathways in transforming growth factor beta 1-induced furin gene transactivation. The Journal of biological chemistry 2001;276:33986-94.
166. Poli M, Luscieti S, Gandini V, et al. Transferrin receptor 2 and HFE regulate furin expression via mitogen-activated protein kinase/extracellular signal-regulated kinase (MAPK/Erk) signaling. Implications for transferrin-dependent hepcidin regulation. Haematologica 2010;95:1832-40.
167. Lotfi CF, Todorovic Z, Armelin HA, Schimmer BP. Unmasking a growth-promoting effect of the adrenocorticotropic hormone in Y1 mouse adrenocortical tumor cells. The Journal of biological chemistry 1997;272:29886-91.
168. Tsuji A, Yoshida S, Hasegawa S, et al. Human subtilisin-like proprotein convertase, PACE4 (SPC4) gene expression is highly regulated through E-box elements in HepG2 and GH4C1 cells. Journal of biochemistry 1999;126:494-502.
169. Pedron T, Girard R, Chaby R. TLR4-dependent lipopolysaccharide-induced shedding of tumor necrosis factor receptors in mouse bone marrow granulocytes. The Journal of biological chemistry 2003;278:20555-64.
170. Tellier E, Negre-Salvayre A, Bocquet B, et al. Role for furin in tumor necrosis factor alpha-induced activation of the matrix metalloproteinase/sphingolipid mitogenic pathway. Molecular and cellular biology 2007;27:2997-3007.
171. Stawowy P, Meyborg H, Stibenz D, et al. Furin-like proprotein convertases are central regulators of the membrane type matrix metalloproteinase-pro-matrix metalloproteinase-2 proteolytic cascade in atherosclerosis. Circulation 2005;111:2820-7.
172. Simon C, Goepfert H, Boyd D. Inhibition of the p38 mitogen-activated protein kinase by SB 203580 blocks PMA-induced Mr 92,000 type IV collagenase secretion and in vitro invasion. Cancer research 1998;58:1135-9.
173. Gum R, Wang H, Lengyel E, Juarez J, Boyd D. Regulation of 92 kDa type IV collagenase expression by the jun aminoterminal kinase- and the extracellular signal-regulated kinase-dependent signaling cascades. Oncogene 1997;14:1481-93.
174. Kim SY, Lee EJ, Woo MS, et al. Inhibition of matrix metalloproteinase-9 gene expression by an isoflavone metabolite, irisolidone in U87MG human astroglioma cells. Biochemical and biophysical research communications 2008;366:493-9.
175. Dubois CM, Blanchette F, Laprise MH, Leduc R, Grondin F, Seidah NG. Evidence that furin is an authentic transforming growth factor-beta1-converting enzyme. The American journal of pathology 2001;158:305-16.
176. Thompson C, McMahon S, Bosse Y, Dubois CM, Stankova J, Rola-Pleszczynski M. Leukotriene D4 up-regulates furin expression through CysLT1 receptor signaling. American journal of respiratory cell and molecular biology 2008;39:227-34.
177. Lai Y, Oslund RC, Bollinger JG, et al. Eosinophil cysteinyl leukotriene synthesis mediated by exogenous secreted phospholipase A2 group X. The Journal of biological chemistry 2010;285:41491-500.

178. Chen B, She S, Li D, et al. Role of miR-19a targeting TNF-alpha in mediating ulcerative colitis. Scandinavian journal of gastroenterology 2013;48:815-24.
179. Liu M, Wang Z, Yang S, et al. TNF-alpha is a novel target of miR-19a. International journal of oncology 2011;38:1013-22.
180. Masuda S, Murakami M, Komiyama K, et al. Various secretory phospholipase A2 enzymes are expressed in rheumatoid arthritis and augment prostaglandin production in cultured synovial cells. The FEBS journal 2005;272:655-72.
181. Yamamoto T, Shimano H, Inoue N, et al. Protein kinase A suppresses sterol regulatory element-binding protein-1C expression via phosphorylation of liver X receptor in the liver. The Journal of biological chemistry 2007;282:11687-95.
182. Delvecchio CJ, Capone JP. Protein kinase C alpha modulates liver X receptor alpha transactivation. The Journal of endocrinology 2008;197:121-30.
183. Wang X, Shen CL, Dyson MT, et al. The involvement of epoxygenase metabolites of arachidonic acid in cAMP-stimulated steroidogenesis and steroidogenic acute regulatory protein gene expression. The Journal of endocrinology 2006;190:871-8.
184. Evans JF, Shen CL, Pollack S, Aloia JF, Yeh JK. Adrenocorticotropin evokes transient elevations in intracellular free calcium ([Ca2+]i) and increases basal [Ca2+]i in resting chondrocytes through a phospholipase C-dependent mechanism. Endocrinology 2005;146:3123-32.
185. Kanashiro CA, Khalil RA. Signal transduction by protein kinase C in mammalian cells. Clinical and experimental pharmacology & physiology 1998;25:974-85.
186. O'Flaherty JT, Chadwell BA, Kearns MW, Sergeant S, Daniel LW. Protein kinases C translocation responses to low concentrations of arachidonic acid. The Journal of biological chemistry 2001;276:24743-50.
187. Han WK, Sapirstein A, Hung CC, Alessandrini A, Bonventre JV. Cross-talk between cytosolic phospholipase A2 alpha (cPLA2 alpha) and secretory phospholipase A2 (sPLA2) in hydrogen peroxide-induced arachidonic acid release in murine mesangial cells: sPLA2 regulates cPLA2 alpha activity that is responsible for arachidonic acid release. The Journal of biological chemistry 2003;278:24153-63.
188. Zhou L, Choi HY, Li WP, Xu F, Herz J. LRP1 controls cPLA2 phosphorylation, ABCA1 expression and cellular cholesterol export. PloS one 2009;4:e6853.

# Vita

Joseph Layne, Ph.D.

Professional Education

December 2013
Doctor of Philosophy, Nutritional Science,
Graduate Center for Nutritional Sciences,
University of Kentucky, Lexington, KY

May 2008
Bachelor of Science, Chemistry/Biochemistry,
Department of Chemistry
Montana State University, Bozeman, MT

Research Experience

December 2013 - Present
Post-doctoral Scholar,
Advisor: Ryan Temel Ph.D., Saha Cardiovascular Research Center & Department of Molecular and Biomedical Pharmacology,
University of Kentucky, Lexington, KY

August 2008 - November 2013
Graduate Research Assistant,
Advisor: Nancy Webb, Ph.D., Graduate Center for Nutritional Sciences & Department of Internal Medicine,
University of Kentucky, Lexington, KY

January 2006 - December 2007
Undergraduate Research Assistant,
Department of Chemistry
Montana State University, Bozeman, MT

Teaching Experience

August 2006 - May 2007
Teaching Assistant, Organic Chemistry,
Department of Chemistry/Biochemistry
Montana State University, Bozeman, MT

Awards

October 2010 – July 2013

Pre-doctoral stipend support from NIH, T32DK007778-11, Oxidative Stress Training Grant

Spring 2008
Dean's List, University of Kentucky

Spring 2006
Dean's List, Montana State University

Publications

**Layne J**, Shridas P, Webb N R. Pro-group X secretory phospholipase $A_2$ is proteolytically activated by furin-like proprotein convertases: Implications for the regulation of adrenal steroidogenesis. (submitted for publication)

Shridas P, Zahoor L, Forrest K, **Layne J**, and Webb N R. Group X secretory phospholipase $A_2$ suppresses glucose-stimulated insulin secretion through a cyclooxygenase-2-dependent mechanism. (submitted for publication)

Zheng Y, Morris A, Sunkara M, **Layne J**, Toborek M, and Hennig B. (2012). Epigallocatechin-gallate stimulates NF-E2-related factor and heme oxygenase-1 via caveolin-1 displacement. The Journal of Nutritional Biochemistry 23, 163-168.

**Layne J**, Majkova Z, Smart E J, Toborek M, and Hennig B. (2011). Caveolae: a regulatory platform for nutritional modulation of inflammatory diseases. The Journal of Nutritional Biochemistry 22, 807-811.

Majkova Z, **Layne J**, Sunkara M, Morris A J, Toborek M, and Hennig B. (2011). Omega-3 fatty acid oxidation products prevent vascular endothelial cell activation by coplanar polychlorinated biphenyls. Toxicology and Applied Pharmacology 251, 41-49.

Abstracts

**Layne J**, Shridas P, Forrest K, Webb N R. Proteolytic activation of group X secretory phospholipase $A_2$ by furin-like proproteinconvertases. Barnstable Brown Obesity and Diabetes Research Day, Lexington, KY. (2013)

**Layne J**, Shridas P, Forrest K, Webb N R. Post-translational regulation of group X secretory phospholipase $A_2$. ATVB, Lake Buena Vista, FL. (2013)

**Layne J**, Shridas P, Forrest K, Webb N R. Post-translational regulation of group X secretory phospholipase $A_2$.Gill Heart Institute Cardiovascular Research Day, Lexington, KY. (2012)

**Layne J**, Shridas P, Forrest K, Webb N R. Post-translational regulation of group X secretory phospholipase $A_2$. Southeast Lipid Research Conference, Calloway Gardens, GA. (2012)

**Layne J**, Shridas P, Bailey W, Forrest K, Webb N R. GX $sPLA_2$ deficiency does not protect mice from high fat diet-induced metabolic dysfunction or adipose tissue inflammation. Barnstable Brown Obesity and Diabetes Research Day, Lexington, KY. (2012)

**Layne J**, Shridas P, Forrest K, Bailey W, Webb N R. The role of group X secretory phospholipase $A_2$ (GX $sPLA_2$) in promoting adipose tissue inflammation in response to high fat diet. Gill Heart Institute Cardiovascular Research Day, Lexington, KY. (2011)

Majkova Z, **Layne J**, Toborek M, Hennig B. Omega-3 fatty acid oxidation products prevent vascular endothelial cell activation by coplanar polychlorinated biphenyls (PCBs). SOT (2010)

Zheng YY, **Layne J**, Toborek M, Hennig B. The roles of caveolin-1 and heme oxygenase-1 in EGCG-mediated protection against TNFα-induced endothelial inflammation. FASEB J (2010)

Seelbach MJ, Chen L, Choi YJ, Wei Y, **Layne J**, Hennig B, Toborek M. Novel model of brain metastasis formation: The influence of polychlorinated biphenyls on blood-brain barrier integrity and brain metastasis. FASEB J (2009)

Invited Presentations

**Layne J.** Post-translational regulation of group X secretory phospholipase $A_2$. Gill Heart Institute Cardiovascular Research Day, Lexington, KY. (2012).

**Layne J.** Group X secretory phospholipase $A_2$ (GX $sPLA_2$) regulates LXR target gene expression in macrophages: functional implications. Gill Heart Institute Cardiovascular Research Day, Lexington, KY. (2011).